NASA TECHNICAL NOTE

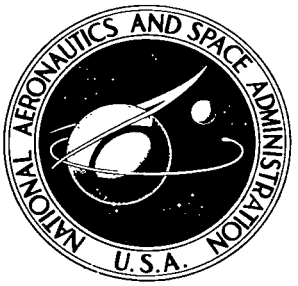

NASA TN D-6191

NASA TN D-6191

INVESTIGATION OF THE AERODYNAMIC CHARACTERISTICS OF A HYPERSONIC TRANSPORT MODEL AT MACH NUMBERS TO 6

by James C. Ellison

Langley Research Center
Hampton, Va. 23365

NATIONAL AERONAUTICS AND SPACE ADMINISTRATION • WASHINGTON, D. C. • APRIL 1971

1. Report No.	2. Government Accession No.	3. Recipient's Catalog No.
NASA TN D-6191		

4. Title and Subtitle
INVESTIGATION OF THE AERODYNAMIC CHARACTERISTICS OF A HYPERSONIC TRANSPORT MODEL AT MACH NUMBERS TO 6

5. Report Date
April 1971

6. Performing Organization Code

7. Author(s)
James C. Ellison

8. Performing Organization Report No.
L-7478

9. Performing Organization Name and Address
NASA Langley Research Center
Hampton, Va. 23365

10. Work Unit No.
722-01-10-04

11. Contract or Grant No.

12. Sponsoring Agency Name and Address
National Aeronautics and Space Administration
Washington, D.C. 20546

13. Type of Report and Period Covered
Technical Note

14. Sponsoring Agency Code

15. Supplementary Notes

16. Abstract

A wind-tunnel investigation was conducted at subsonic, supersonic, and hypersonic speeds to determine the aerodynamic characteristics of a blended wing-body configuration. Data were obtained for the configuration with a single vertical tail, a flow-through inlet, and elevons deflected from 5° to -20°. At a Mach number of 6 and a Reynolds number of 21.6×10^{6}, the configuration had a maximum lift-drag ratio of 5.0 with no trim penalty. Based on the selected center-of-gravity position of 56.4 percent of the model length, the configuration was stable in all directions over the Mach number range. Results of analytical methods agreed with the data at zero elevon deflection for the range of angle of attack from 0° to 6° at all Mach numbers.

17. Key Words (Suggested by Author(s))	18. Distribution Statement
Blended wing-body Wind-tunnel investigation Aerodynamic characteristics	Unclassified – Unlimited

19. Security Classif. (of this report)	20. Security Classif. (of this page)	21. No. of Pages	22. Price*
Unclassified	Unclassified	79	$3.00

*For sale by the National Technical Information Service, Springfield, Virginia 22151

INVESTIGATION OF THE AERODYNAMIC CHARACTERISTICS OF A HYPERSONIC TRANSPORT MODEL AT MACH NUMBERS TO 6

By James C. Ellison
Langley Research Center

SUMMARY

A wind-tunnel investigation has been conducted on a model of a hypersonic transport configuration at Mach numbers from 0.36 to 6 and at Reynolds numbers from 6.67×10^6 to 21.6×10^6 (depending on Mach number) based on model length. The model was composed of a blended wing-body with strakes. The fuselage had a Sears-Haack area distribution, a width-height ratio of 2, negative camber over the forward portion, and a fineness ratio of 13.

Data were obtained for the model with the elevons deflected from -20° to 5° and for the model without the inlet and without the vertical tail at zero elevon deflection. The wind-tunnel results are compared with the results of several analytical methods.

Based on a fixed center-of-gravity position, the model was longitudinally stable or neutrally stable at all test conditions and could be trimmed at all Mach numbers. At a Mach number of 6 and a Reynolds number of 21.6×10^6, the maximum value of lift-drag ratio was 5.0 with no penalty due to trim. The model was directionally stable and had positive effective dihedral over the Mach number range of the investigation. Results obtained from analytical methods were considered adequate for preliminary design studies at zero elevon deflection for angles of attack between 0° and 6°.

INTRODUCTION

Preliminary optimizations of trade-offs between aerodynamic and structural design interactions on hydrogen-fueled, hypersonic transports resulted in configurations with large-volume, low-fineness-ratio fuselages which aerodynamically dominated the remaining components of the airplane. (See refs. 1 and 2.) Conventional, distinct wing-body designs, with small body width and large volume compared with the wing area, produce drag penalties which result in poor hypersonic maximum lift-drag ratio. (See refs. 3 and 4.) In an attempt to improve the overall performance under large volume restrictions, a departure from conventional design was adopted to evolve a configuration

that features (1) a body width-height ratio of 2 to improve the lifting capability of the fuselage, (2) negative camber in the forward fuselage to minimize trim drag penalties on maximum lift-drag ratio, (3) strakes to retard windward pressure bleed-off at angle of attack, and (4) wing-body blending to minimize adverse component interference effects. The configuration has been the subject of preliminary weight and balance and structural and aerodynamic studies similar to those reported in references 3 and 4. This report presents the results of an experimental investigation conducted over the speed range from subsonic to hypersonic.

SYMBOLS

Longitudinal data are presented about the stability axes and lateral data are presented about the body axes. The moment reference point was taken at 56.4 percent of the body length.

b	wing span (30.48 cm)
C_D	drag coefficient, $\frac{\text{Drag}}{qS}$
$C_{D,o}$	drag coefficient at zero lift
$C_{D,min}$	minimum drag coefficient
$\frac{dC_D}{dC_L^2}$	drag-due-to-lift parameter
C_L	lift coefficient, $\frac{\text{Lift}}{qS}$
C_{L_α}	lift-curve slope at zero lift, $\frac{dC_L}{d\alpha}$
C_l	rolling-moment coefficient, $\frac{\text{Rolling moment}}{qSb}$
$C_{l_\beta} = \frac{\Delta C_l}{\Delta \beta}$, per deg	
C_m	pitching-moment coefficient, $\frac{\text{Pitching moment}}{qS\bar{c}}$
$C_{m_{C_L}}$	longitudinal stability parameter, $\frac{dC_m}{dC_L}$
C_n	yawing-moment coefficient, $\frac{\text{Yawing moment}}{qSb}$

$C_{n_\beta} = \frac{\Delta C_n}{\Delta \beta}$, per deg

C_Y side-force coefficient, $\frac{\text{Side force}}{qS}$

$C_{Y_\beta} = \frac{\Delta C_Y}{\Delta \beta}$, per deg

c wing chord, cm

$\bar{c}$ mean aerodynamic chord (27.56 cm)

L/D lift-drag ratio

$(L/D)_{max}$ maximum lift-drag ratio

l length of model (81.28 cm)

M Mach number

q dynamic pressure, N/cm^2

R Reynolds number based on model length

r_{le} average leading-edge radius of strakes and wings (0.0204 cm)

S reference area, planform area of wing including body intercept $(687\ cm^2)$

t/c wing thickness-chord ratio (0.03)

x,y,z longitudinal, lateral, and vertical coordinate, respectively, cm

α angle of attack, deg

β angle of sideslip, deg

ΔC_m C_m at δ_e minus C_m at $\delta_e \approx 0^o$

δ_e elevon deflection (positive, trailing edge down)

APPARATUS AND TESTS

Facilities

The data at $M = 0.36$ were obtained in the Langley low-turbulence pressure tunnel; the data at Mach numbers of 1.50, 2.00, 2.36, and 2.86 were obtained in the Langley Unitary Plan wind tunnel; and the data at a Mach number of 6.00 were obtained in the Langley 20-inch hypersonic tunnel (Mach 6). Details of facilities are given in reference 5.

Model Description

Details of the model and pertinent dimensions are shown in figure 1 (the dashed lines indicate the afterbody shape prior to modifications necessary to accommodate the balances), and details of the inlet and vertical tails are shown in figure 2. The coordinates of the cross sections shown in figure 1 are given in table I. All results are related

TABLE I.- CROSS-SECTION COORDINATES

x = 5.418 cm		x = 43.35 cm		x = 48.77 cm		x = 73.15 cm	
y, cm	z, cm	y, cm	z, cm	y, cm	z, cm	y, cm	z, cm
0.000	0.621	0.000	0.000	0.000	0.000	0.000	0.000
.161	.631	.341	.002	.410	.020	.480	.021
.251	.641	.761	.036	.750	.059	.839	.099
.352	.661	1.052	.084	1.149	.128	1.148	.186
.422	.681	1.383	.173	1.538	.218	1.495	.344
.492	.701	1.664	.251	1.865	.346	1.880	.603
.602	.750	1.905	.340	2.252	.506	2.165	.860
.712	.800	2.166	.459	2.588	.685	2.575	1.331
.823	.860	2.498	.627	2.963	.935	2.872	1.918
.943	.940	2.830	.856	3.278	1.173	2.976	2.201
1.033	1.020	3.101	1.055	3.620	1.502	3.059	2.544
1.144	1.150	3.343	1.274	3.903	1.819	3.092	2.825
1.234	1.290	3.635	1.553	4.147	2.106	3.096	3.106
1.324	1.411	3.897	1.862	4.320	2.391	3.295	3.180
1.444	1.481	4.129	2.171	4.573	2.708	3.543	3.276
1.645	1.550	4.301	2.460	4.759	2.863	3.792	3.332
1.475	1.631	4.543	2.699	4.956	2.998	4.032	3.377
1.355	1.681	4.774	2.899	5.154	3.103	4.382	3.405
1.224	1.721	5.005	3.017	5.344	3.137	4.110	3.459
1.124	1.761	5.206	3.116	5.603	3.184	3.628	3.508
1.044	1.782	5.477	3.205	7.772	3.396	3.174	3.629
.954	1.812	5.738	3.234	5.582	3.624	2.658	3.857
.864	1.822	4.838	3.579	5.069	3.722	2.365	3.991
.684	1.852	4.238	3.733	4.483	3.888	2.102	4.095
.574	1.862	3.528	3.907	3.738	4.070	1.607	4.274
.483	1.872	2.977	4.020	3.133	4.185	1.295	4.338
.353	1.893	2.257	4.145	1.966	4.387	.983	4.391
.253	1.893	1.506	4.259	1.323	4.451	.601	4.442
.133	1.903	.805	4.313	.631	4.474	.280	4.465
.000	1.903	.000	4.317	.000	4.489	.000	4.479

to the modified configuration and no attempt was made to account for the boattail of a full-scale configuration. The model consisted of a fuselage having a fineness ratio of 13, a Sears-Haack longitudinal area distribution (ref. 6) and a body width-height ratio of 2. The fuselage was blended with negatively cambered strakes and a wedge-slab-wedge delta wing having leading- and trailing-edge sweep angles of 65° and -15°, respectively. A diamond vertical tail with 2° included angle was used for the subsonic investigation and a wedge vertical tail with a 4° included angle was used for the other test Mach numbers. It is anticipated that the flight configuration might have actuators that could change the vertical tail to reduce the base drag at subsonic speeds. The propulsion package was simulated by a flow-through inlet of constant area, 1.5 percent of the reference area. The model elevons, which had as area of 20 percent of the reference area, could be deflected from 5° to -20° at 5° increments to study the trim and control characteristics of the configuration. The relative proportions of the configuration were arrived at through sizing, weight and balance, and aerodynamic/structural trade-off studies and are representative of a vehicle with a gross weight of 226 800 kilograms capable of Mach 6 cruise and a range of 9260 kilometers.

Tests

The conditions under which the model was tested are presented in table II:

TABLE II.- TEST PROGRAM

M	R	Configuration	α, deg	β, deg	Transition
0.36	9.4×10^6	Complete, elevon deflected	-6 to 21	0	Fixed
		Complete, $\delta_e = 0^{\circ}$	-6 to 21	4	Fixed
		No inlet	-6 to 21	0	Fixed
		Vertical tail off	-6 to 21	4	Fixed
1.50, 2.00, 2.36, 2.86	6.67×10^6	Complete, elevon deflected	-4 to 14	0	Fixed
		Complete, $\delta_e = 0^{\circ}$	-4 to 14	0, 8	Fixed
		No inlet	-4 to 14	0	Fixed
		Vertical tail off	-4 to 14	0, 3	Fixed
6.00	21.6×10^6	Complete, elevon deflected	-2 to 12	0	Free
		Complete, $\delta_e = 0^{\circ}$	-2 to 12	-4	Free
		No inlet	-2 to 12	0	Free
		Vertical tail off	-2 to 12	0, -4	Free

A six-component strain-gage balance was used to measure the forces and moments on the model throughout the test program. For the tests at a Mach number of 6.00 the true angle of attack was set by optical means in which a prism mounted on the model reflected a point source of light on a calibrated screen. For the tests at the other Mach numbers the angle of attack was set by a calibrated counter and the data were corrected for changes due to load deflections.

Base pressure (M = 0.36 and 6.00) and balance cavity pressure (M = 1,50 to 2.86) were measured and the axial force was corrected to the condition of free-stream static pressure.

Except for the tests at a Mach number of 6.00 the model had 0.159-cm-wide strips of No. 60 carborundum grit located 3.05 cm from the nose and 1.02 cm (streamwise) from the wing, inlet, and vertical-tail leading edges to induce boundary-layer transition. Based on the results of reference 7, no corrections were made for grit drag. At M = 6.00 transition is estimated to end on the windward surface at a Reynolds number of 2×10^6 according to reference 8; this corresponds to about 7.6 cm from the leading edges for the conditions of the present investigation.

The area distribution of the inlet was constant and the internal drag was assumed to be entirely skin-friction drag. An estimate of the skin-friction-drag coefficient (0.0009) was calculated and this correction was applied to the supersonic data. However, the estimates calculated for Mach numbers of 0.36 and 6.00 were less than the accuracy in C_D and were considered negligible.

The moment reference center for the model was located at $0.06\bar{c}$ $(0.564l)$, which is about $0.1\bar{c}$ ahead of center-of-gravity position calculated for the full-scale airplane, for all Mach numbers.

Accuracy of Data

The possible errors resulting from inaccuracies within the balances and uncertainties in measured quantities are estimated to be as follows:

	M = 0.36	M = 1.50 to 2.86	M = 6.00
α	$\pm 0.05^o$	$\pm 0.05^o$	$\pm 0.10^o$
C_L	±0.02	±0.004	±0.002
C_D	±0.003	±0.001	±0.001
L/D	1.5	0.25	0.40
C_m	±0.005	±0.001	±0.0002

ANALYTICAL METHODS

The computer program described in reference 9 employs linearized potential flow concepts in the form of a vortex lattice and was utilized to calculate the lift-curve slope $\left(C_{L_\alpha}\right)$ and the longitudinal stability parameter $\left(C_{m_{C_L}}\right)$ at zero lift for Mach numbers from 0.20 to 0.80. Calculation of the total drag was predicted by $C_D = C_{D,o} + C_L \tan \alpha$

where the drag coefficient at zero lift $(C_{D,o})$ was determined by the method of reference 10 and $C_L \tan \alpha$ was determined from the results of the computer program (ref. 9).

A linearized supersonic-wing theory which has been incorporated into a computer program (ref. 11) was employed to calculate the aerodynamic characteristics at Mach numbers of 1.50 and 2.00. (This program requires supersonic flow at the trailing edge which limited its use to Mach numbers below 2.30 for the present configuration.) For Mach numbers of 2.00 and above, three sets of results were obtained by adding tangent-cone-theory results for the fuselage, strakes, and vertical tail to results for the wing obtained from tangent-cone theory (Method I), shock-expansion theory (Method II), and tangent-wedge theory (Method III). These methods were obtained by utilizing a computer program presented in reference 12. All skin-friction-drag calculations (M = 1.50 and above) were obtained by the method of Spalding and Chi (ref. 13) for a turbulent boundary layer.

RESULTS AND DISCUSSION

Basic Results

The longitudinal aerodynamic characteristics for the complete configuration with elevons deflected from -20^o to 5^o are presented in figures 3 to 7. At the Mach number of 0.36 no indication of stall occurred up to 20^o angle of attack; and, in general, the configuration showed no unusual aerodynamic characteristics over the angle-of-attack and Mach number ranges of the investigation. In addition, the model was longitudinally stable at all angles of attack, all elevon deflection angles, and all Mach numbers except 0.36 where the model was neutrally stable at the highest angles of attack for all elevon deflection angles less than 5^o. The negative camber designed into the forward portion of the fuselage and strakes produced a positive pitching moment at zero lift at all Mach numbers and elevon deflection angles except 5^o at Mach numbers of 0.36 and 1.50. In general, at all Mach numbers, the elevons showed good control power over the ranges of angle of attack and angle of elevon deflection.

Effects of Inlet and Vertical Tail

The effects of removing the inlet and vertical tail on the longitudinal characteristics of the configuration with $\delta_e = 0^o$ are presented in figures 8 to 11. The incremental changes in C_L, C_D, and C_m due to removal of the inlet or the vertical tail were, in general, less than the accuracy of the data except at $M = 6.00$ where removal of the inlet and vertical tail produced positive and negative increments, respectively, in C_m. At all Mach numbers above 1.50, removal of the vertical tail increased (within the accuracy of the data) the maximum L/D more than did removal of the inlet.

Lateral Directional Stability Characteristics

The stability parameters C_{l_β}, C_{n_β}, and C_{Y_β} for the complete configuration and for the configuration without the vertical tail were obtained by taking the difference in lateral coefficients measured at angles of sideslip of 0° and a nonzero angle (see table II) and are presented as a function of angle of attack in figure 12. With the vertical tail the model was directionally stable and possessed positive effective dihedral at all Mach numbers. Without the vertical tail the model was directionally stable for angles of attack below 10° and displayed positive effective dihedral for positive angles of attack at all Mach numbers except 6.00. This behavior probably occurred because of the small side area of the forward fuselage, compared with that of the rear of the fuselage, which resulted from the noncircular cross section. A reduction in vertical-tail size could probably be made and a gain in maximum L/D realized. (See fig. 10.) An unusual phenomenon occurred at Mach numbers of 0.36 and 1.50 where the directional stability increased with angle of attack. (See figs. 12(a) and 12(b).) A similar result occurred in the study of reference 14 and was attributed to the effects of vortex flow from the wings.

Comparison of Analytical With Experimental Results

Analytical results of C_m, C_D, and C_L are compared with the experimental results for the configuration ($\delta_e = 0^\circ$) without the inlet in figure 13. At $M = 0.36$ and angles of attack up to about 3° the calculated values of C_L agreed with the data; however, at the higher angles of attack the experimental values were greater than the calculated values. This result probably occurs because the analytical method used (ref. 9) did not account for vortex lift which occurs at these angles of attack. (See refs. 15 and 16.) The calculated drag coefficient at zero lift agrees with the data; but, because of the larger angle of attack required to obtain a given value of C_L, the calculated drag coefficients at angles of attack above 6° were greater than the experimental values. (See fig. 13(a).) The slope of the pitching-moment curve $C_{m_{C_L}}$ obtained analytically agreed with the experimental value, but the underestimated value of C_L suggests that this agreement is fortuitous.

The linear theory method of reference 11 was used for Mach numbers of 1.50 and 2.00, and tangent-cone theory (Method I), tangent-cone shock-expansion theory (Method II), and tangent-cone tangent-wedge theory (Method III) were used at Mach numbers of 2.00 through 6.00 to calculate values of C_L, C_D, and C_m over the angle-of-attack range. All of the methods gave better results for C_L, C_D, and C_m at angles of attack below 6° than at the higher angles of attack. Since hypersonic transport configurations are expected to trim around $\alpha = 5^\circ$, these methods are considered adequate for preliminary design studies. Values of C_m calculated by these methods did not agree with the data over the angle-of-attack range. At angles of attack above 6° none of the methods provided

adequate agreement with the data; and, in addition, the results of the various methods did not agree. The method which gave the closest agreement, although not always adequate, over the angle-of-attack range was the tangent-cone shock-expansion theory (Method II).

Using Method II, the increments in pitching-moment coefficient due to elevon deflection were calculated for the configuration without the inlet and the results are compared with experimental values (assuming the inlet has no effect on the increments) in figure 14. The comparison indicates that values of ΔC_m can be calculated to agree within 15 percent of the experimental values for the negative deflection angles investigated; however, at $\delta_e = 5^o$ the calculated results deviated from the experimental results by as much as 50 percent.

The experimental trimmed and untrimmed ($\delta_e = 0^o$) characteristics for the complete configuration are presented as a function of C_L in figure 15. In addition, the analytical values for the configuration without the inlet, calculated by tangent-cone shock-expansion Method II for the trimmed condition are shown for comparison (assuming contributions due to the inlet are negligible, based on fig. 11) in figures 15(c) to 15(f). For the center-of-gravity position selected, no trim penalties occurred at a Mach number of 6.00 (fig. 15(f)) where the trimmed $(L/D)_{max} = 5.0$. At the Mach numbers below 6.00 significant time penalties occurred in C_L and L/D. The analytical and experimental values of trimmed $(L/D)_{max}$ agreed within 10 percent, but the agreement between the values of the other characteristics was inadequate.

Effects of Mach Number

Experimental and calculated values of the lift-curve slope, the drag-due-to-lift factor, and the mininum drag coefficient for the configuration without the inlet are presented as a function of Mach number for $\delta_e = 0^o$ in figure 16. The calculated values of the lift-curve slope and drag-due-to-lift factor agreed with the experimental values at all Mach numbers except 0.36 and the values of the minimum drag coefficient were within 10 percent of the experimental values at all Mach numbers.

Variations of $(L/D)_{max}$, δ_e, and $C_{m_{C_L}}$ (static margin) with Mach number are presented in figure 17 for the untrimmed ($\delta_e = 0^o$) and trimmed conditions. At Mach numbers below 6 significant trim penalties occurred in $(L/D)_{max}$ as a result of the large variation in $C_{m_{C_L}}$ (20 percent) over the Mach number range. A fuel-management program would be required throughout the flight Mach number range to reduce the variation in static margin and the corresponding trim penalties. The calculated values of these parameters were within about 10 percent of the experimental values.

CONCLUSIONS

A wind-tunnel investigation has been conducted on a model of a hypersonic transport configuration at Mach numbers from 0.36 to 6 and at Reynolds numbers from 6.67×10^6 to 21.6×10^6 based on model length and dependent on Mach number. Basically, the configuration was a blended wing-body with strakes, an inlet, and a single vertical tail. The fuselage had a Sears-Haack area distribution with a width-height ratio of 2, negative camber over the forward portion, and a fineness ratio of 13. The data have been presented as aerodynamic coefficients and compared with the results of various analytical methods.

Based on the results of this investigation the following conclusions were made.

1. For the center-of-gravity location of 0.06 mean aerodynamic chord (0.564 model length), the complete configuration was longitudinally stable or neutrally stable at all test conditions.

2. The movement in the aerodynamic center with Mach number produced trim penalties at all Mach numbers except 6 and reduced maximum lift-drag ratio by as much as 1.5 (at Mach 1.5). At Mach 6 and a Reynolds number of 21.6×10^6, the maximum lift-drag ratio had a value of 5.0.

3. The nonsymmetrical cross section and the high-fineness-ratio fuselage provided a low side profile which contributed to the configuration being directionally stable and having positive effective dihedral over the Mach number range.

4. Estimates of the lift and drag coefficients at zero elevon deflection and angles of attack below 6° over the Mach number range were considered adequate for preliminary design studies.

Langley Research Center,
National Aeronautics and Space Administration,
Hampton, Va., February 23, 1971.

REFERENCES

1. Drake, Hubert M.; Gregory, Thomas J.; and Peterson, Richard H.: Hypersonic Technology Problems Identified in Mission Studies. Conference on Hypersonic Aircraft Technology, NASA SP-148, 1967, pp. 1-19.

2. Gregory, Thomas J.; Peterson, Richard H.; and Wyss, John A.: Performance Tradeoffs and Research Problems for Hypersonic Transports. J. Aircraft, vol. 2, no. 4, July-Aug. 1965, pp. 266-271.

3. Penland, Jim A.; Edwards, Clyde L. W.; Witcofski, Robert D.; and Marcum, Don C., Jr.: Comparative Aerodynamic Study of Two Hypersonic Cruise Aircraft Configurations Derived From Trade-Off Studies. NASA TM X-1436, 1967.

4. Small, William J.; Kirkham, Frank S.; and Fetterman, David E.: Aerodynamic Characteristics of a Hypersonic Transport Configuration at Mach 6.86. NASA TN D-5885, 1970.

5. Schaefer, William T., Jr.: Characteristics of Major Active Wind Tunnels at the Langley Research Center. NASA TM X-1130, 1965.

6. Sears, William R.: On Projectiles of Minimum Wave Drag. Quart. Appl. Math., vol. IV, no. 4, Jan. 1947, pp. 361-366.

7. Braslow, Albert L.; Hicks, Raymond M.; and Harris, Roy V.: Use of Grit-Type Boundary-Layer-Transition Trips on Wind-Tunnel Models. NASA TN D-3579, 1966.

8. Whitehead, Allen H., Jr.; and Keyes, J. Wayne: Flow Phenomena and Separation Over Delta Wings With Trailing-Edge Flaps at Mach 6. AIAA J., vol. 6, no. 12, Dec. 1968, pp. 2380-2387.

9. Margason, Richard J.; and Lamar, John E.: Vortex-Lattice FORTRAN Program for Estimating Subsonic Aerodynamic Characteristics of Complex Planforms. NASA TN D-6142, 1971.

10. McDonnell Douglas Corp.: USAF Stability and Control Datcom. Air Force Flight Dyn. Lab., U.S. Air Force, Oct. 1960. (Revised June 1969.)

11. Middleton, Wilbur D.; and Carlson, Harry W.: A Numerical Method for Calculating the Flat-Plate Pressure Distributions on Supersonic Wings of Arbitrary Planform. NASA TN D-2570, 1965.

12. Gentry, Arvel E.; and Smyth, Douglas N.: Hypersonic Arbitrary-Body Aerodynamic Computer Program (Mark III Version). Rep. DAC 61552 (Air Force Contract Nos. F33615 67 C 1008 and F33615 67 C 1602), Douglas Aircraft Co., Apr. 1968. Vol. I – User's Manual. (Available from DDC as AD 851 811.) Vol. II – Program Formulation and Listings. (Available from DDC as AD 851 812.)

13. Spalding, D. B.; and Chi, S. W.: The Drag of a Compressible Turbulent Boundary Layer on a Smooth Flat Plate With and Without Heat Transfer. J. Fluid Mech., vol. 18, pt. 1, Jan. 1964, pp. 117-143.

14. Isaacs, D.: Tests at Subsonic and Supersonic Speeds on a Slender Cambered Wing With Fin, Underwing Engine Nacelles and Trailing-Edge Controls. R. & M. No. 3593, Brit. A.R.C., 1969.

15. Polhamus, Edward C.: A Concept of the Vortex Lift of Sharp-Edge Delta Wings Based on a Leading-Edge-Suction Analogy. NASA TN D-3767, 1966.

16. Polhamus, Edward C.: Predictions of Vortex-Lift Characteristics Based on a Leading-Edge Suction Analogy. AIAA Pap. No. 69-1133, Oct. 1969.

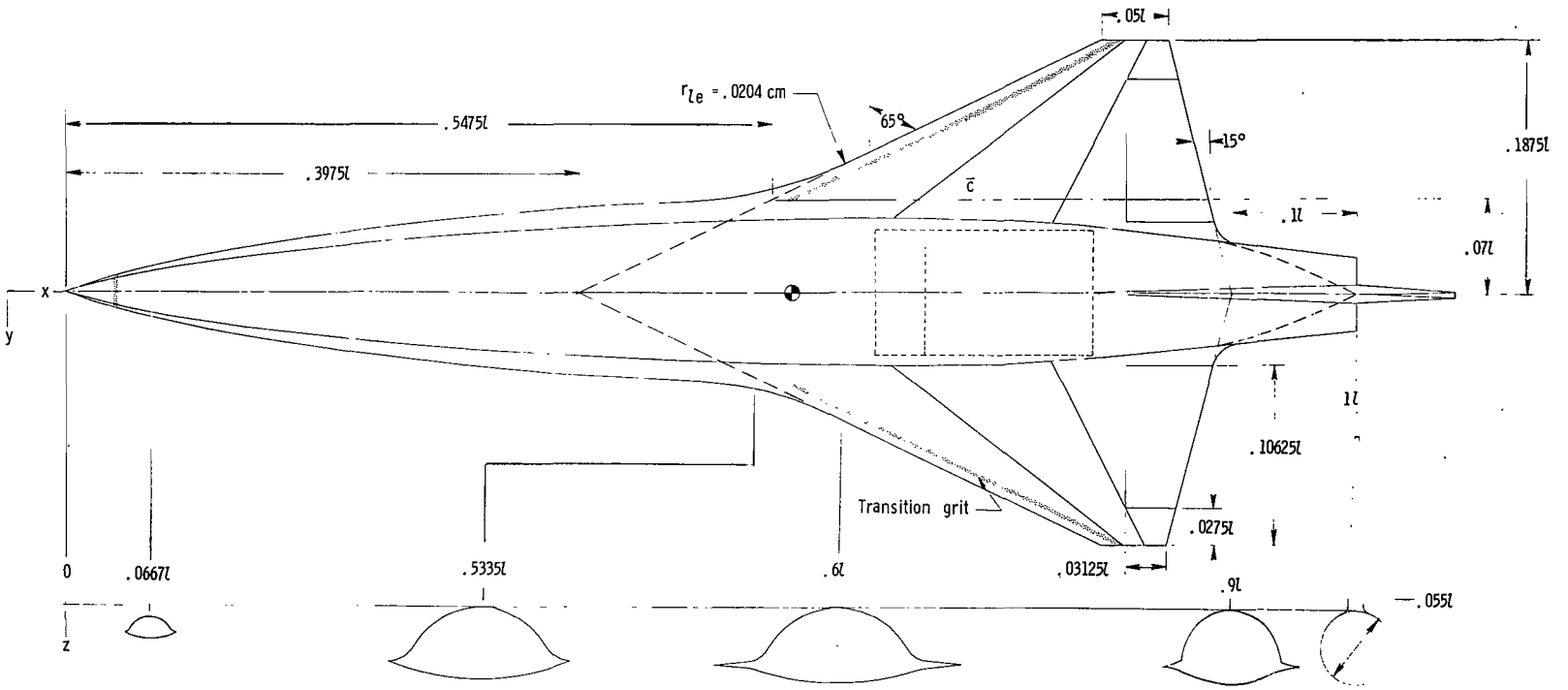

(a) Planform view.

Figure 1.- Details of model. (All linear dimensions are given in terms of the model length ℓ of 81.28 cm.)

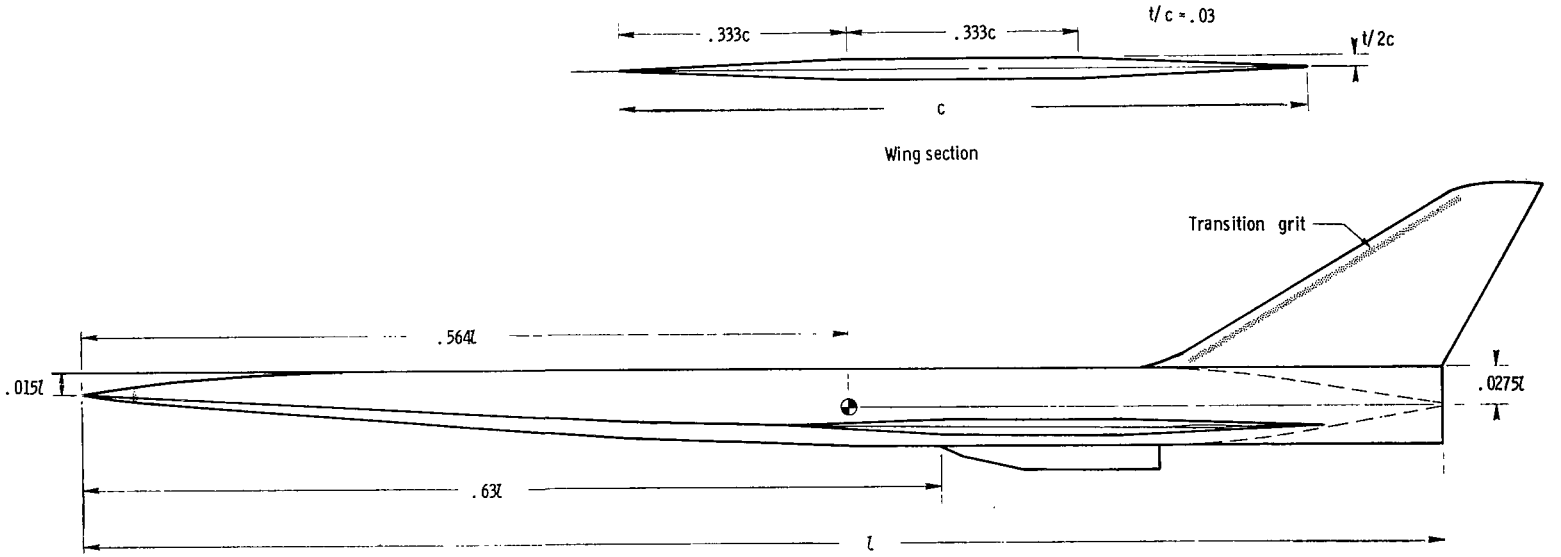

(b) Side view.

Figure 1.- Concluded.

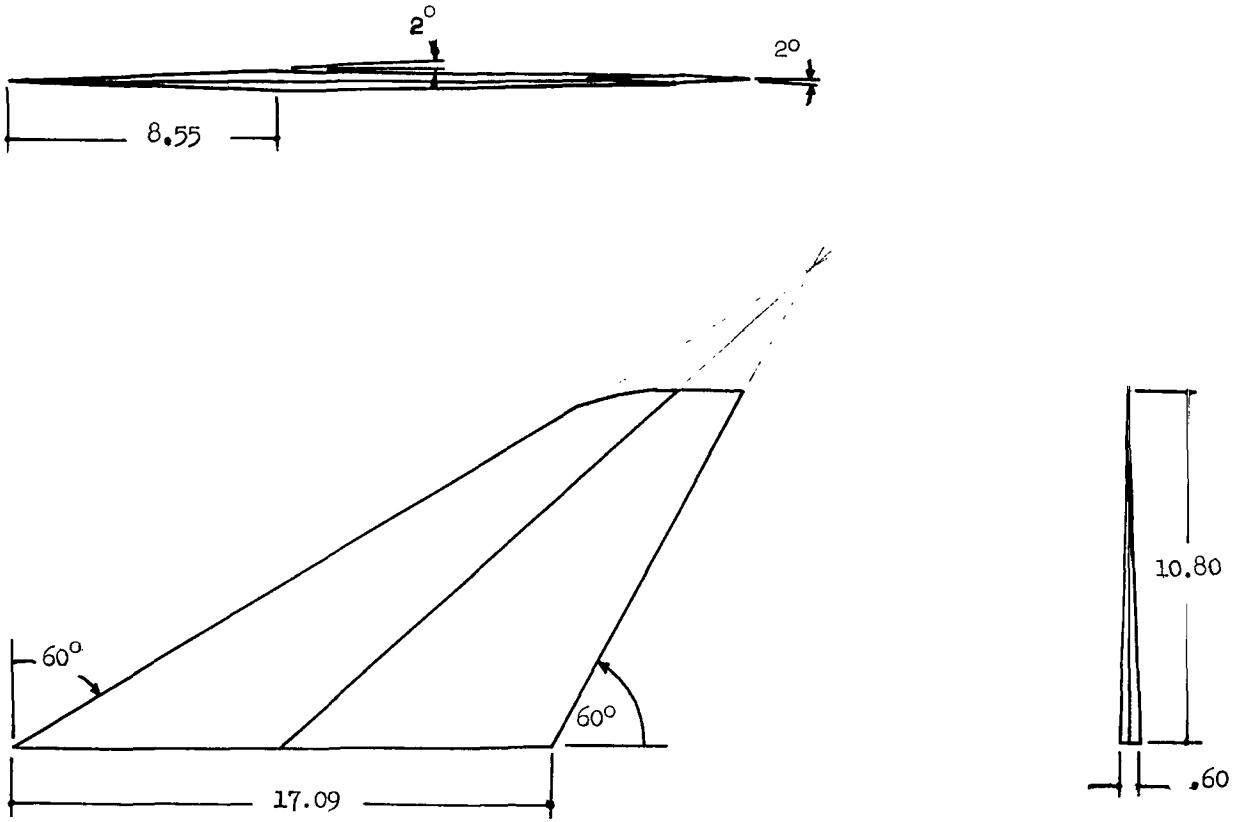

(a) M = 0.36 vertical tail.

Figure 2.- Vertical tails and inlet details. (All dimensions are in centimeters.)

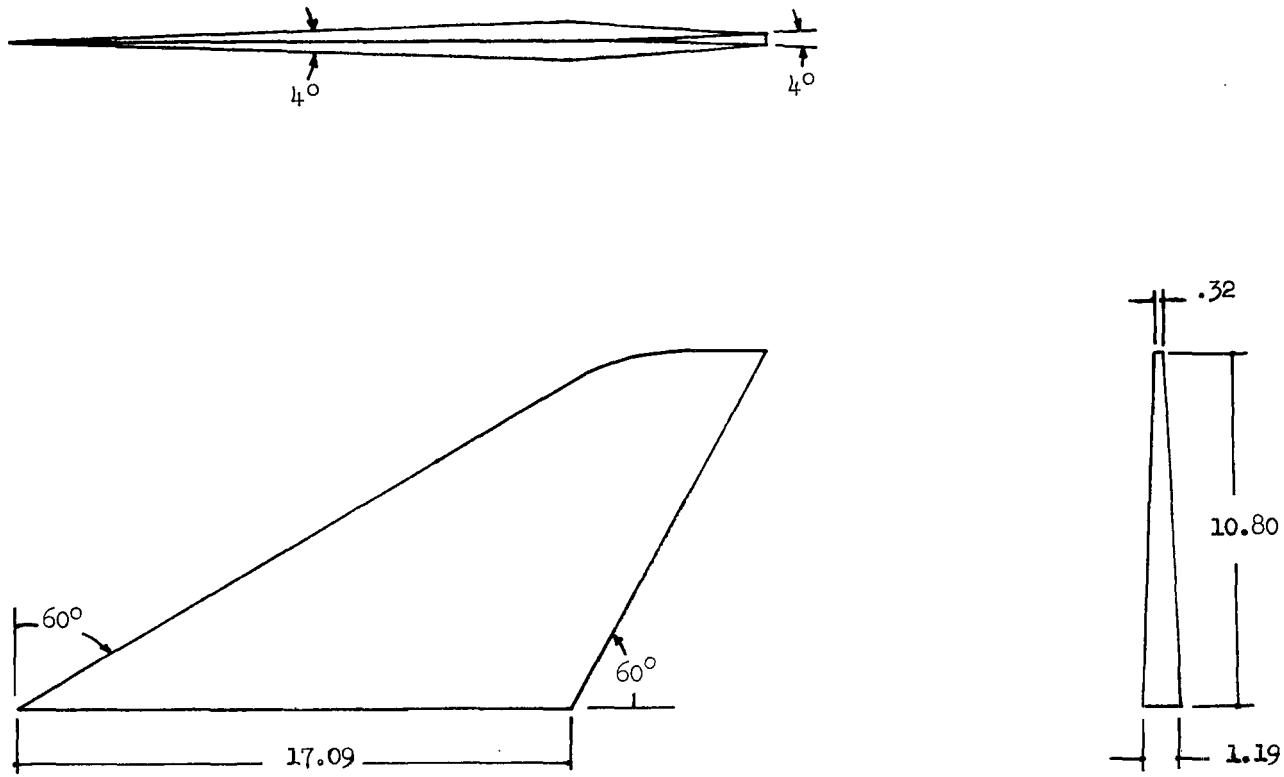

(b) M = 1.50 to 6.00 vertical tail.

Figure 2.- Continued.

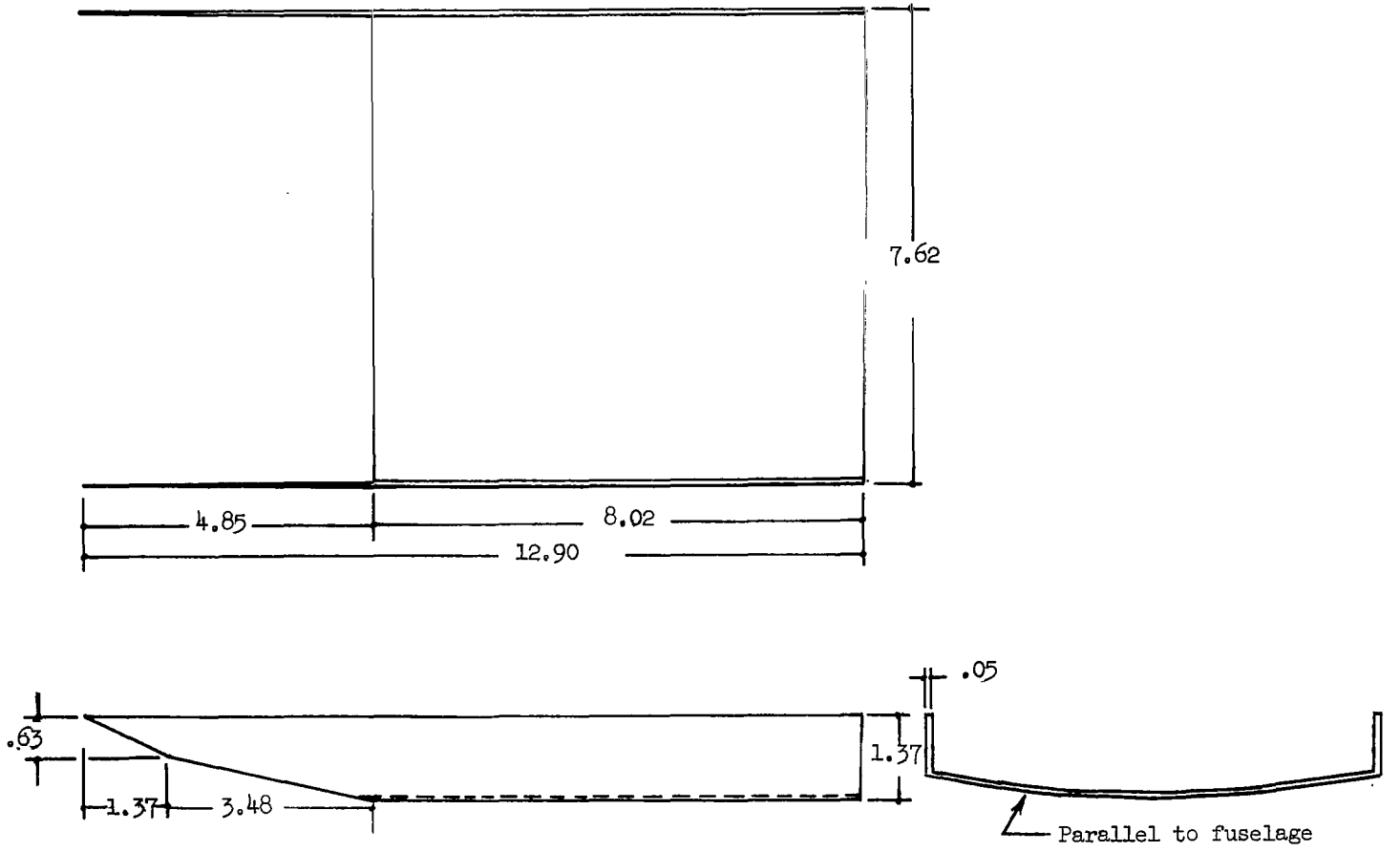

(c) Inlet.

Figure 2.- Concluded.

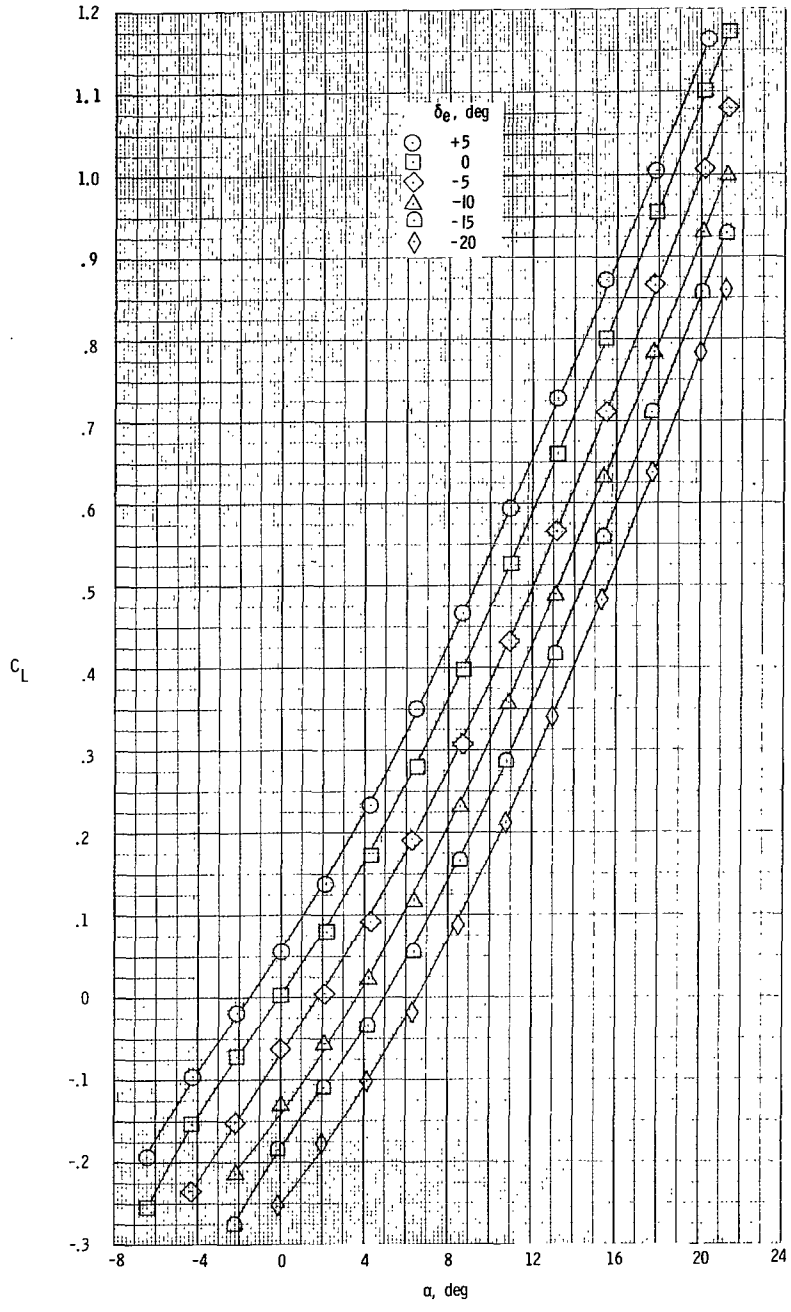

(a) M = 0.36.

Figure 3.- Lift coefficient as a function of elevon deflection and angle of attack for complete configuration.

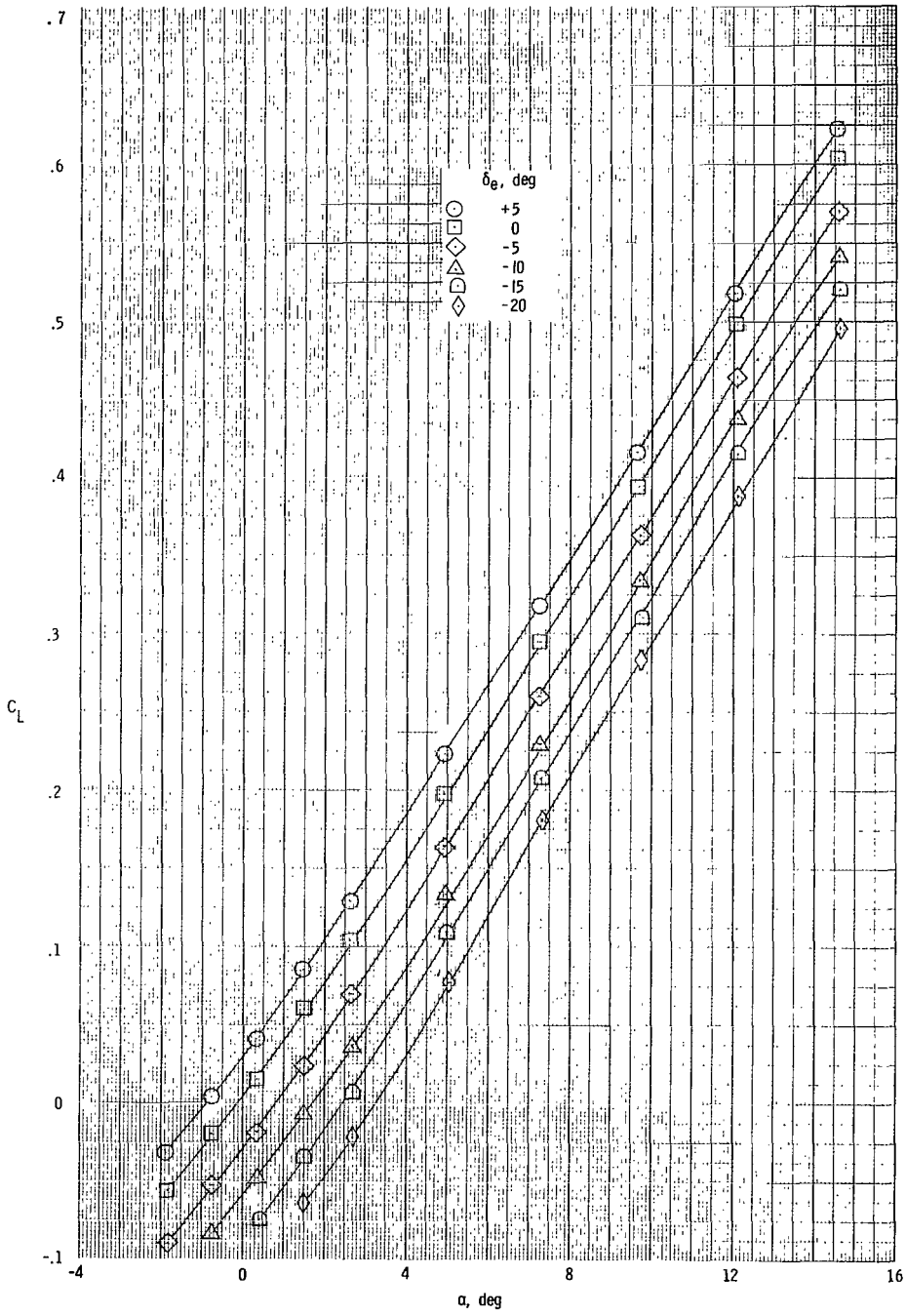

(b) M = 1.50.

Figure 3.- Continued.

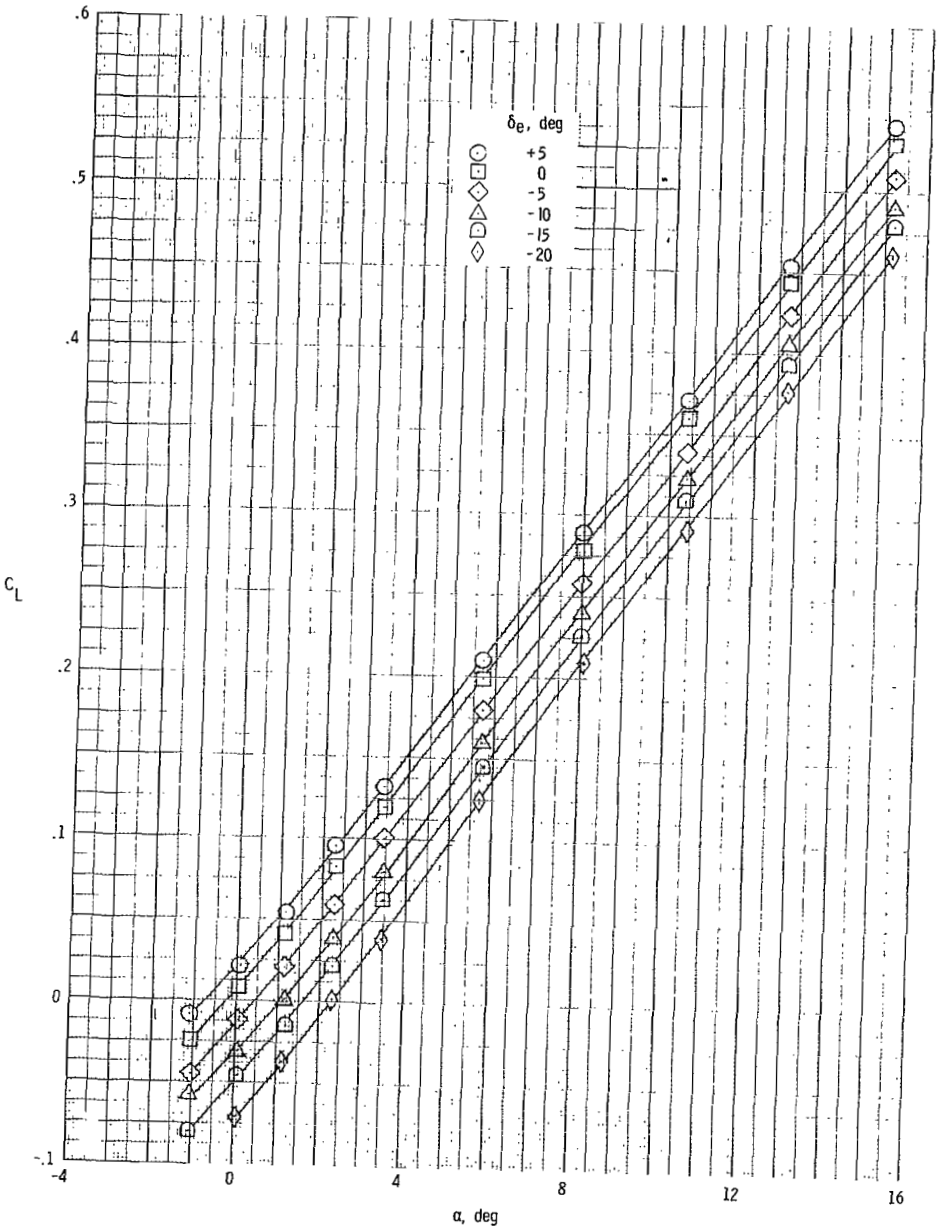

(c) M = 2.00.

Figure 3.- Continued.

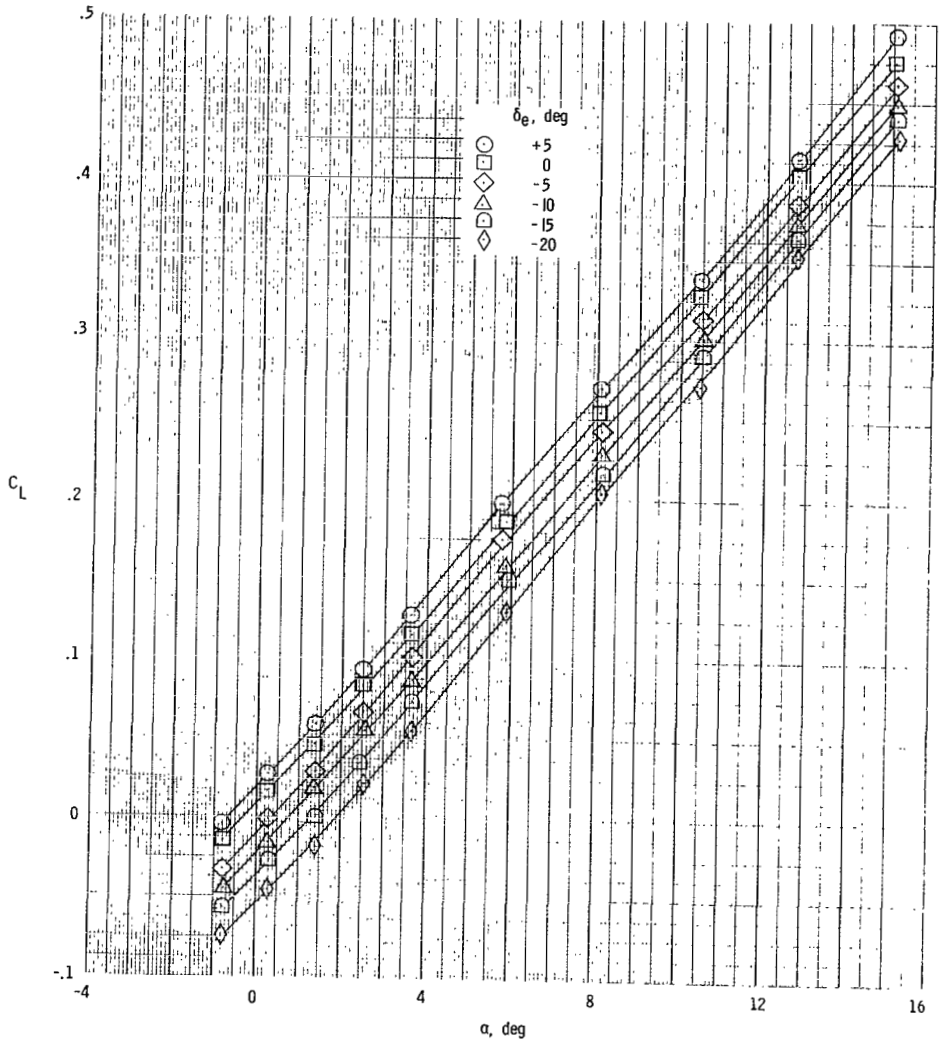

(d) $M = 2.36$.

Figure 3.- Continued.

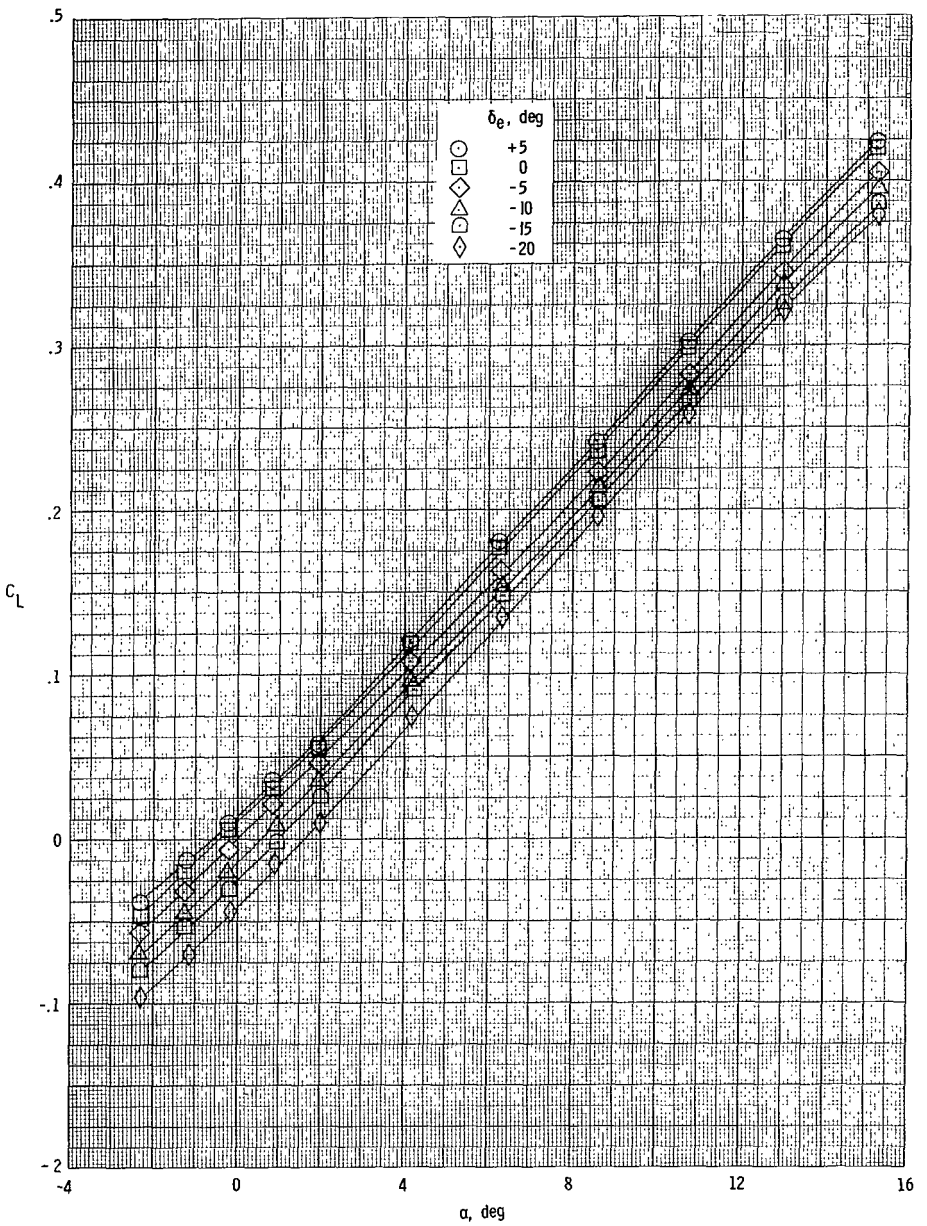

(e) M = 2.86.

Figure 3.- Continued.

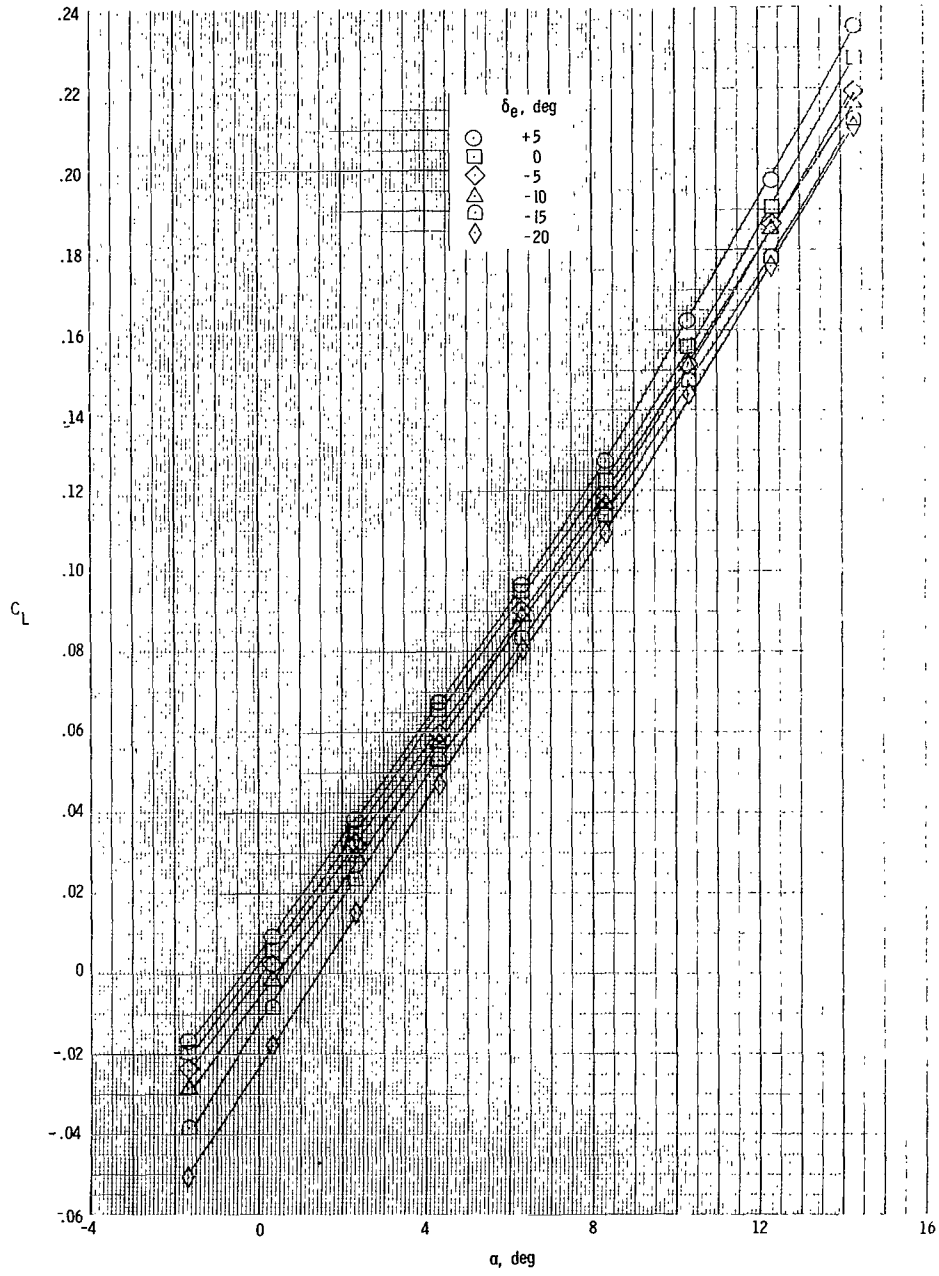

(f) M = 6.00.

Figure 3.- Concluded.

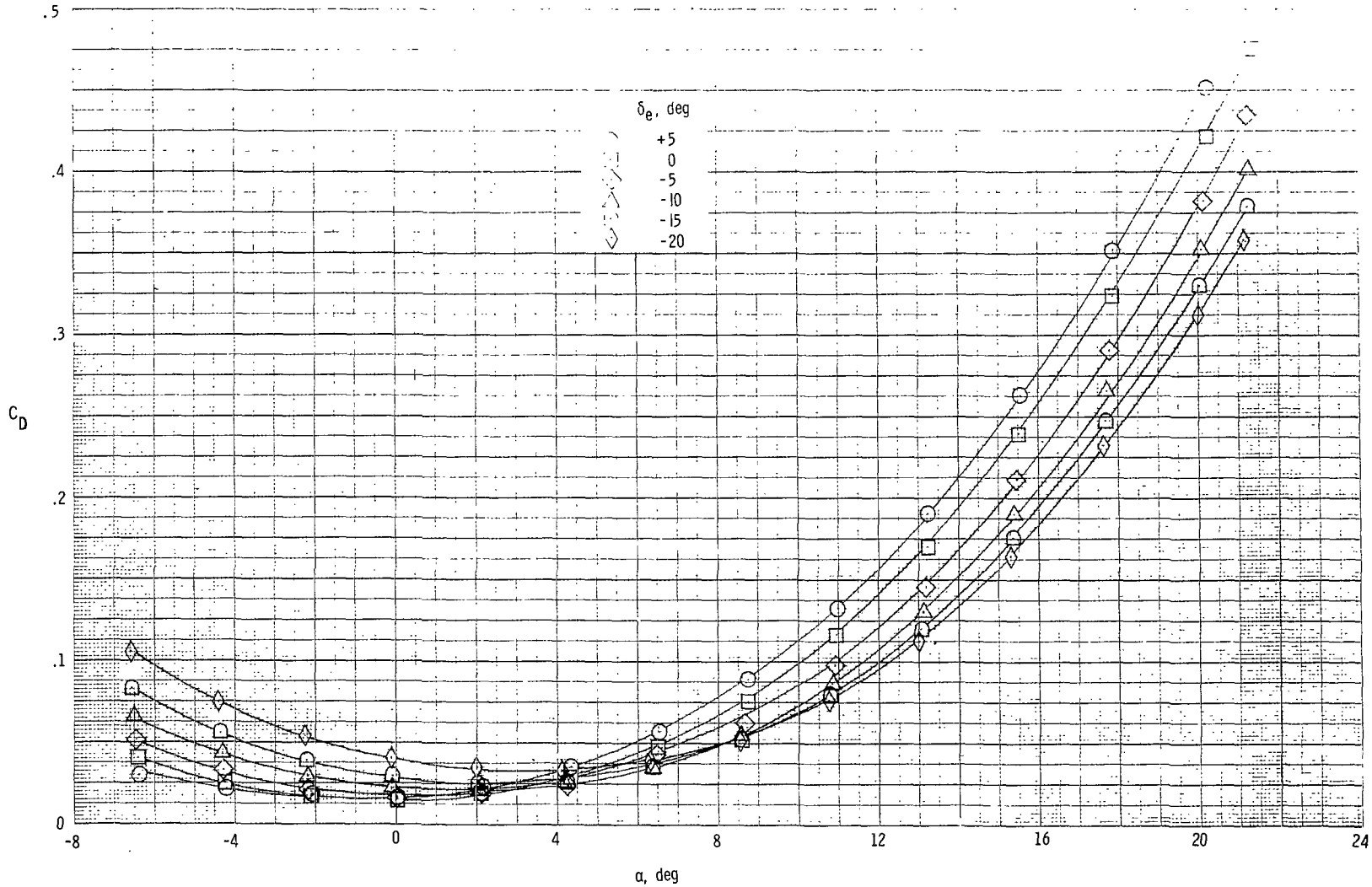

(a) M = 0.36.

Figure 4.- Drag coefficient as a function of elevon deflection and angle of attack for complete configuration.

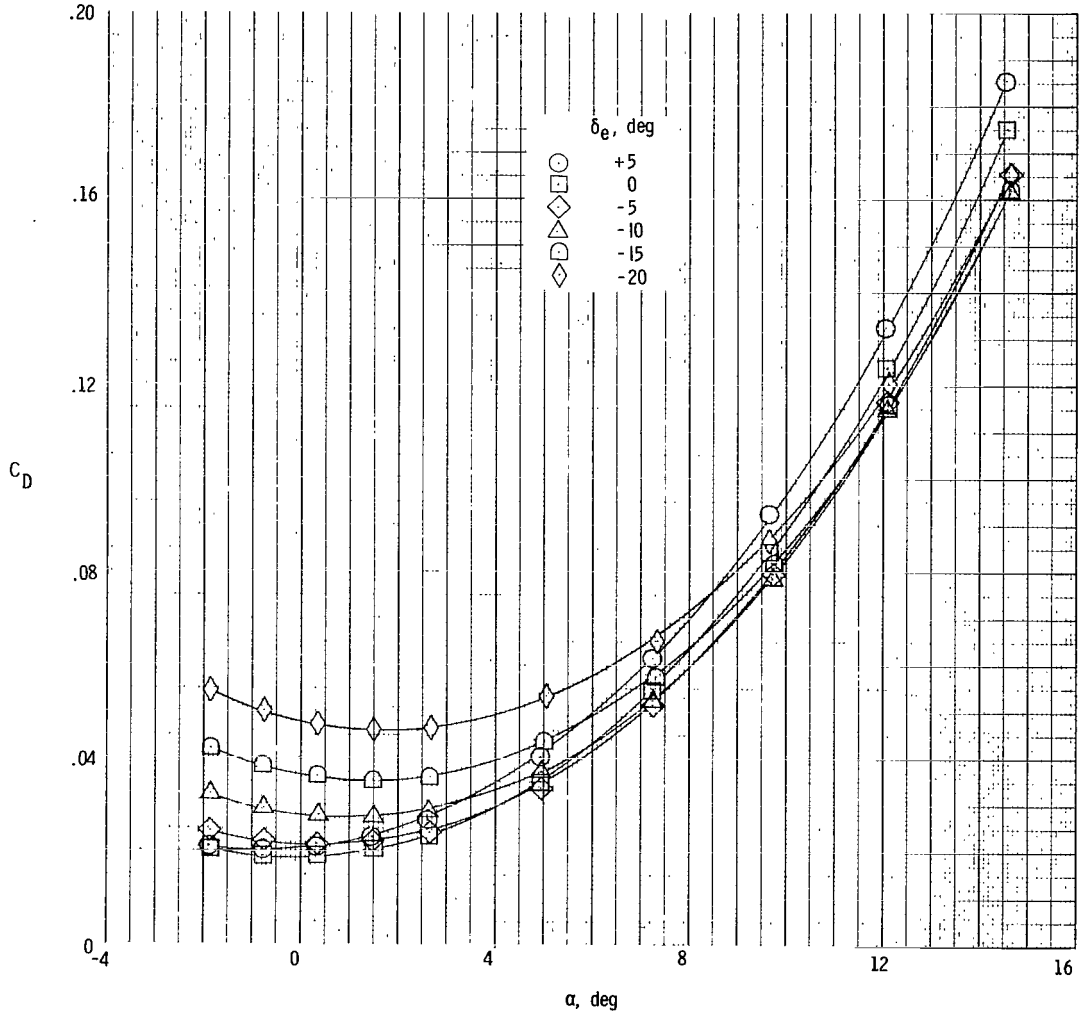

(b) M = 1.50.

Figure 4.- Continued.

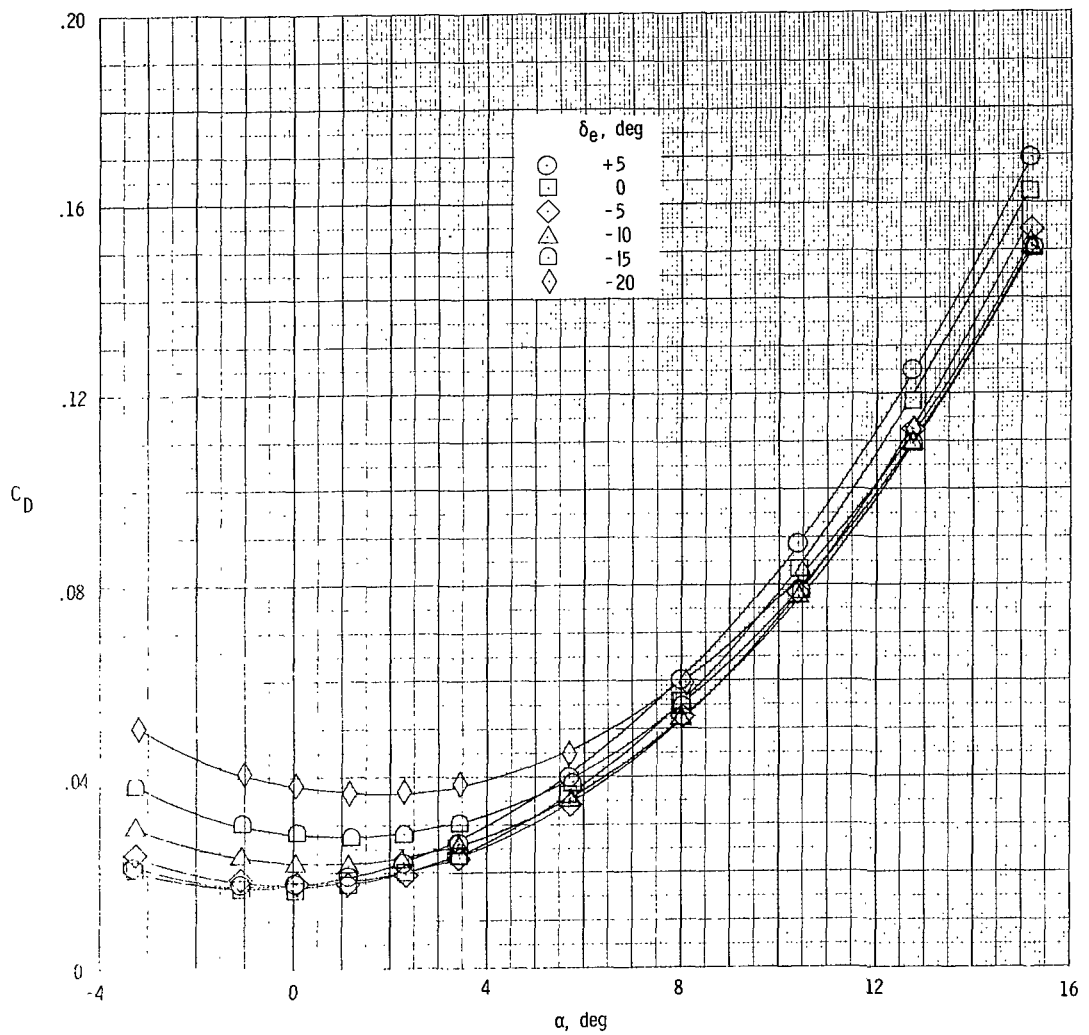

(c) M = 2.00.

Figure 4.- Continued.

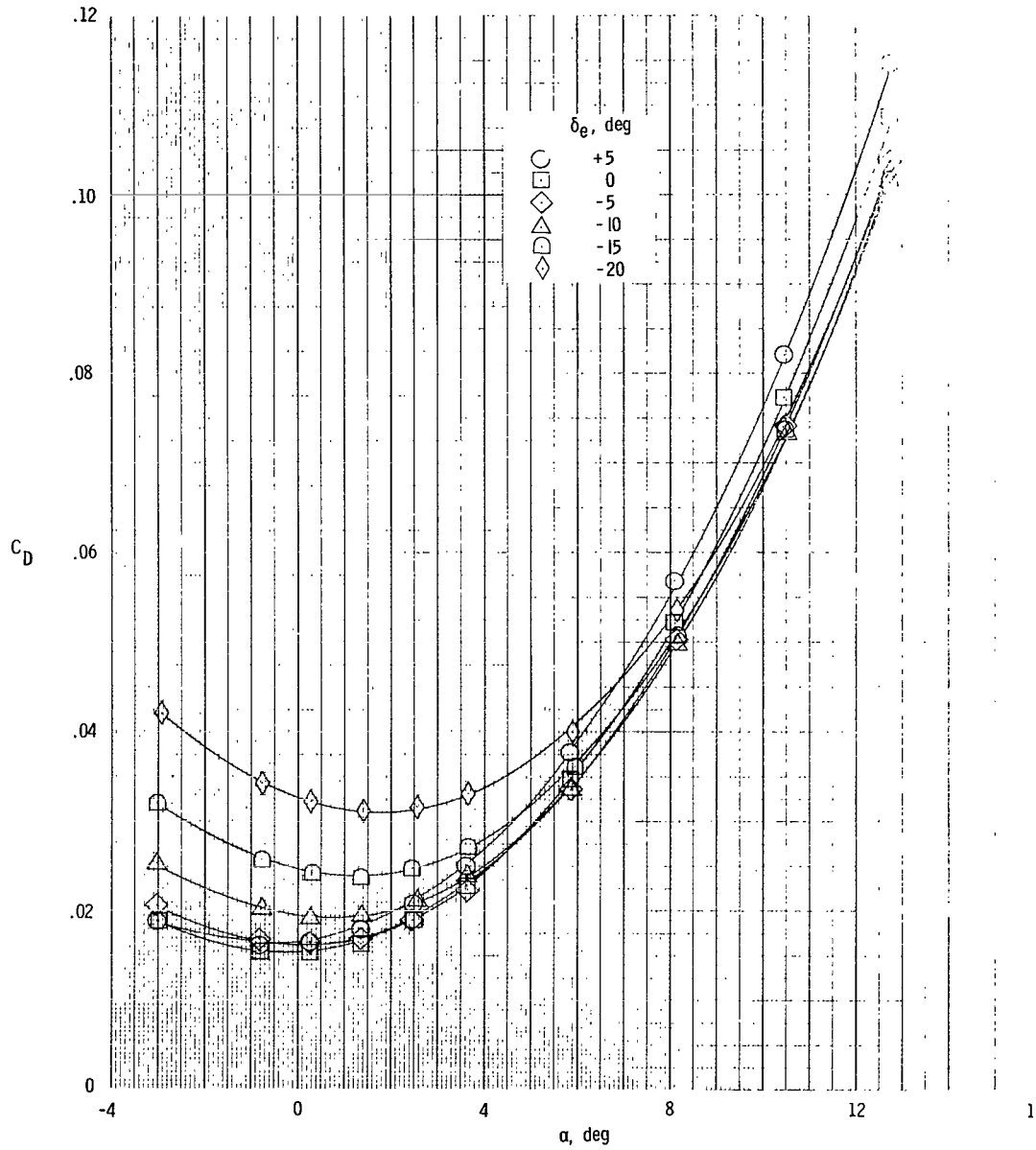

(d) M = 2.36.

Figure 4.- Continued.

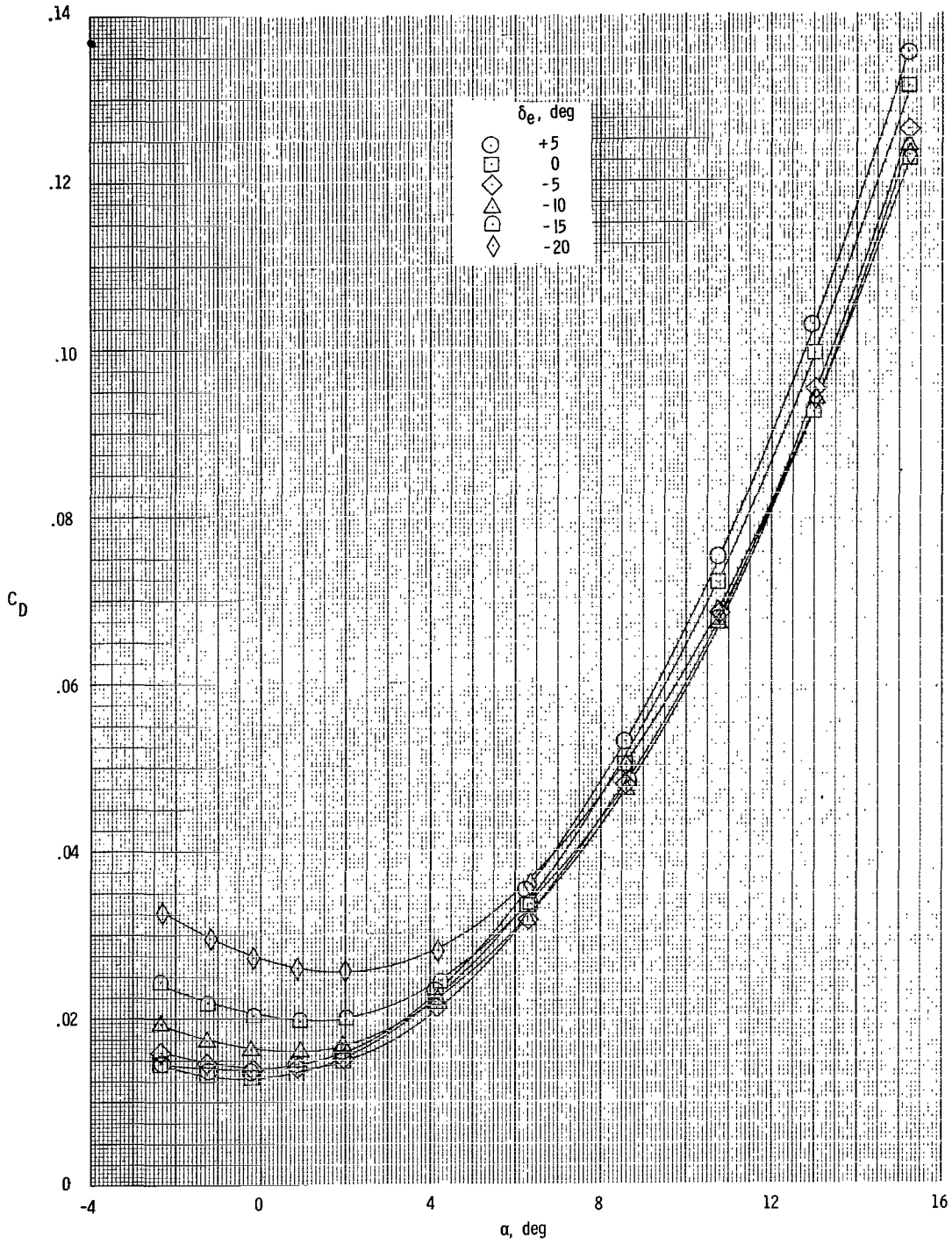

(e) M = 2.86.

Figure 4.- Continued.

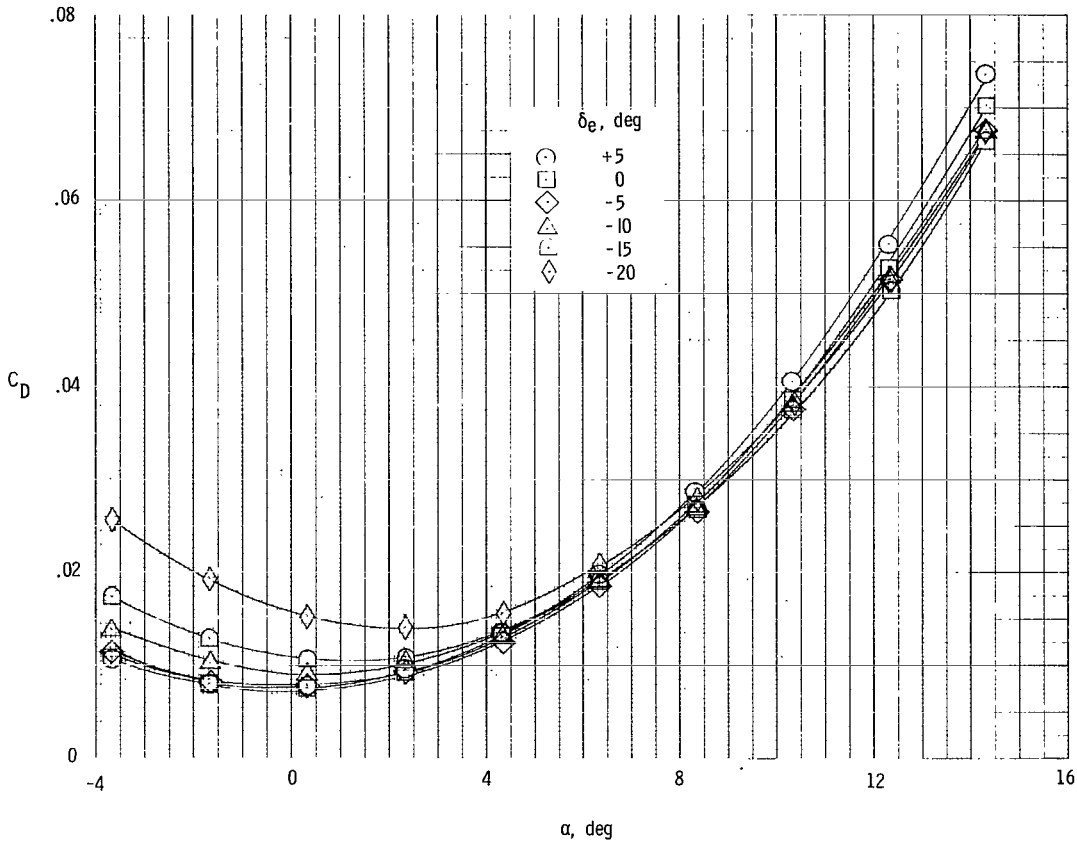

(f) M = 6.00.

Figure 4.- Concluded.

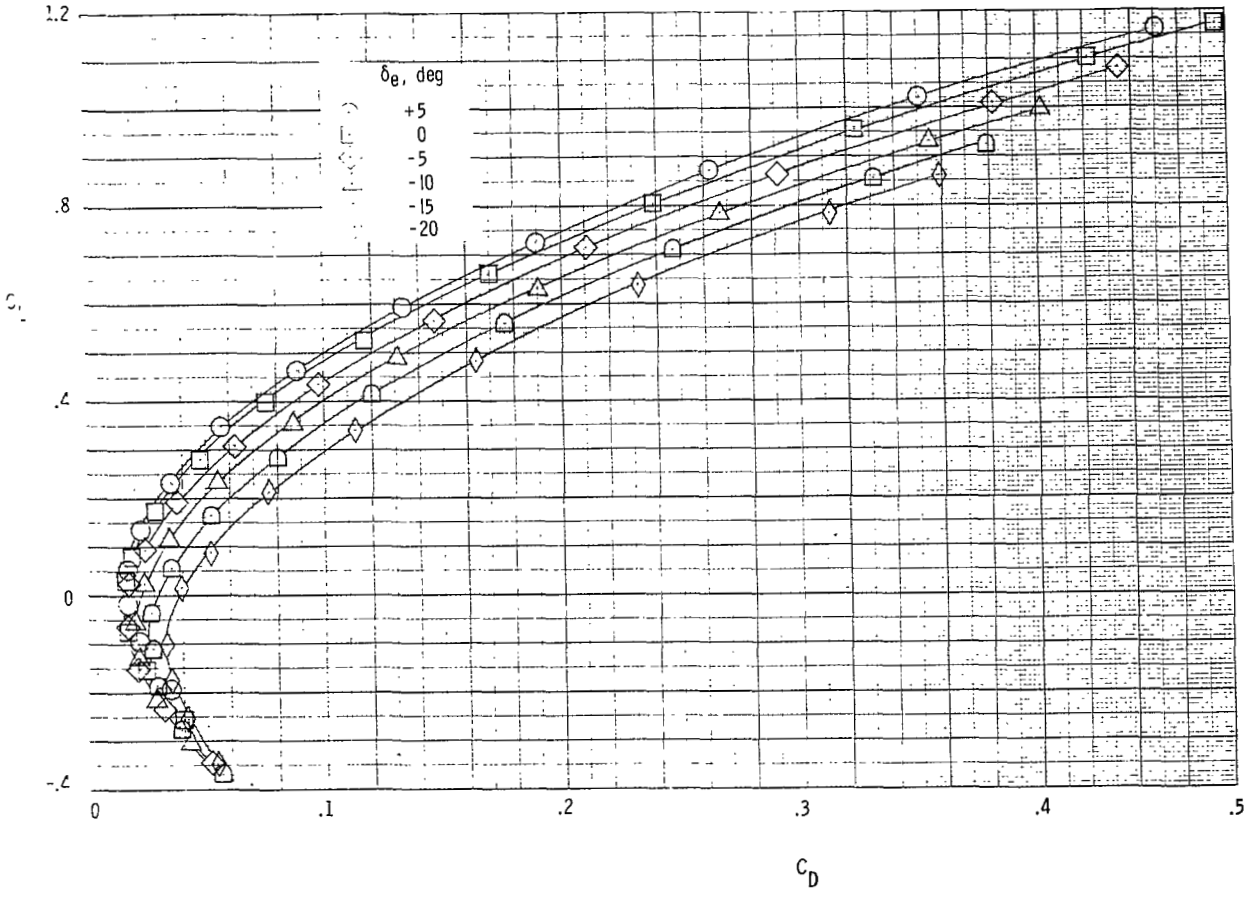

(a) M = 0.36.

Figure 5.- Lift-drag polar for complete configuration.

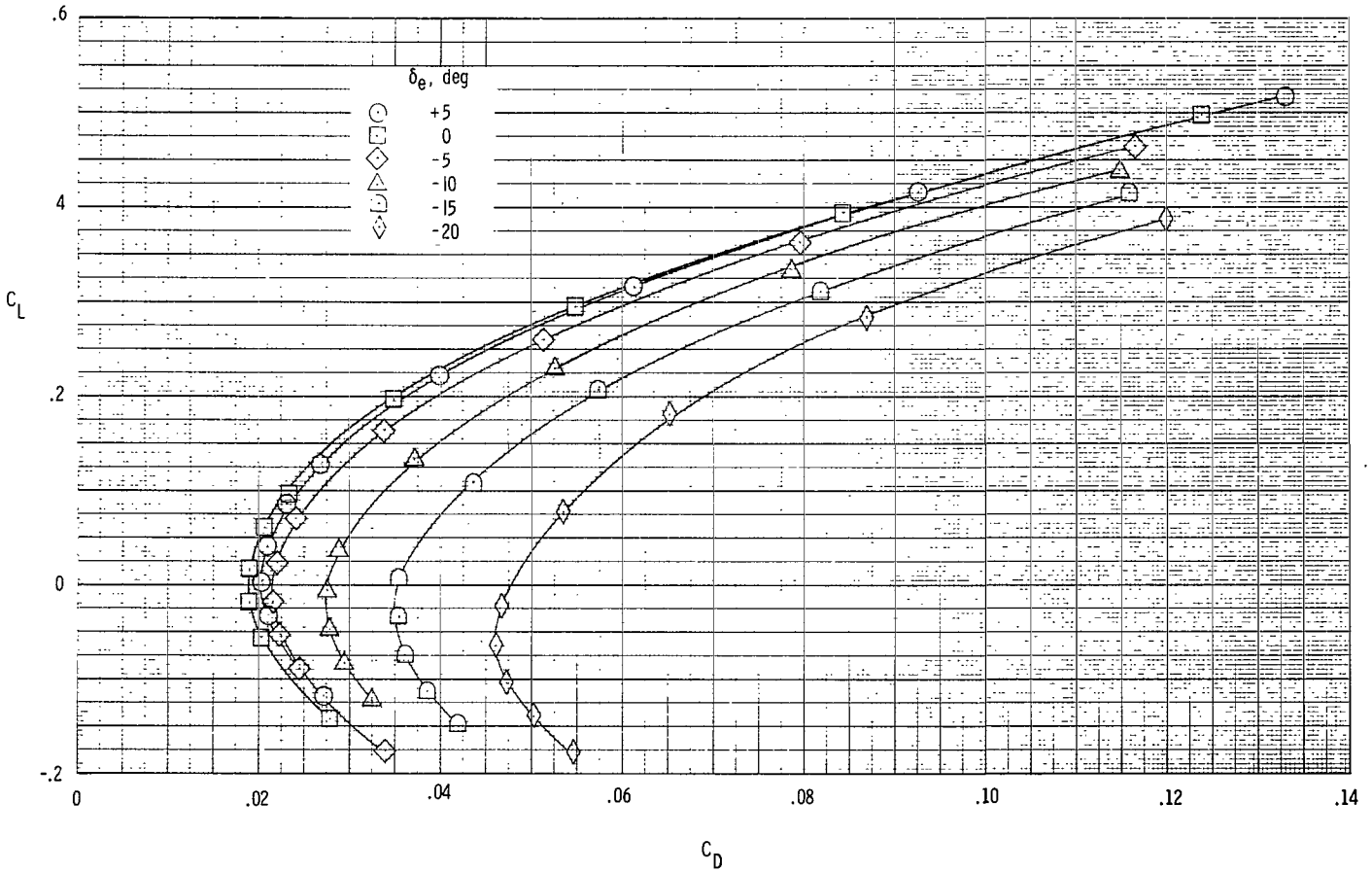

(b) M = 1.50.

Figure 5.- Continued.

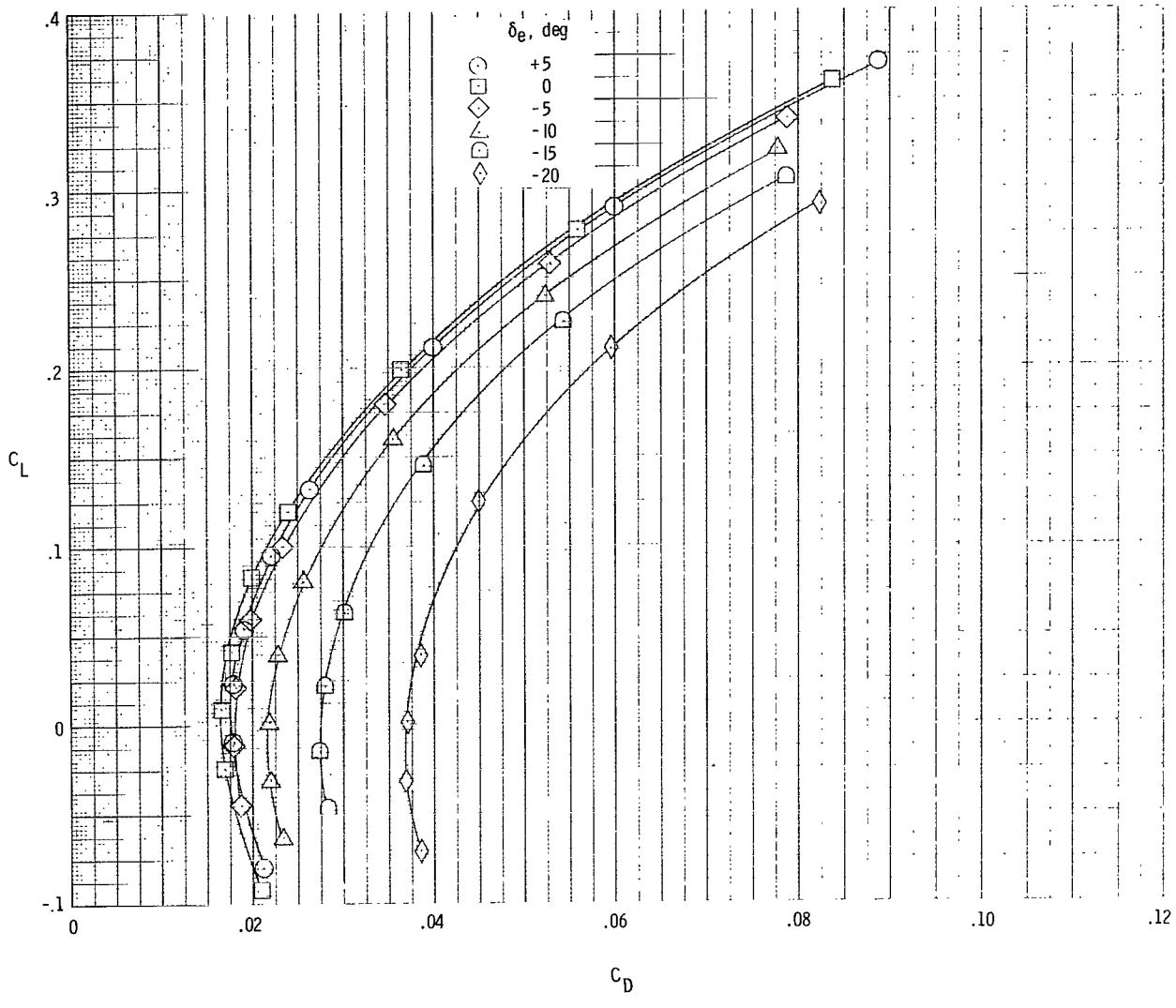

(c) M = 2.00.

Figure 5.- Continued.

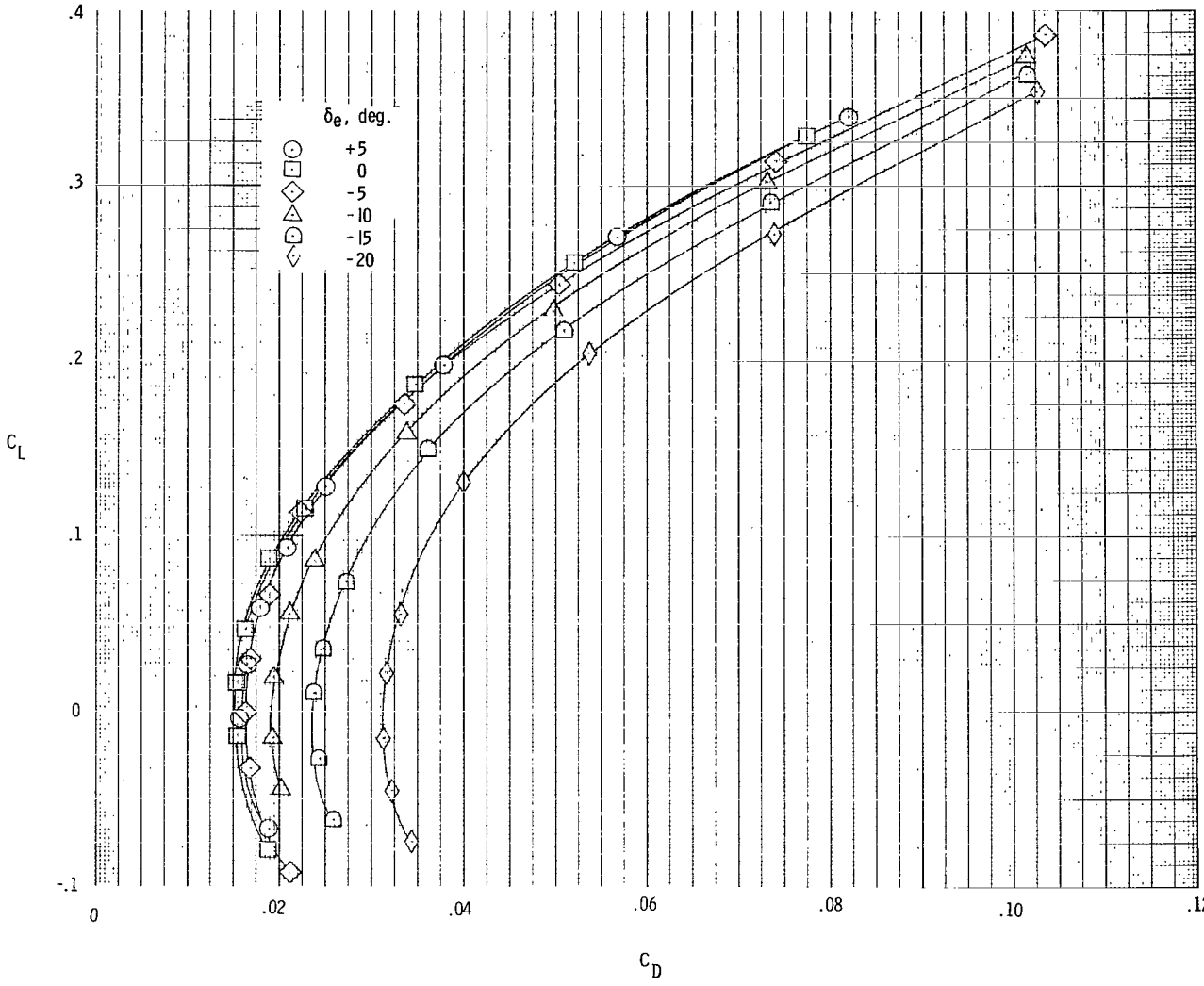

(d) M = 2.36.

Figure 5.- Continued.

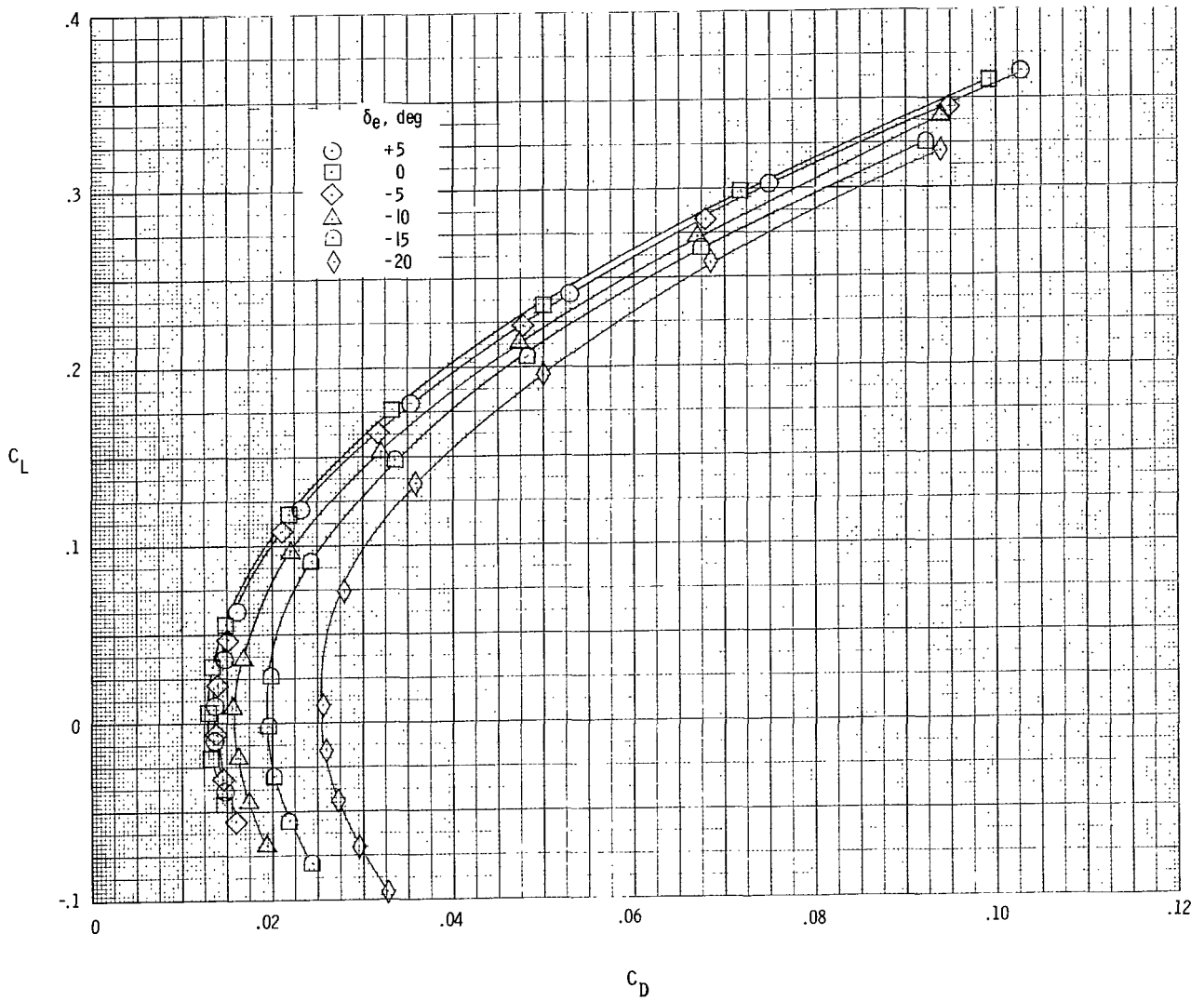

(e) M = 2.86.

Figure 5.- Continued.

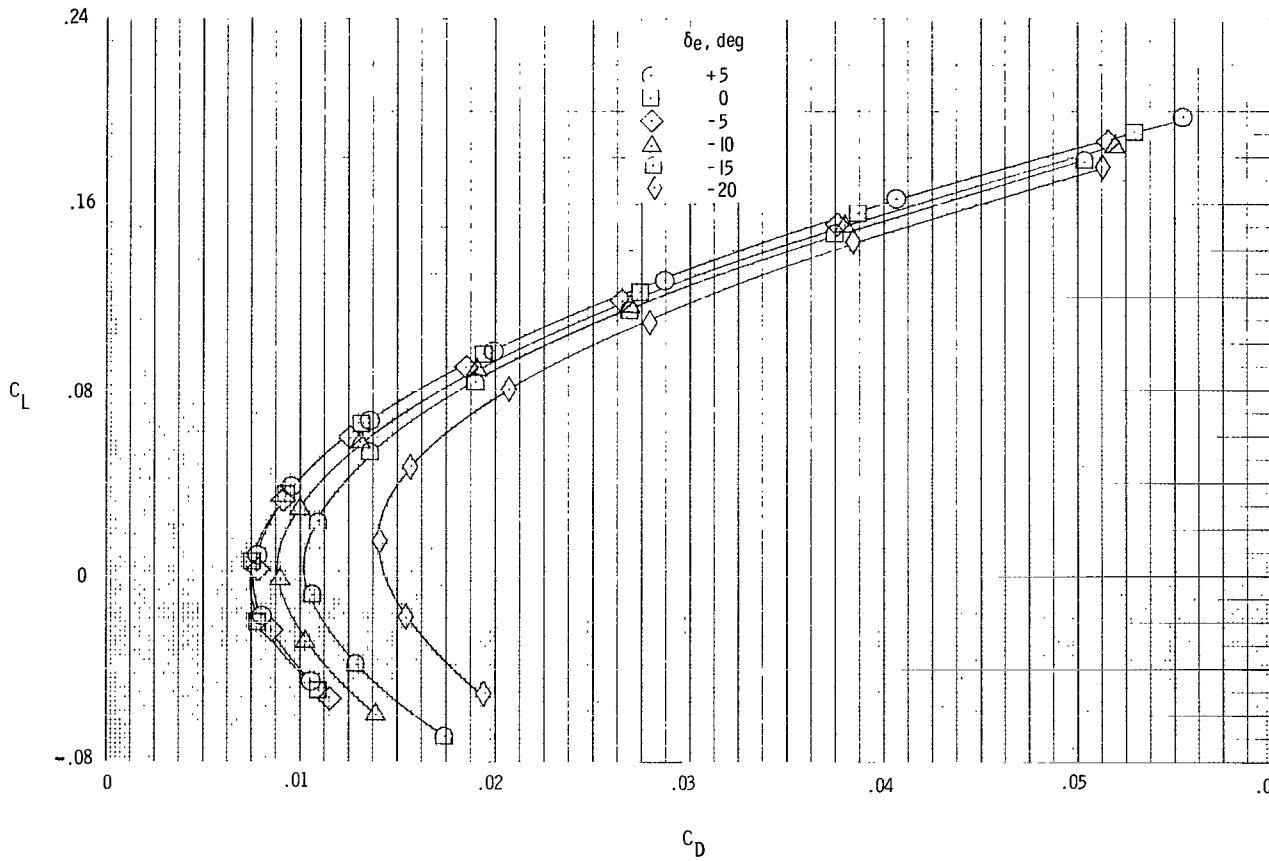

(f) M = 6.00.

Figure 5.- Concluded.

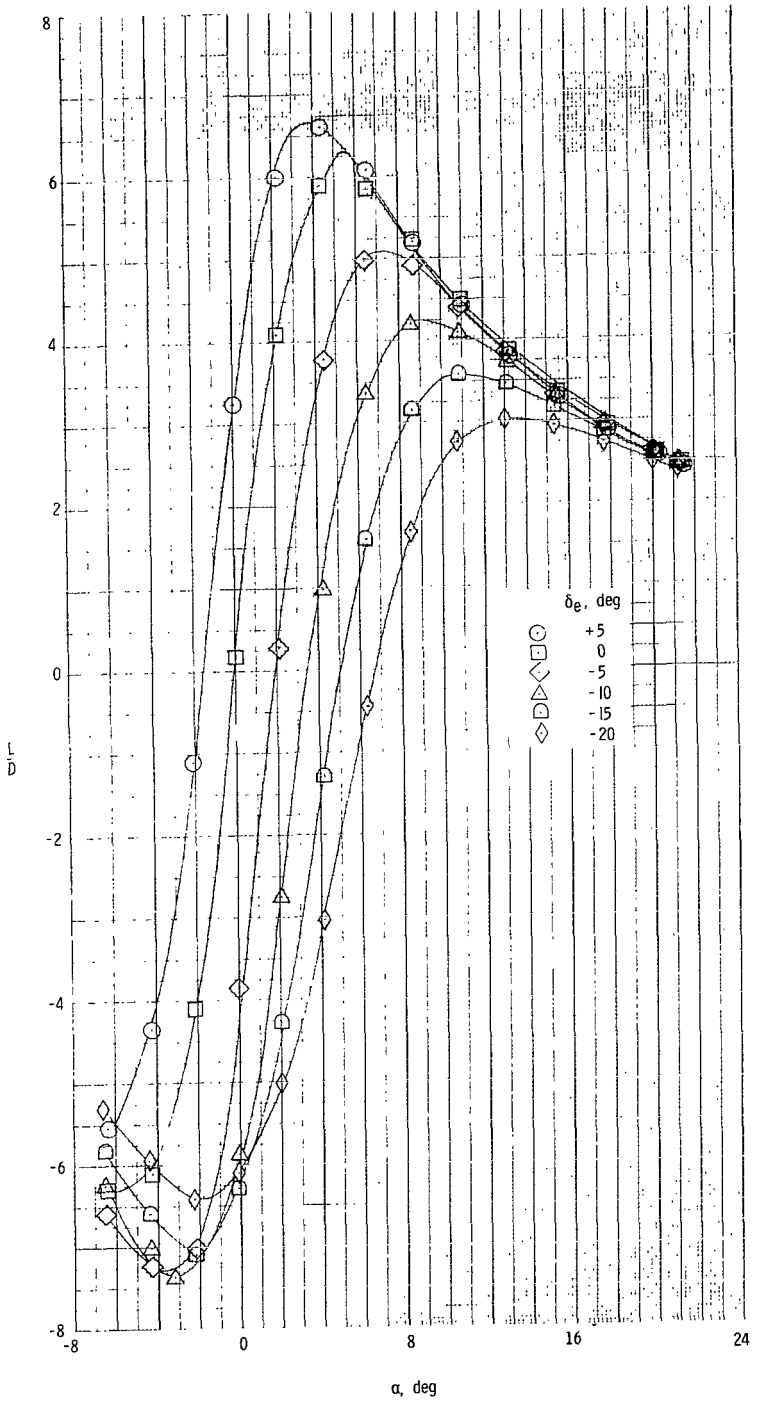

(a) M = 0.36.

Figure 6.- Lift-drag ratio as a function of elevon deflection and angle of attack for complete configuration.

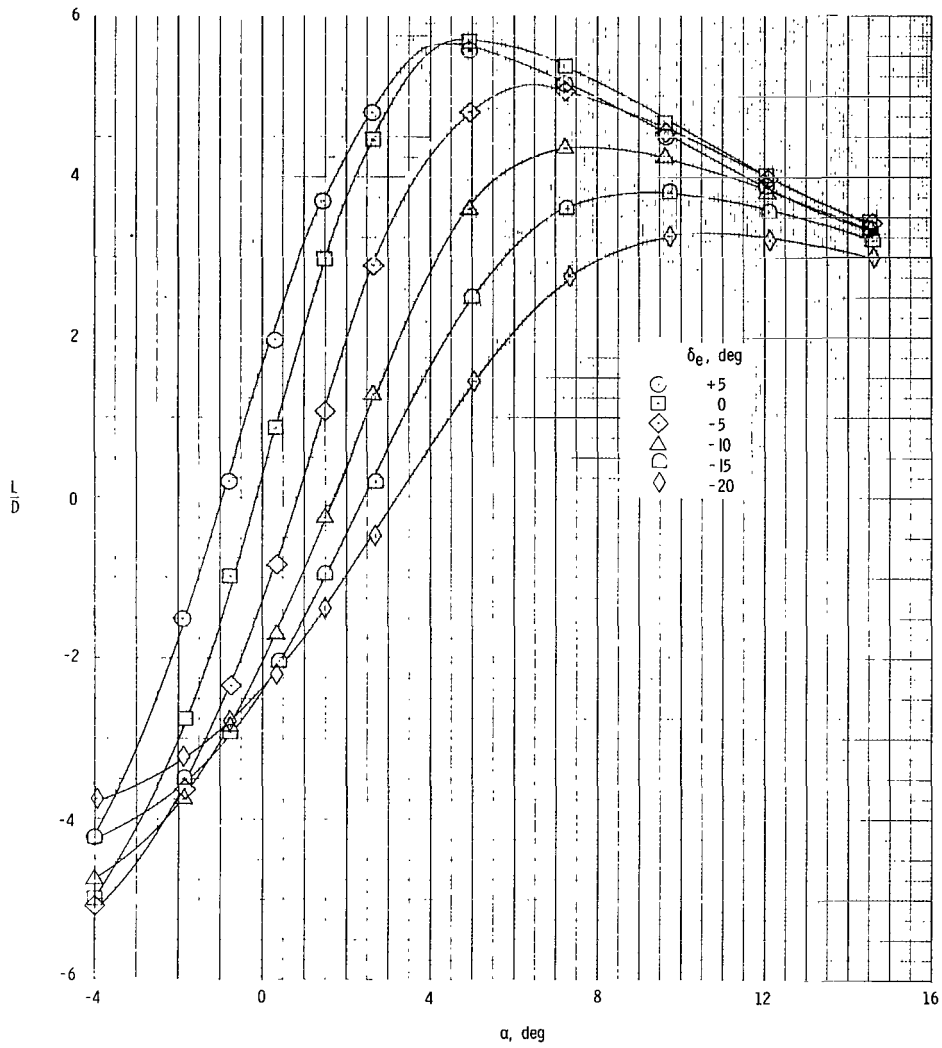

(b) M = 1.50.

Figure 6.- Continued.

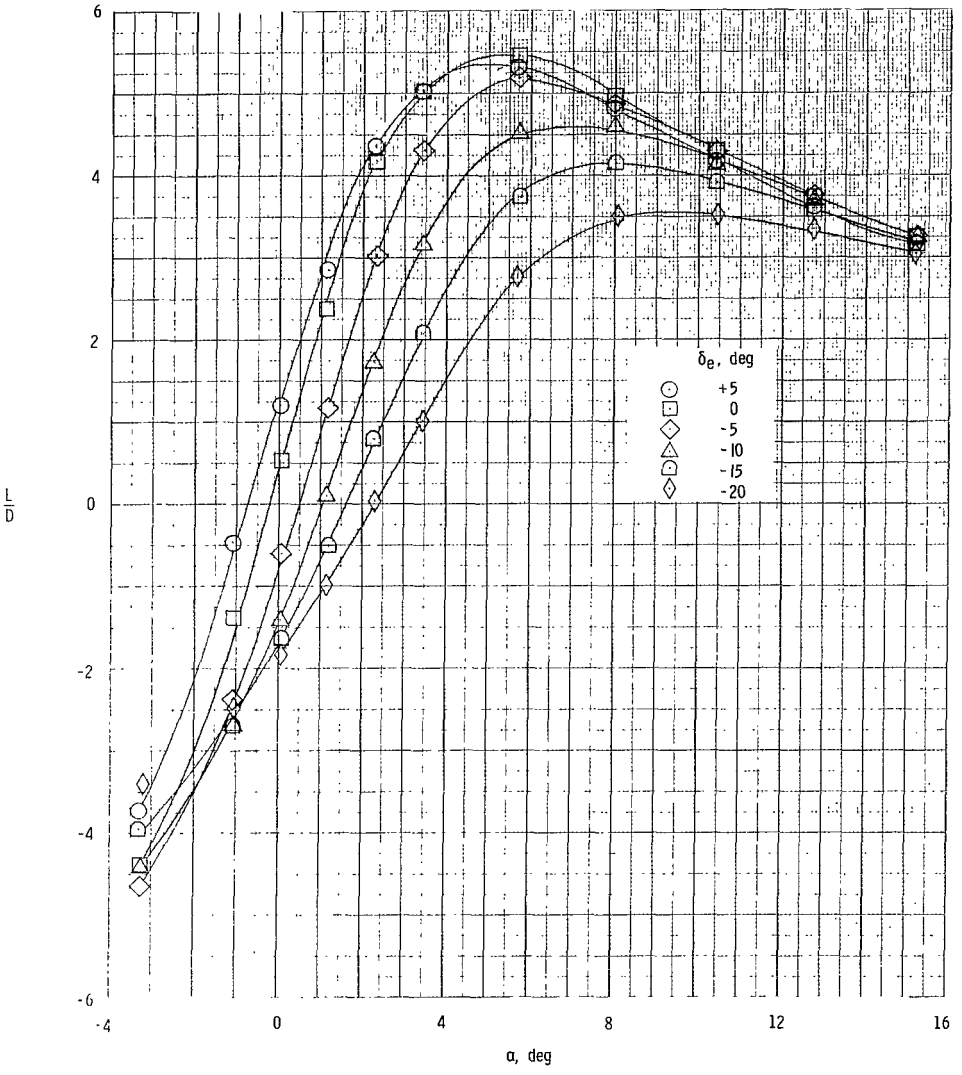

(c) M = 2.00.

Figure 6.- Continued.

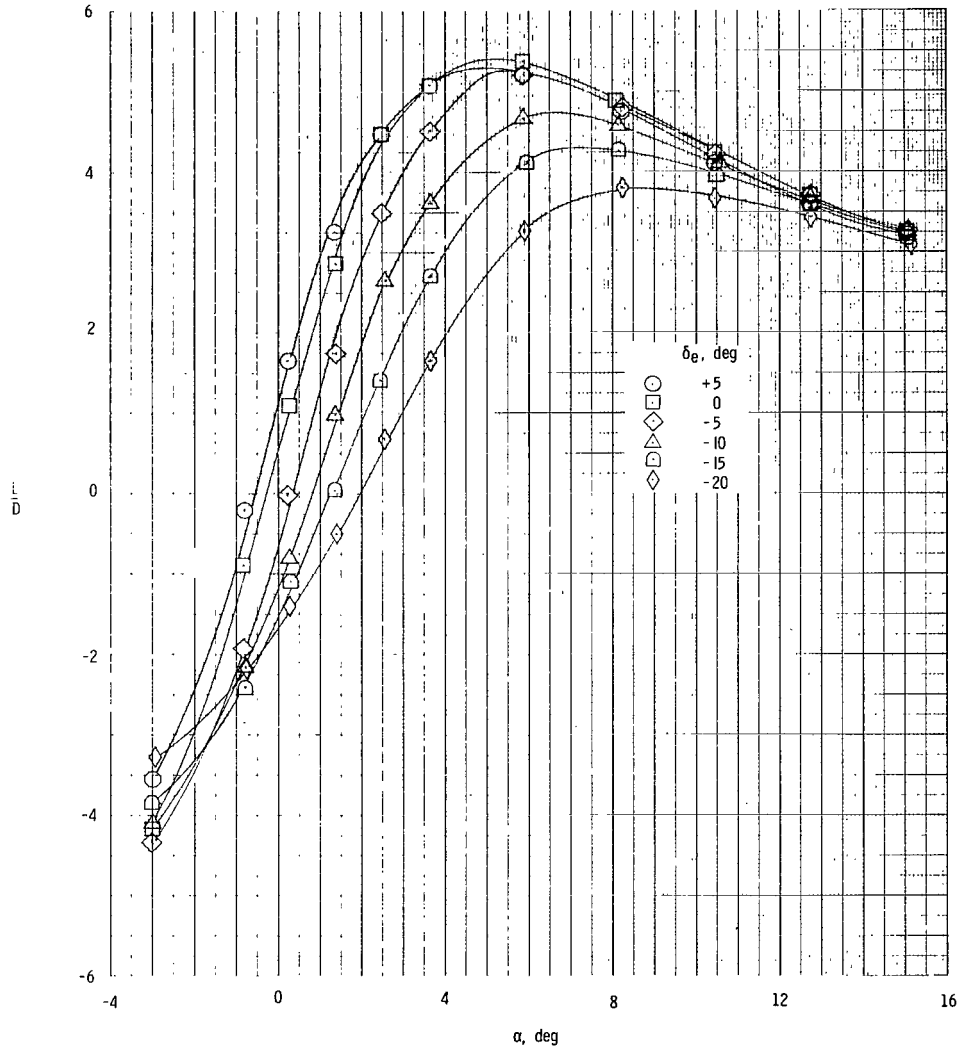

(d) M = 2.36.

Figure 6.- Continued.

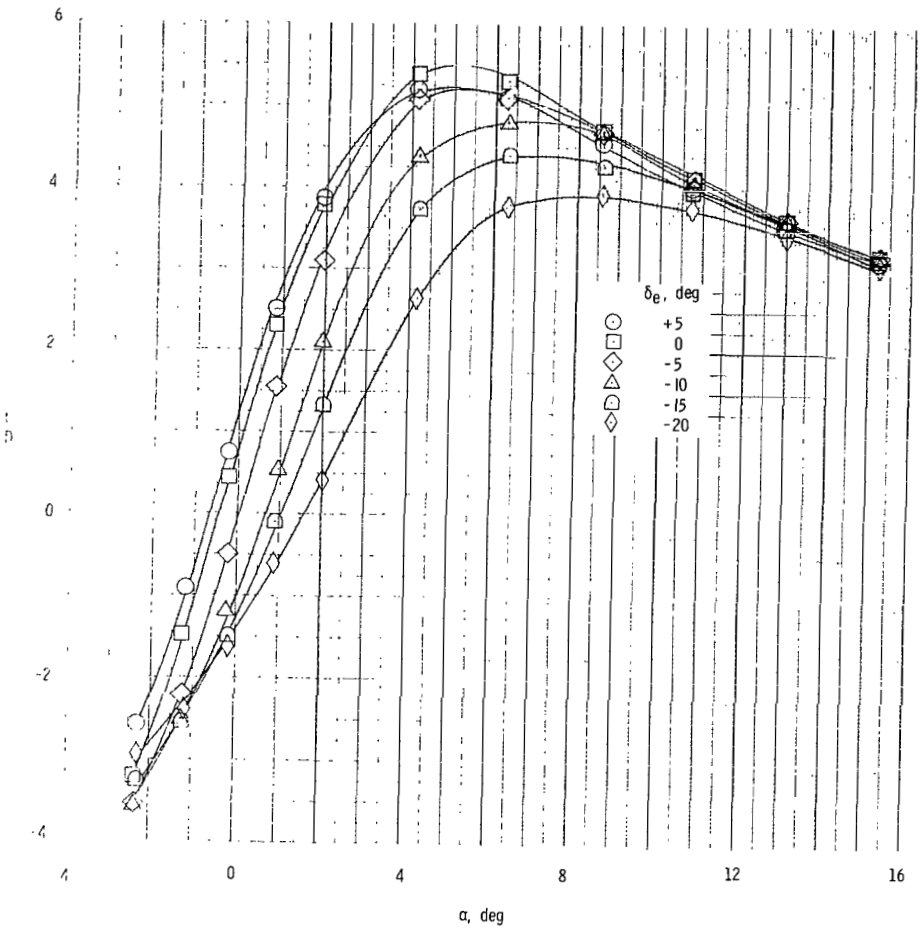

(e) M = 2.86.

Figure 6.- Continued.

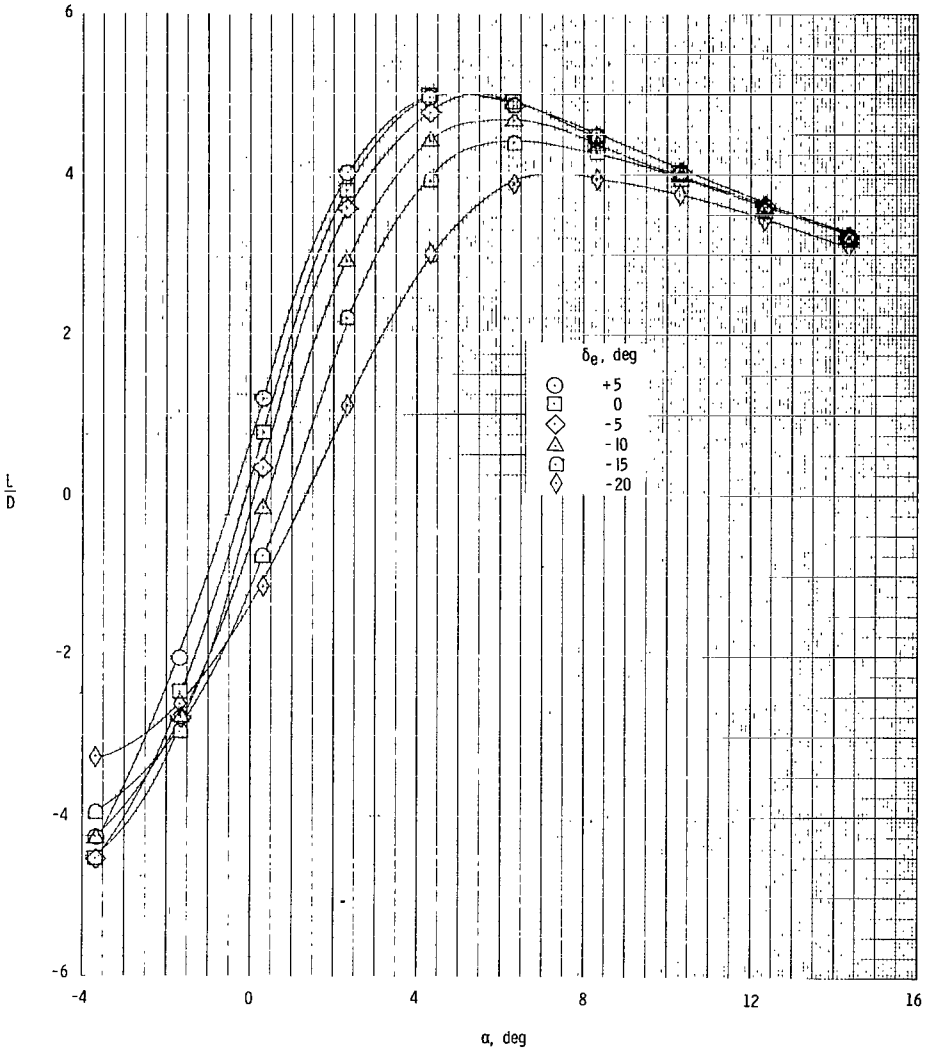

(f) M = 6.00.

Figure 6.- Concluded.

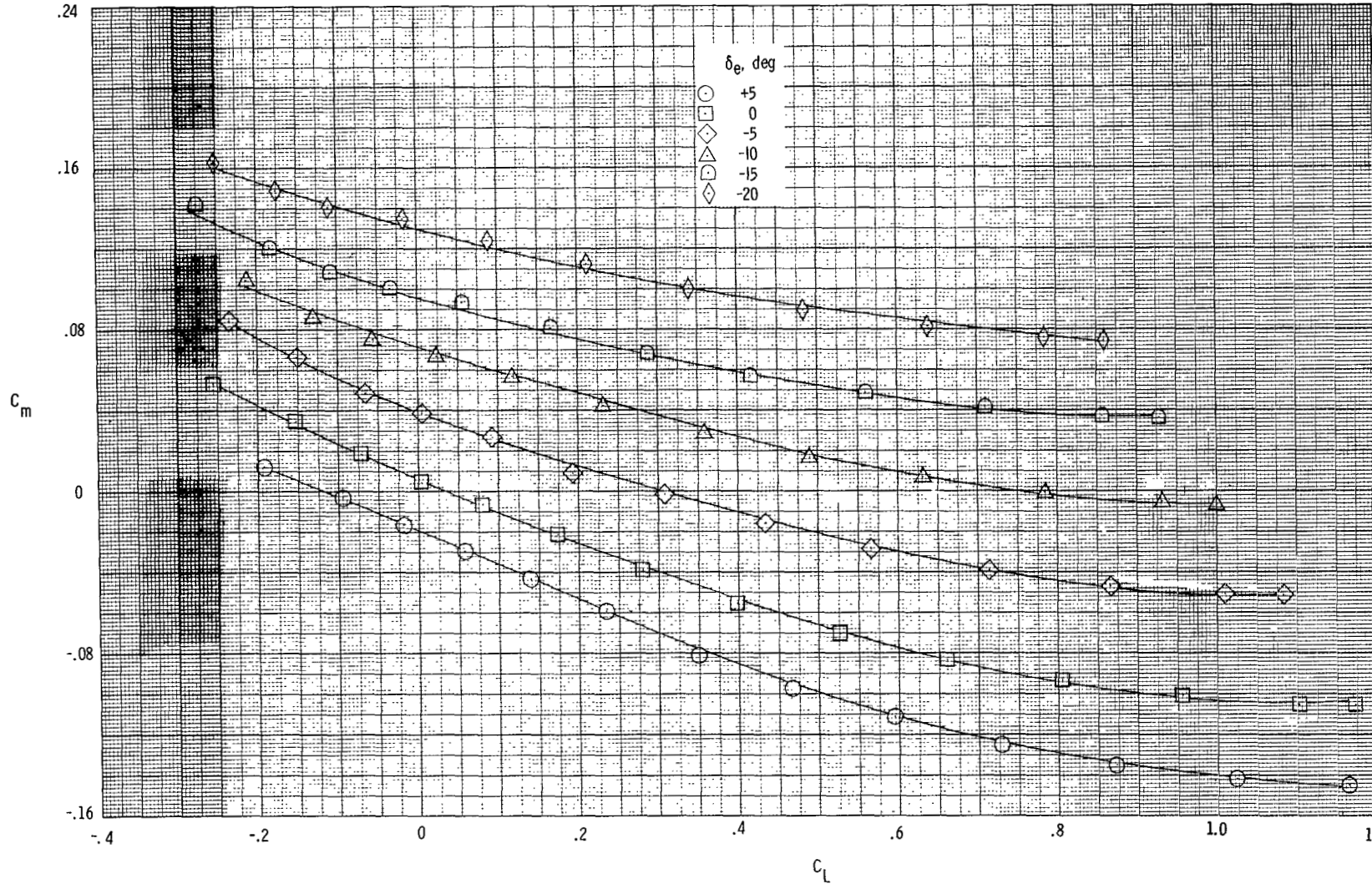

(a) M = 0.36.

Figure 7.- Pitching-moment coefficient as a function of elevon deflection and lift coefficient for complete configuration.

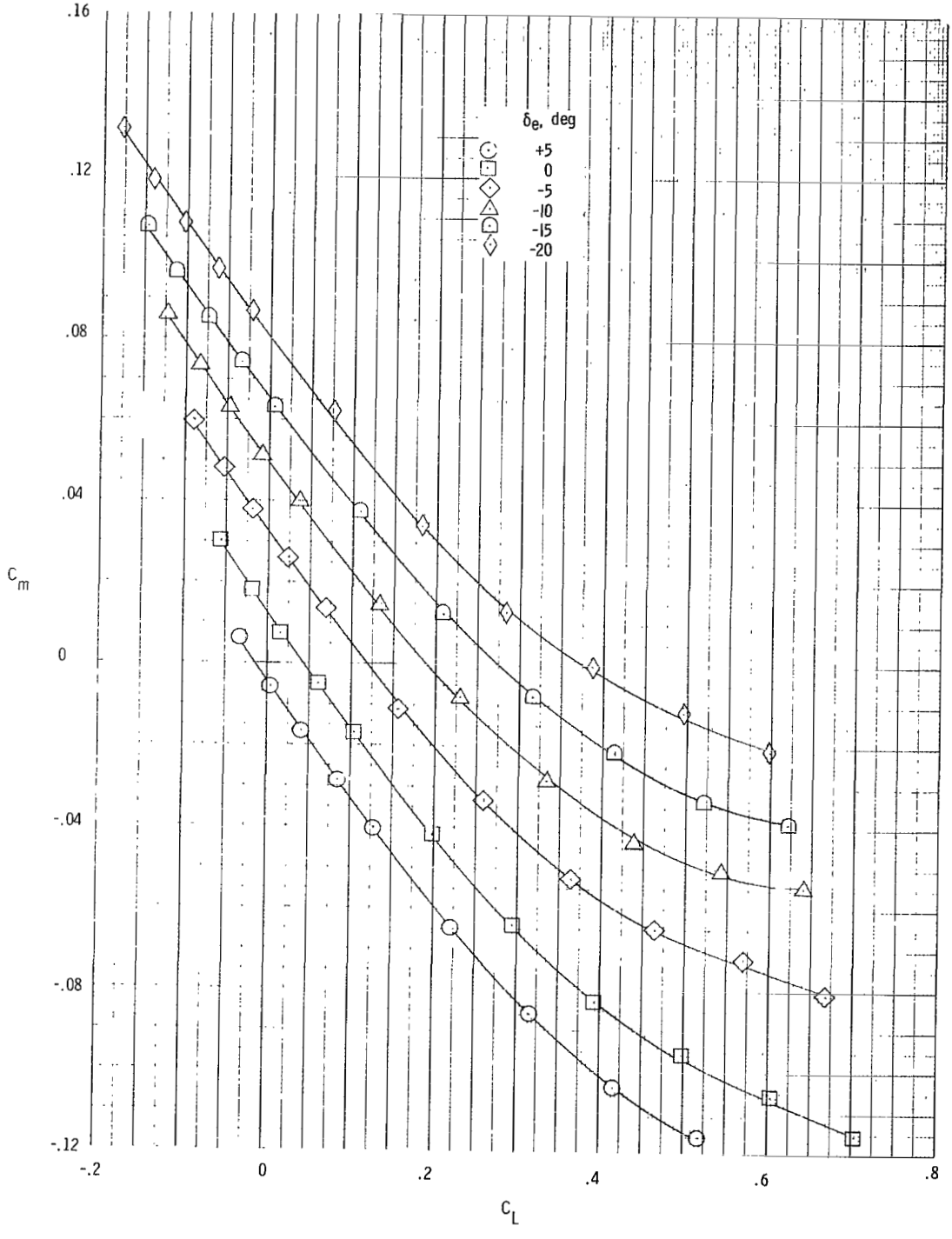

(b) M = 1.50.

Figure 7.- Continued.

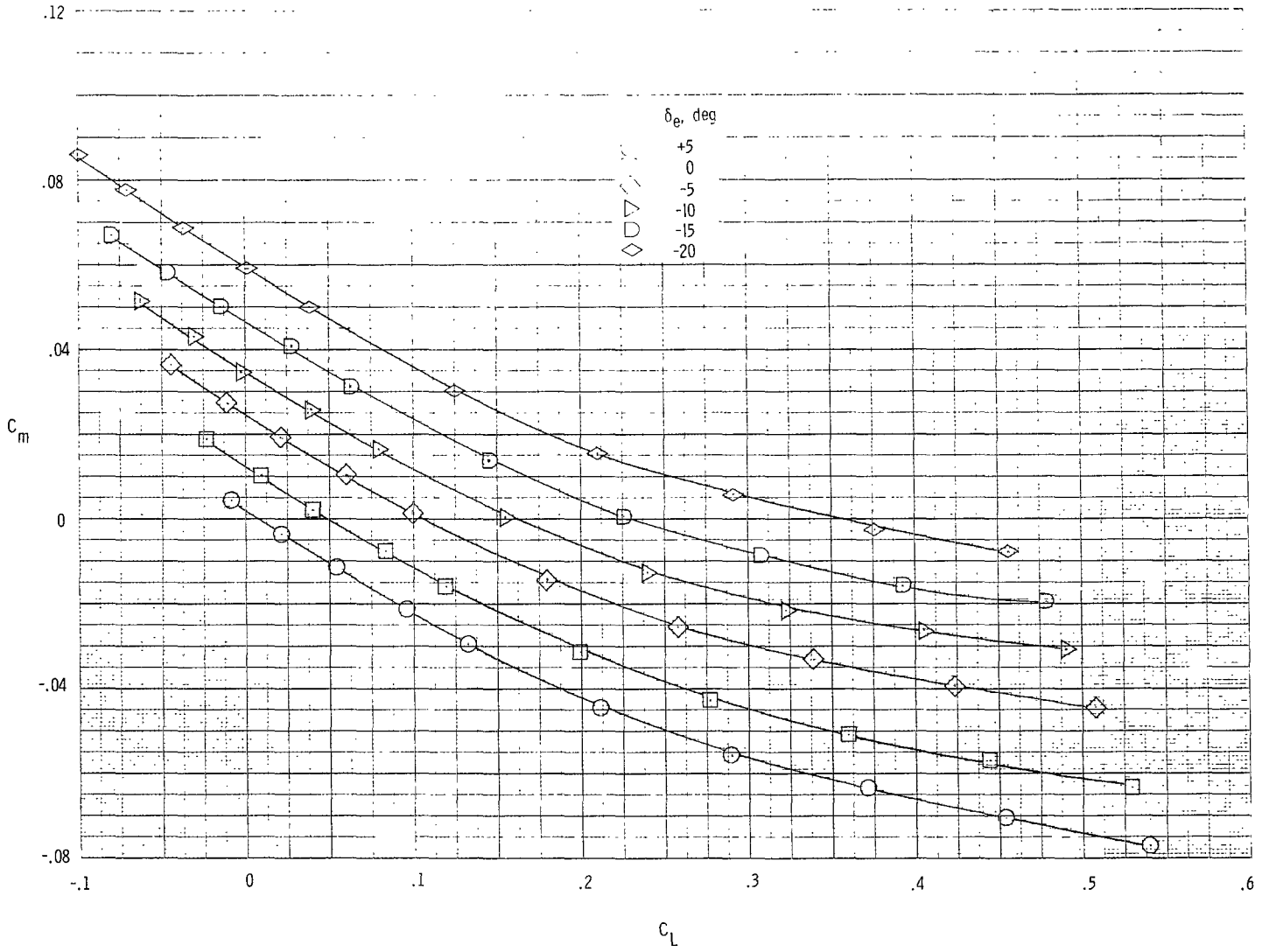

(c) M = 2.00.

Figure 7.- Continued.

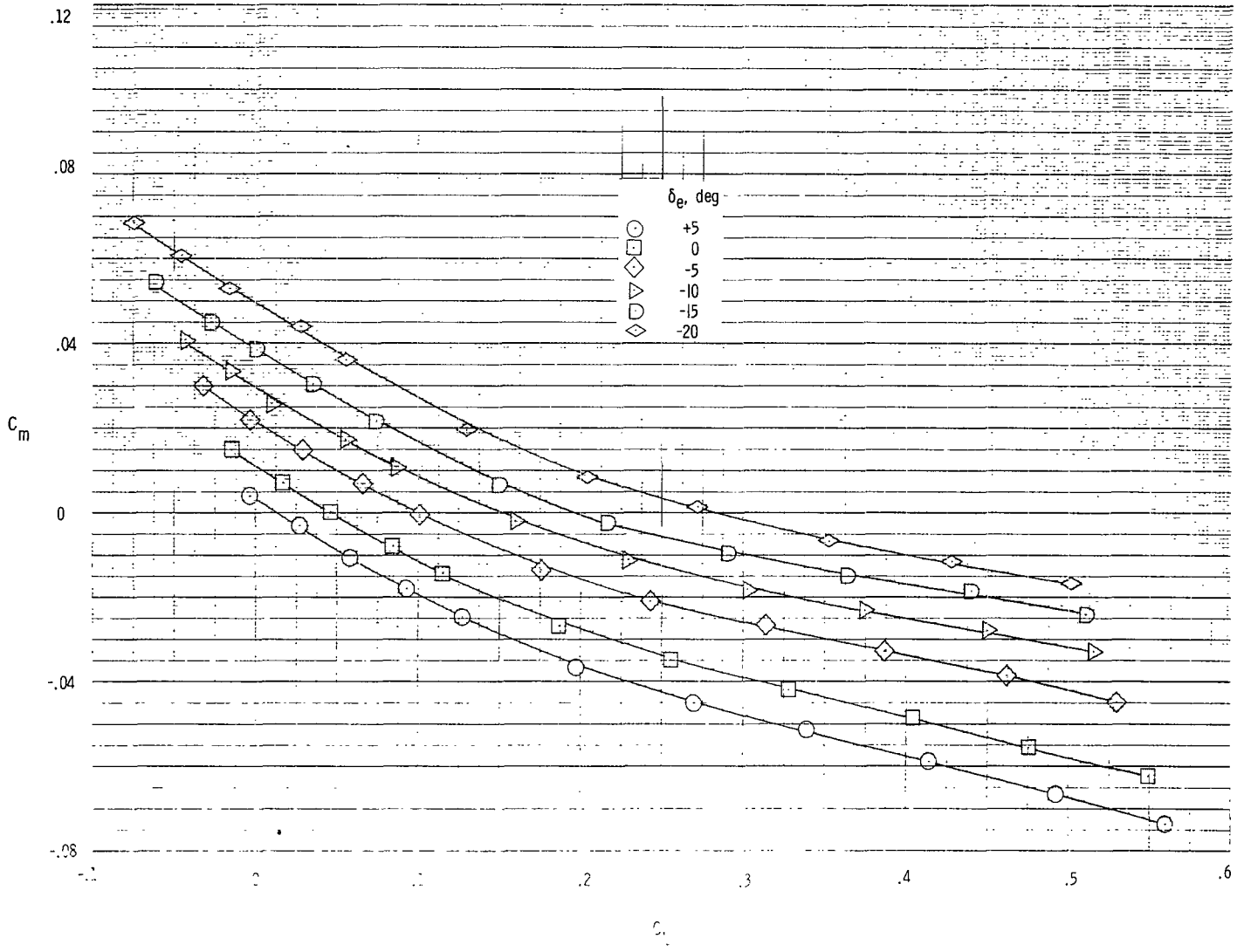

(d) M = 2.36.

Figure 7.- Continued.

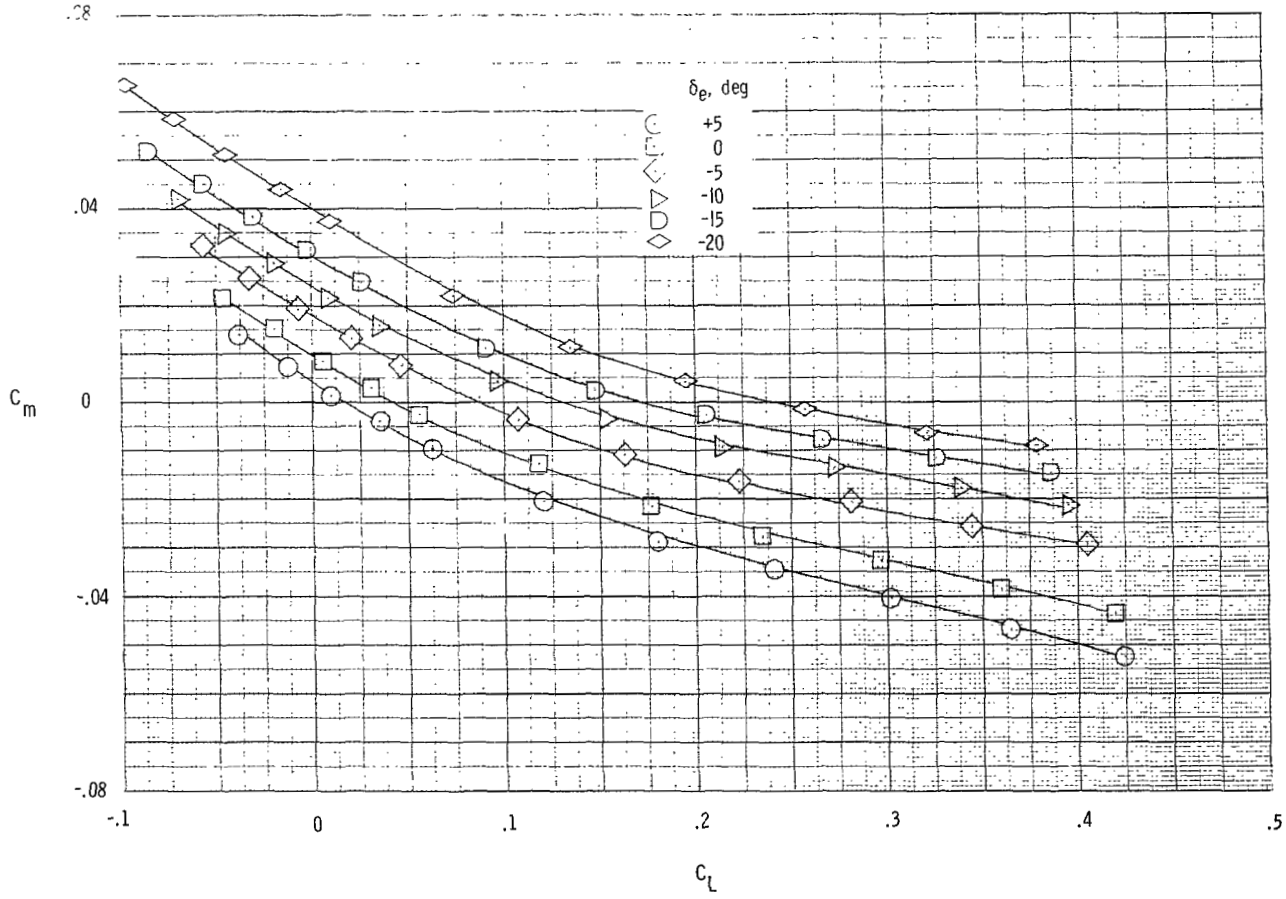

(e) M = 2.86.

Figure 7.- Continued.

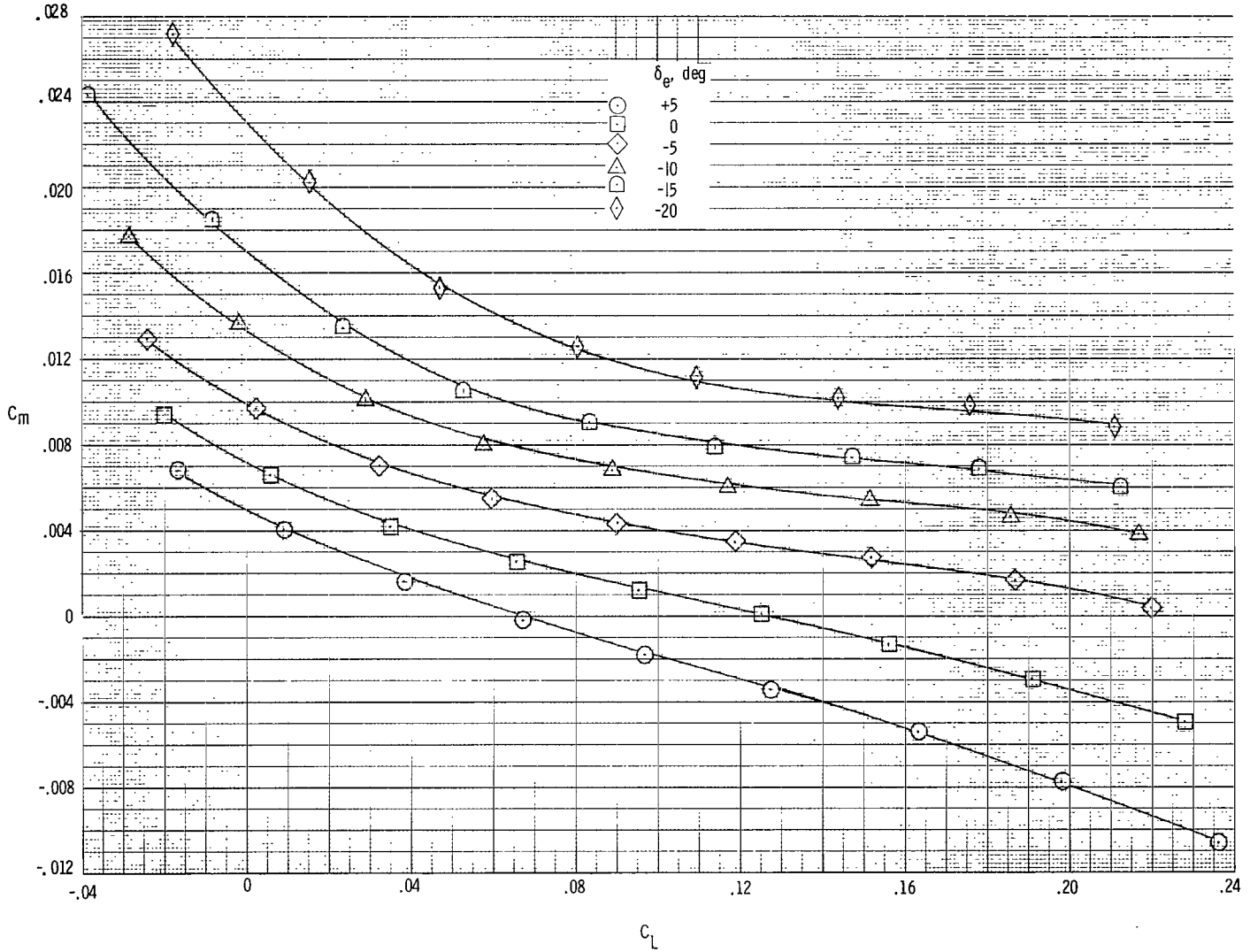

(f) M = 6.00.

Figure 7.- Concluded.

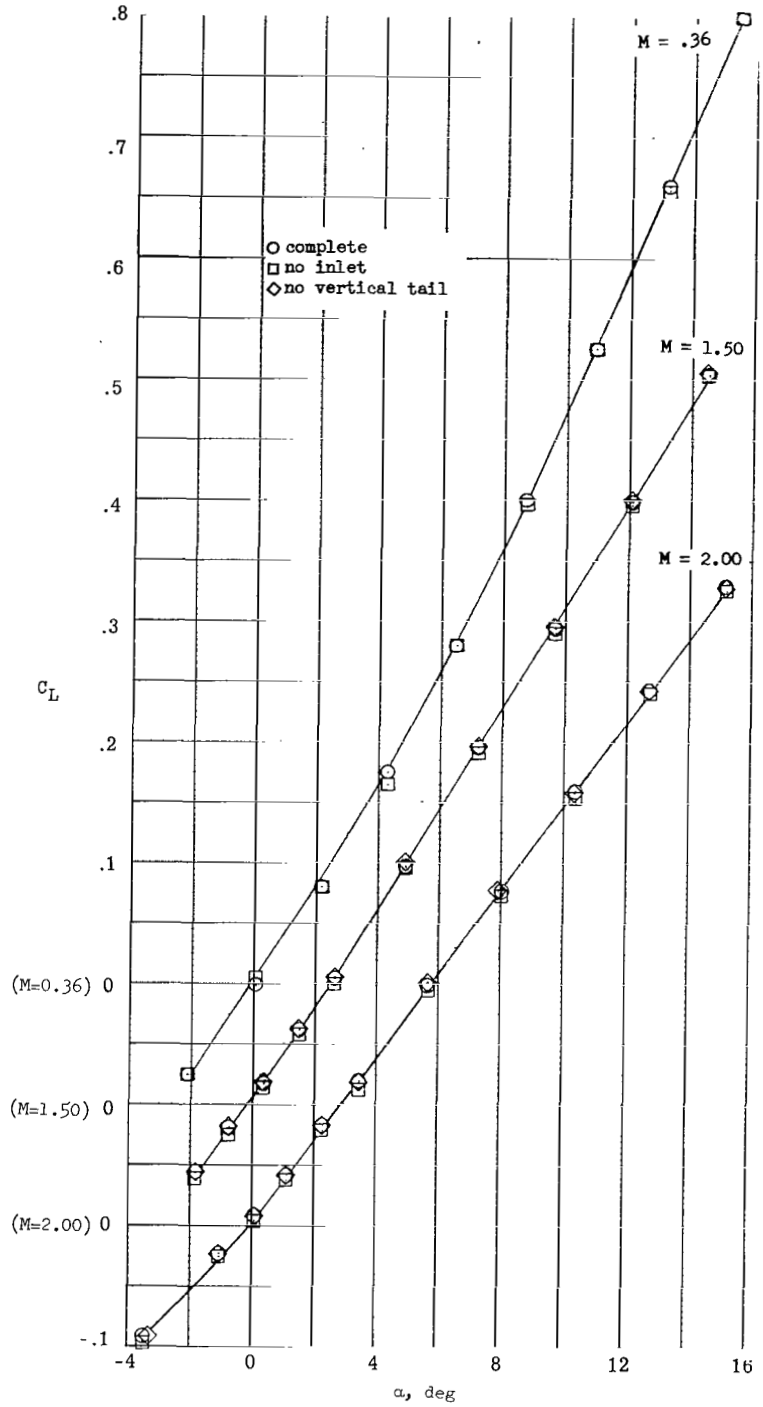

(a) M = 0.36, 1.50, and 2.00.

Figure 8.- Lift coefficient as a function of angle of attack. $\delta_e = 0^o$.

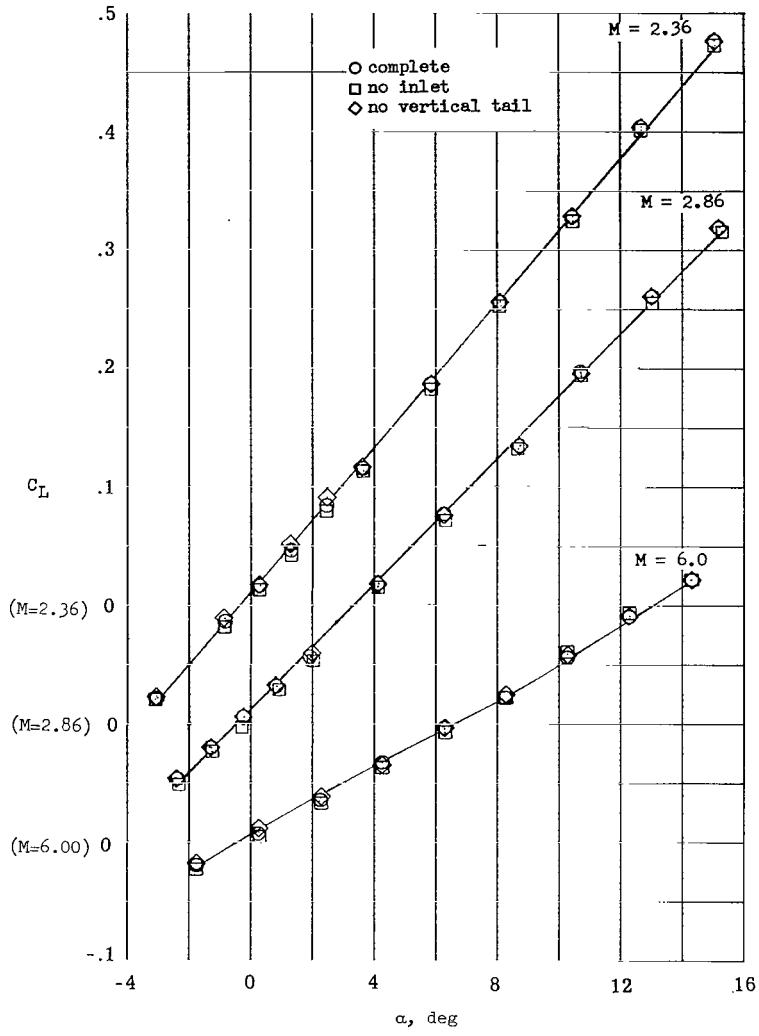

(b) M = 2.36, 2.86, and 6.00.

Figure 8.- Concluded.

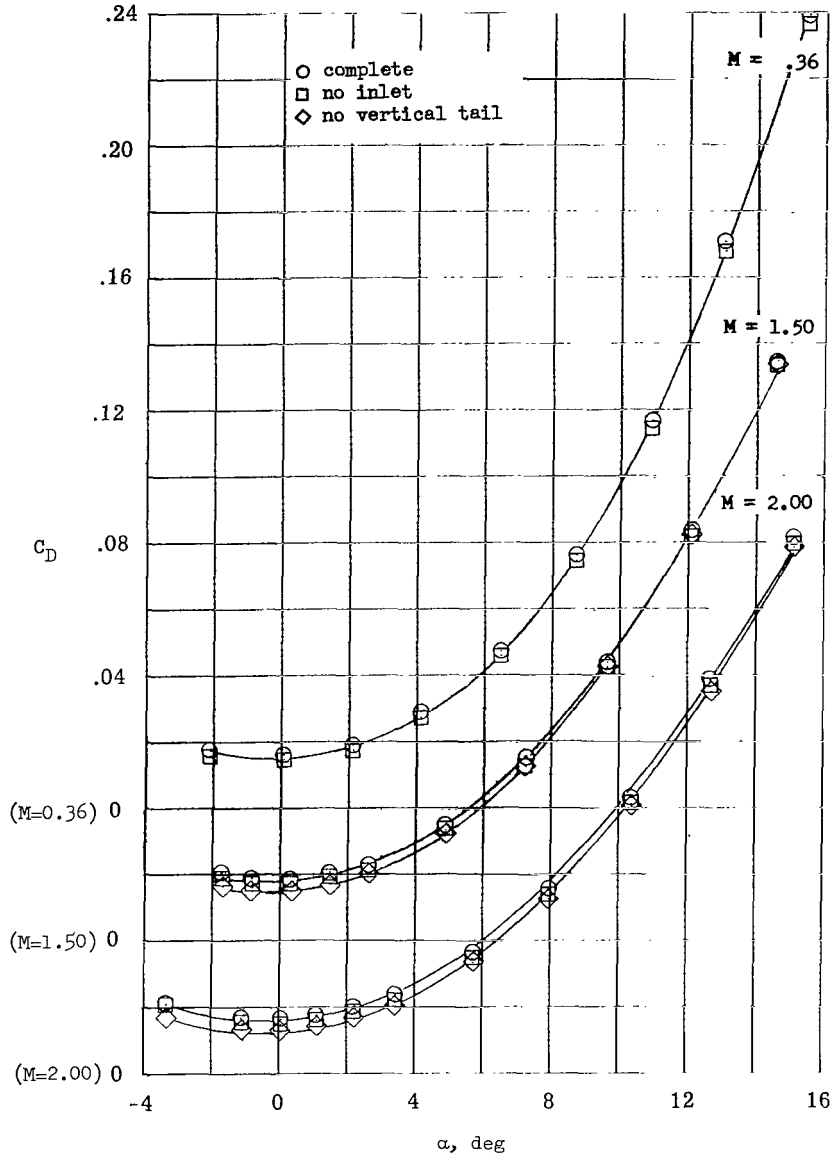

(a) M = 0.36, 1.50, and 2.00.

Figure 9.- Drag coefficient as a function of angle of attack. $\delta_e = 0^o$.

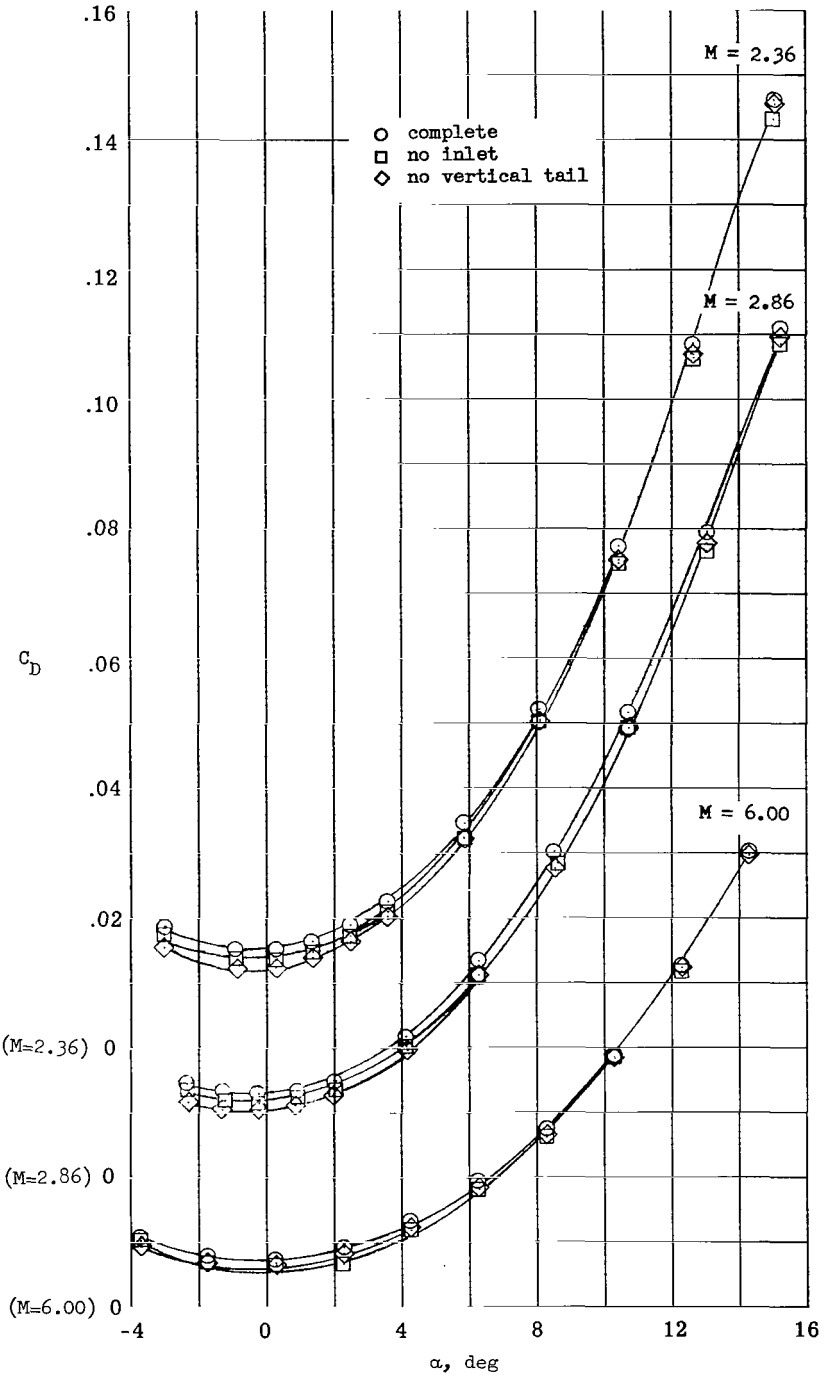

(b) M = 2.36, 2.86, and 6.00.

Figure 9.- Concluded.

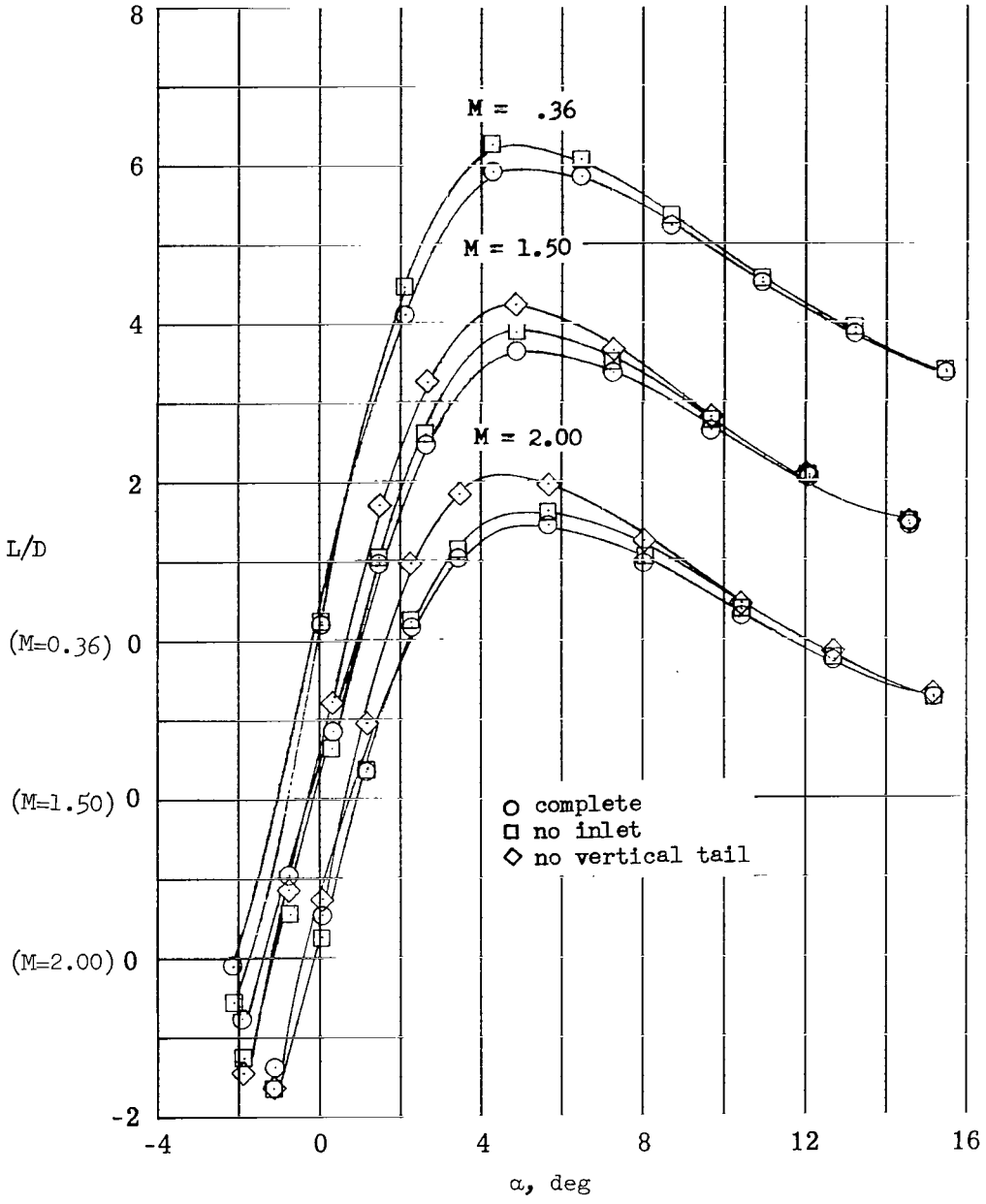

(a) M = 0.36, 1.50, and 2.00.

Figure 10.- Lift-drag ratio as a function of angle of attack. $\delta_e = 0^o$.

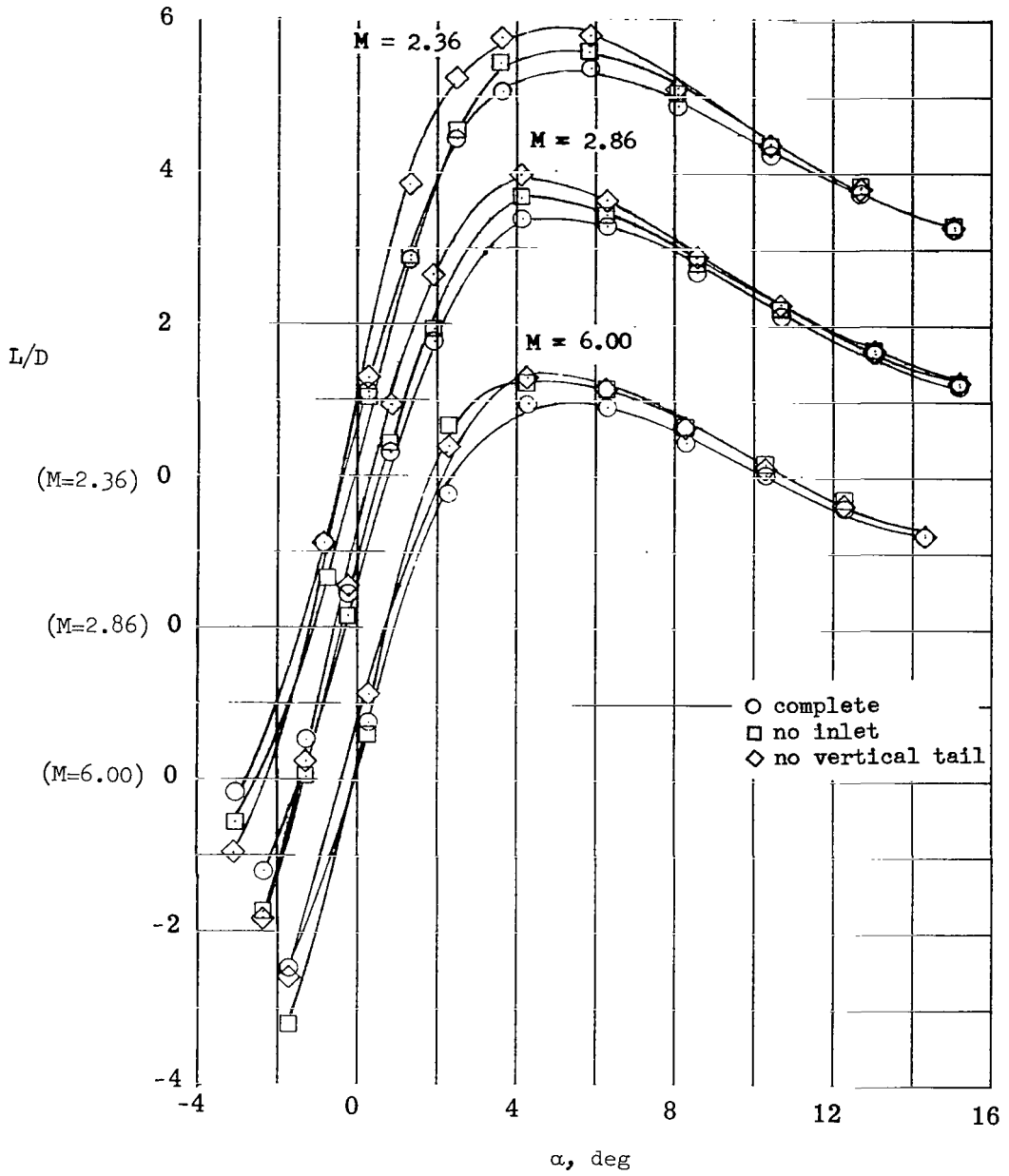

(b) M = 2.36, 2.86, and 6.00.

Figure 10.- Concluded.

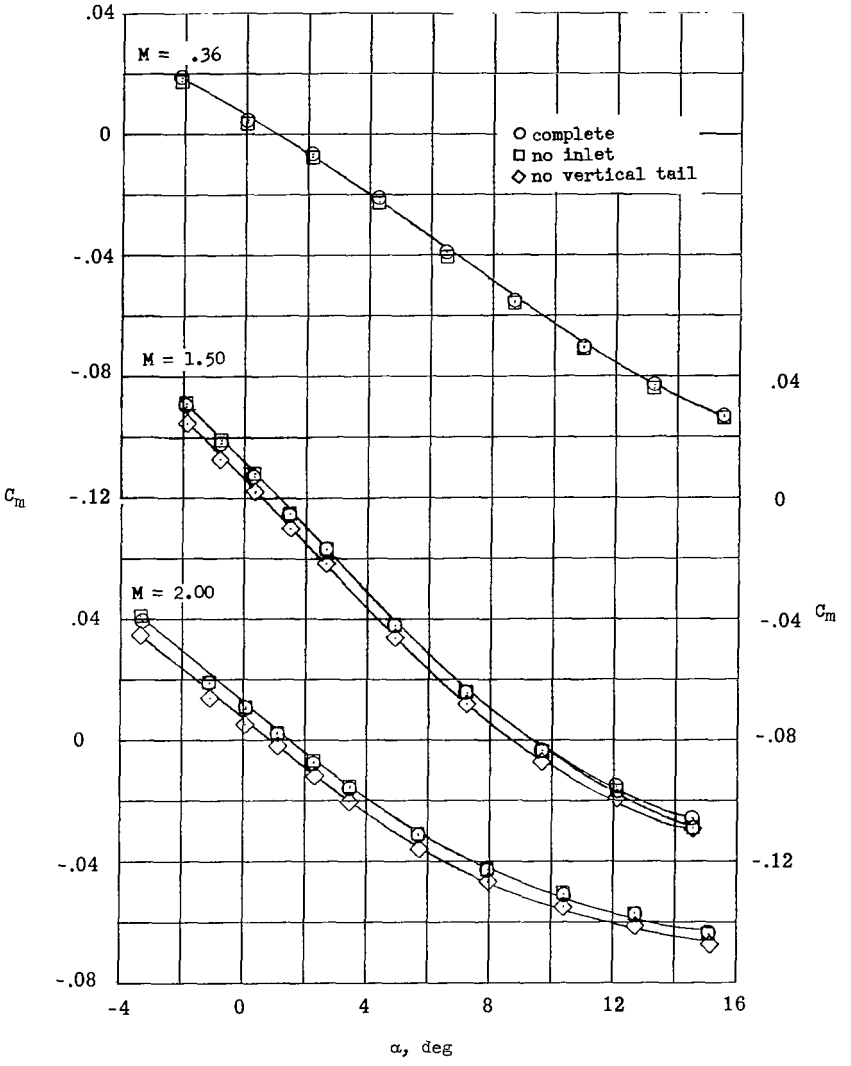

(a) M = 0.36, 1.50, and 2.00.

Figure 11.- Pitching-moment coefficient as a function of angle of attack. $\delta_e = 0^o$.

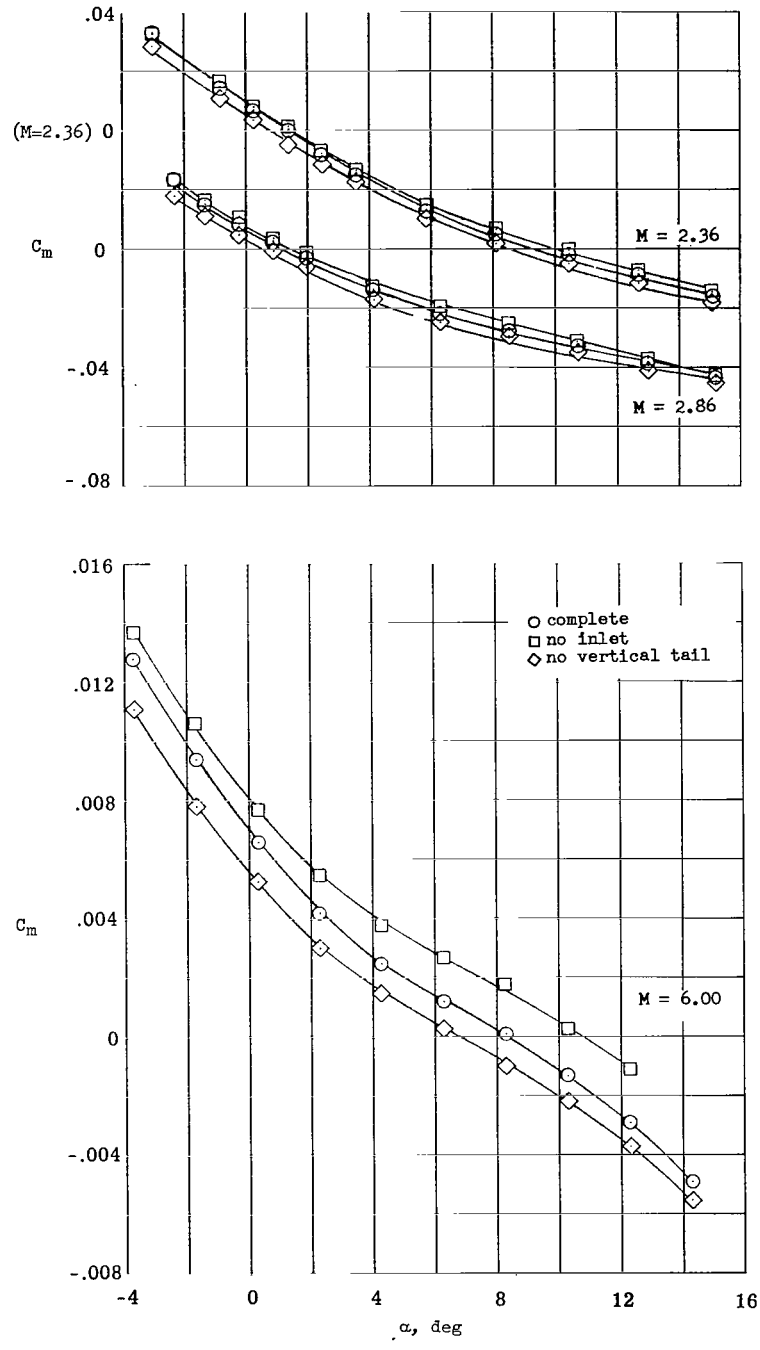

(b) M = 2.36, 2.86, and 6.00.

Figure 11.- Concluded.

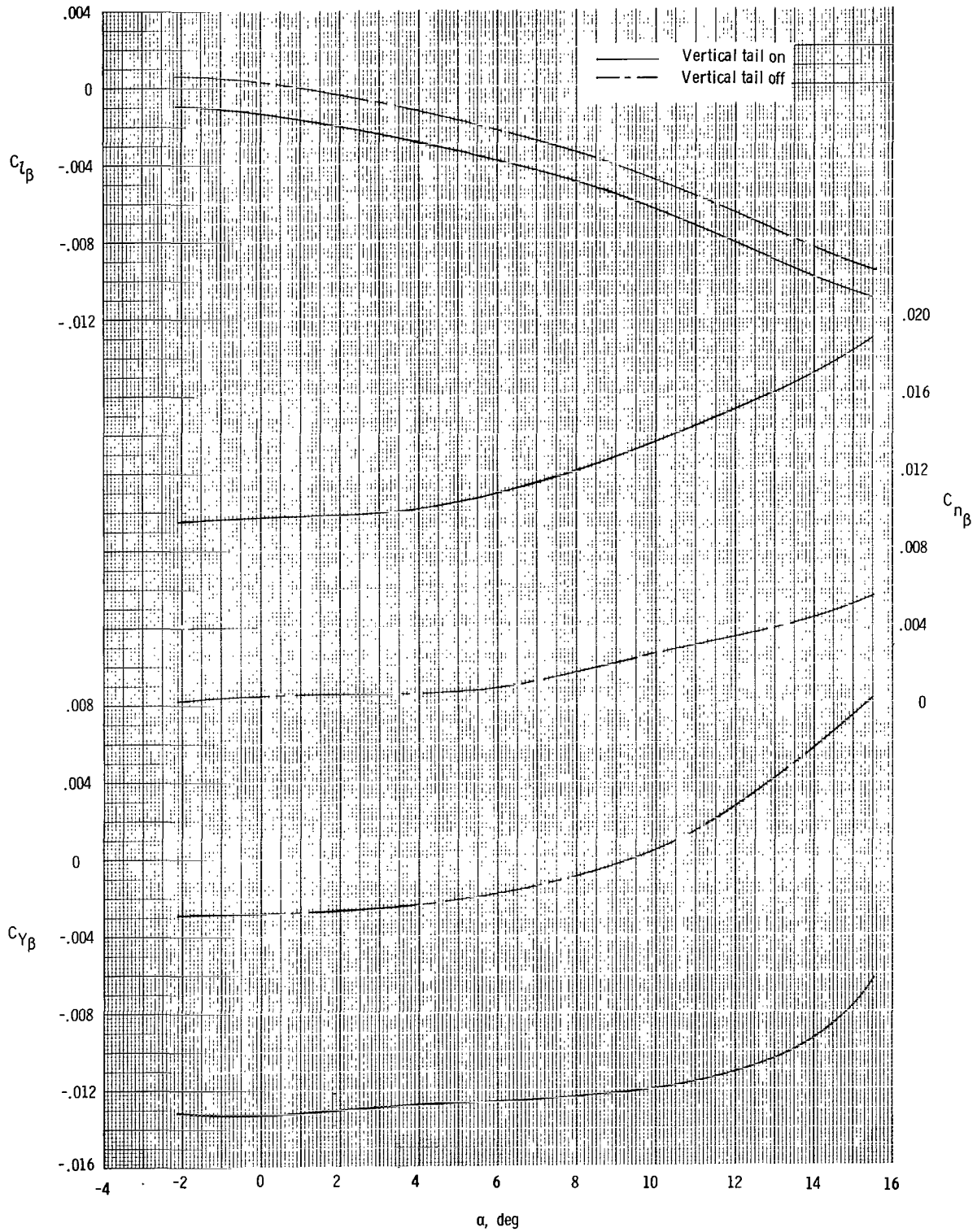

(a) M = 0.36.

Figure 12.- Experimental lateral-directional stability parameters for configuration without inlet. $\delta_e = 0^o$.

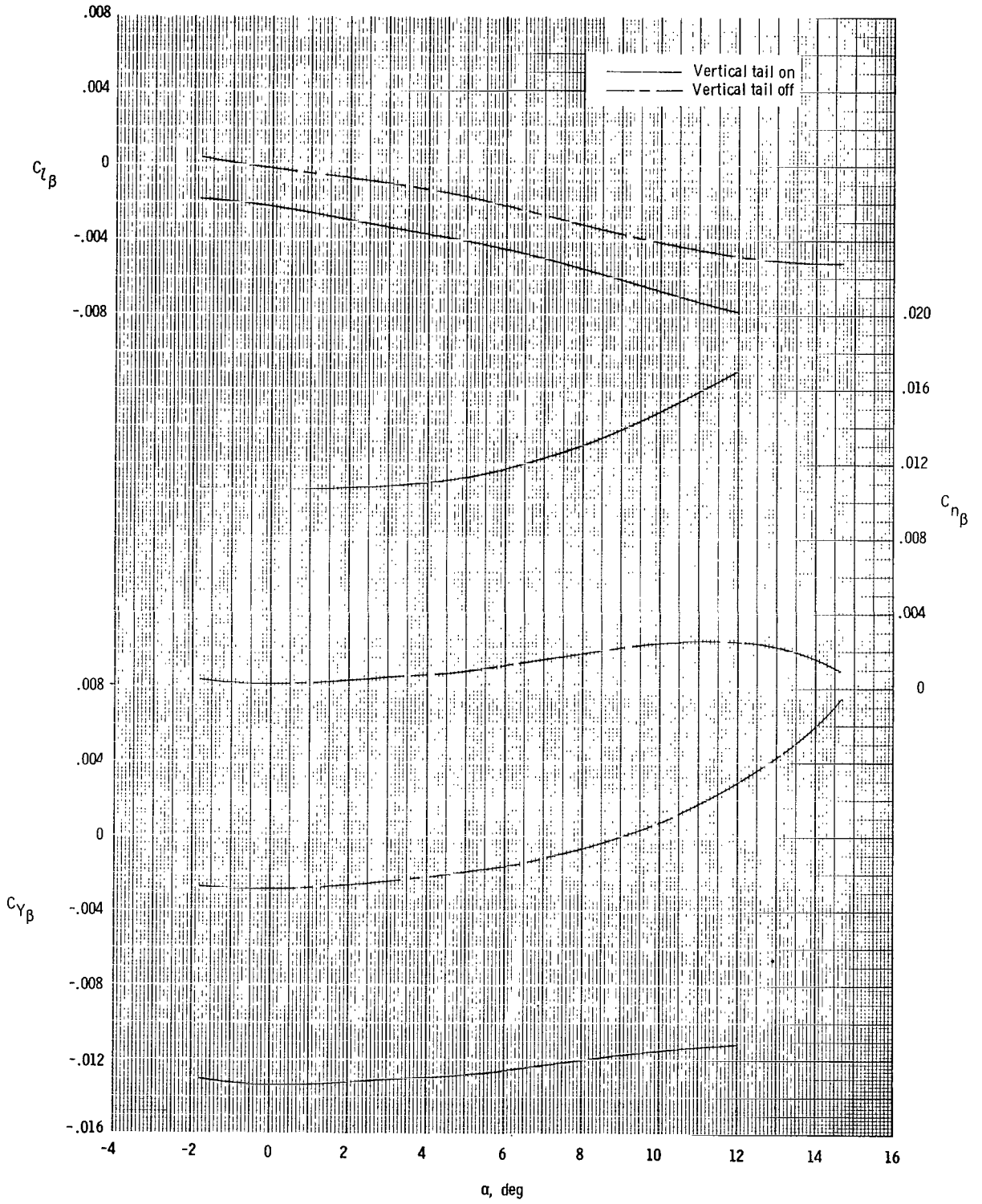

(b) M = 1.50.

Figure 12.- Continued.

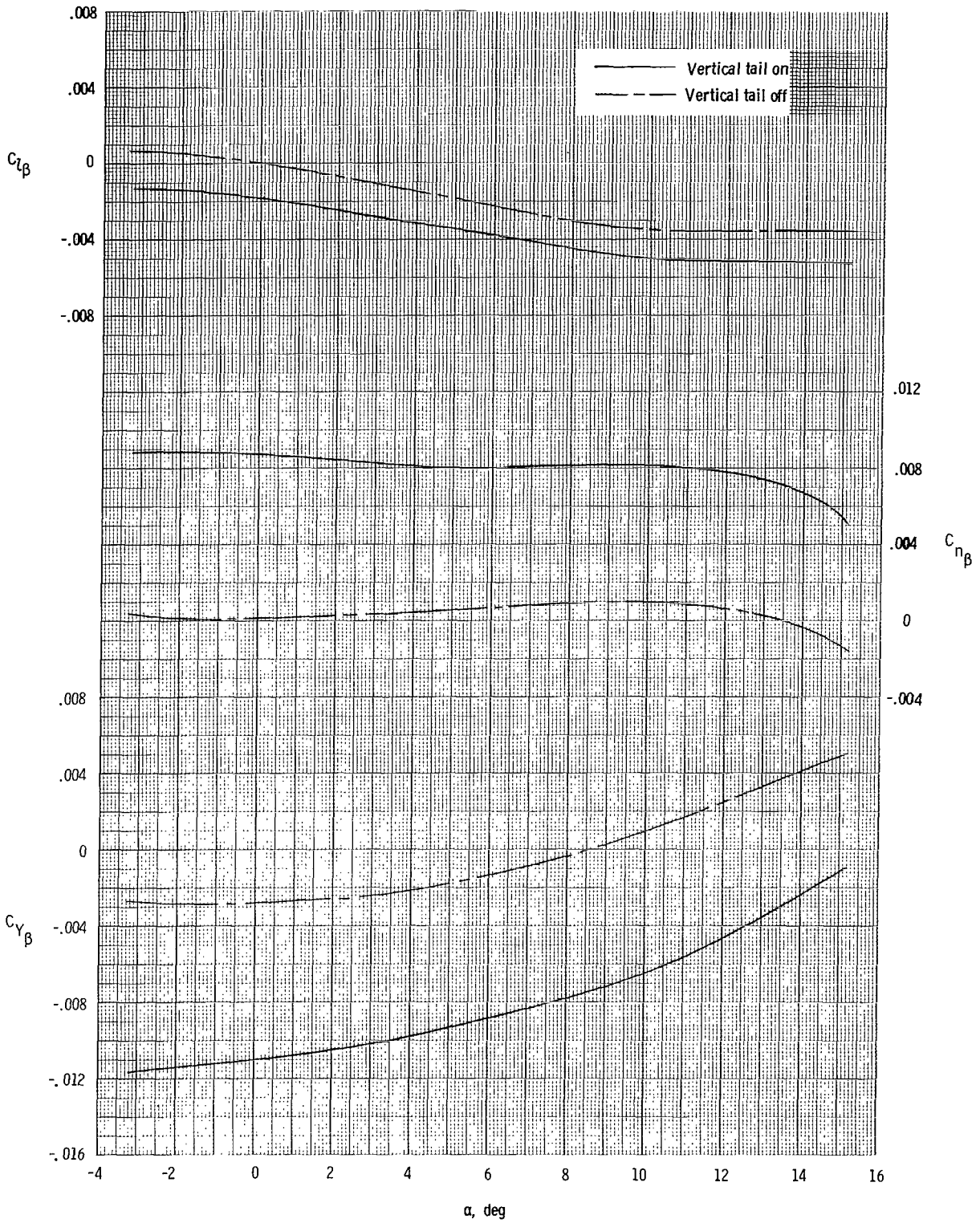

(c) M = 2.00.

Figure 12.- Continued.

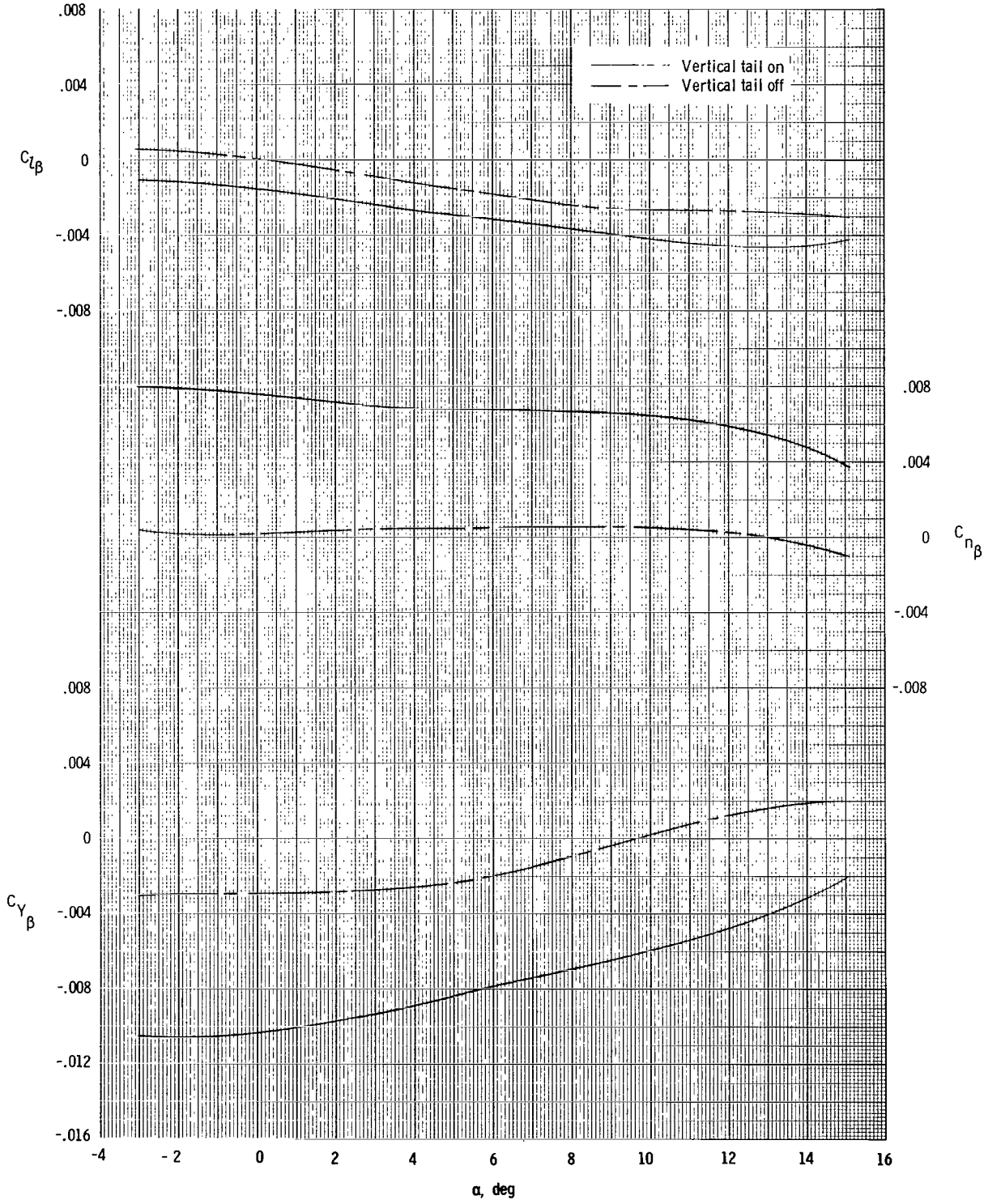

(d) M = 2.36.

Figure 12.- Continued.

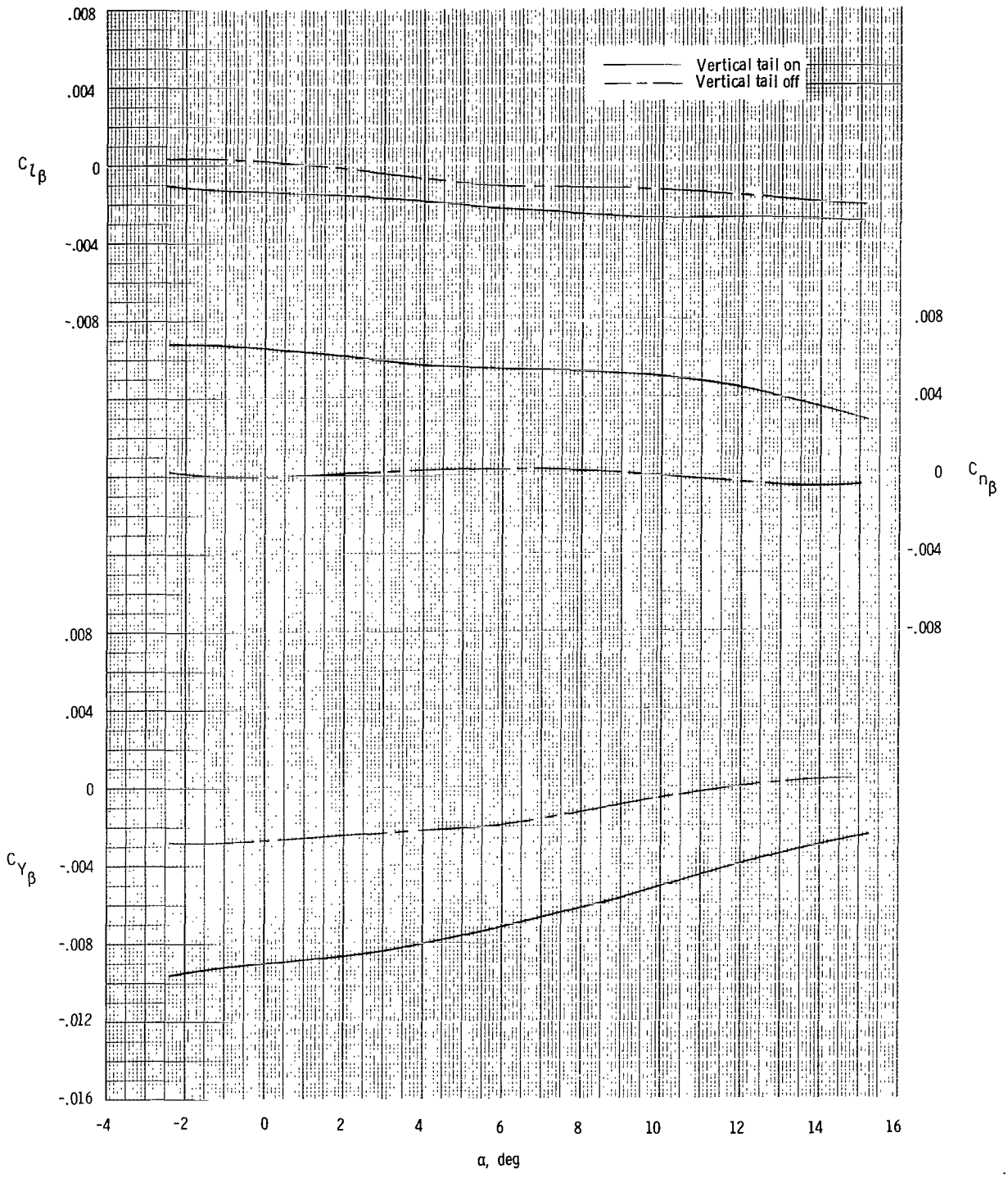

(e) M = 2.86.

Figure 12.- Continued.

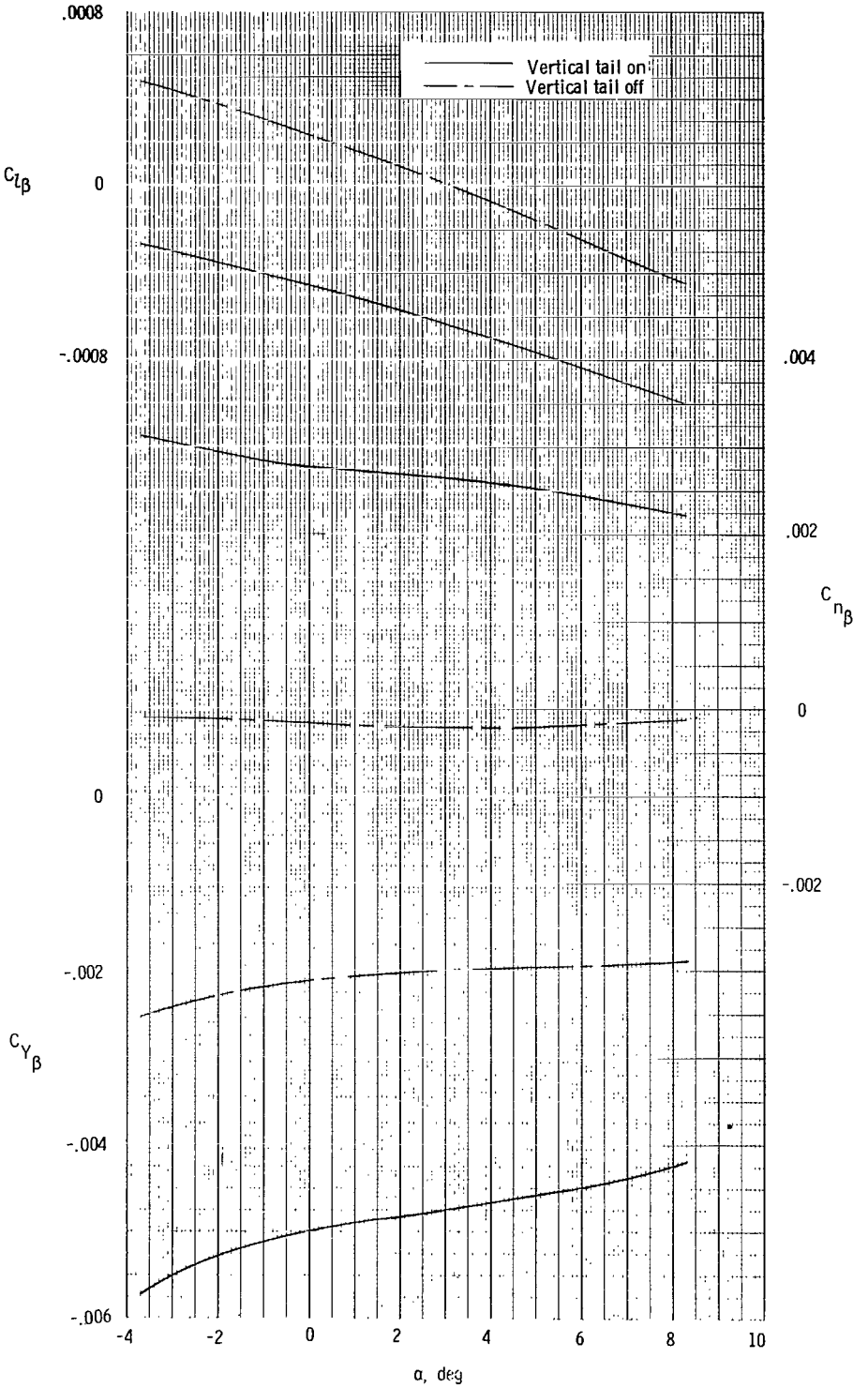

(f) M = 6.00.

Figure 12.- Concluded.

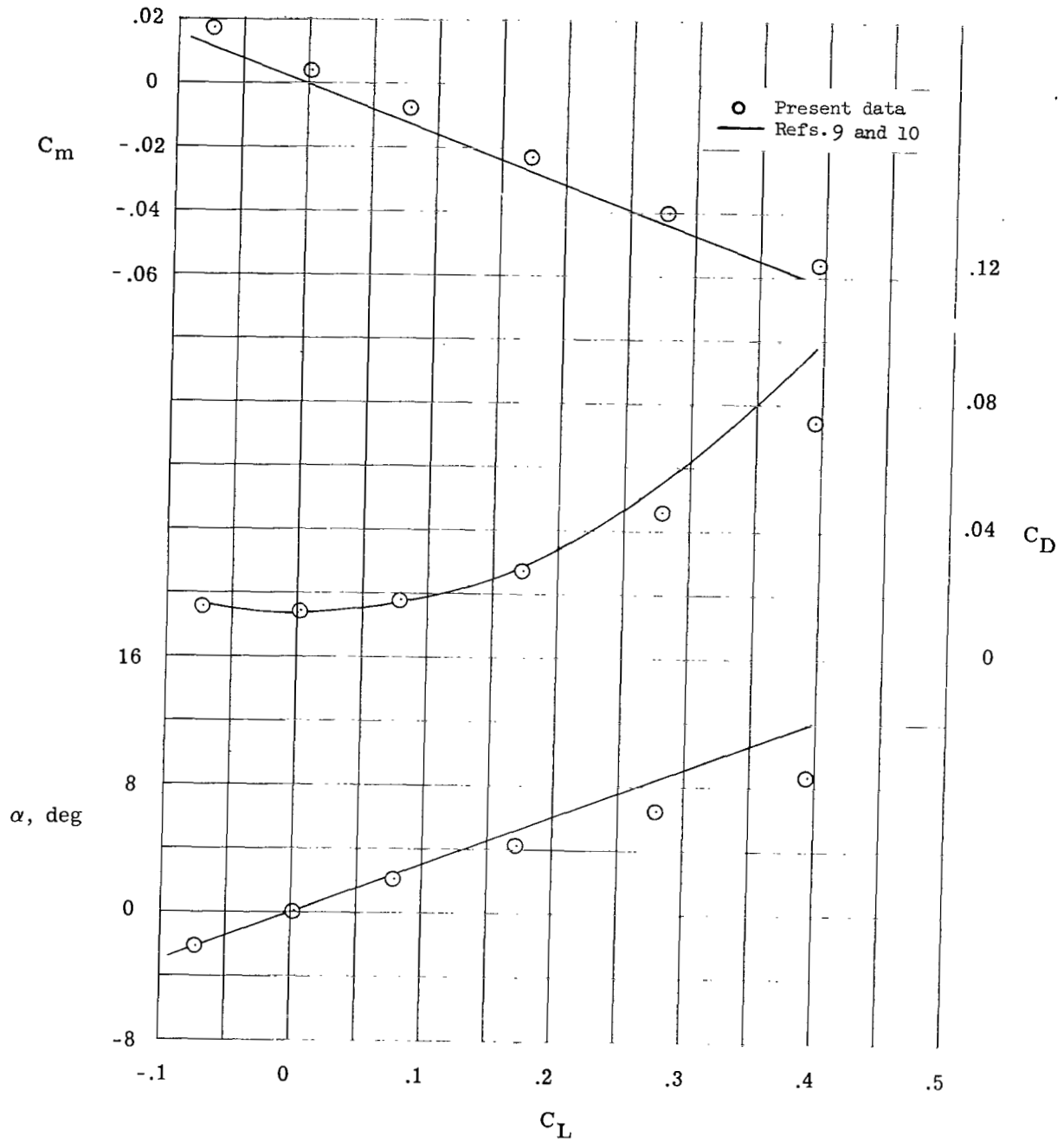

(a) M = 0.36.

Figure 13.- Comparison of longitudinal characteristics for configuration without inlet. $\delta_e = 0^o$.

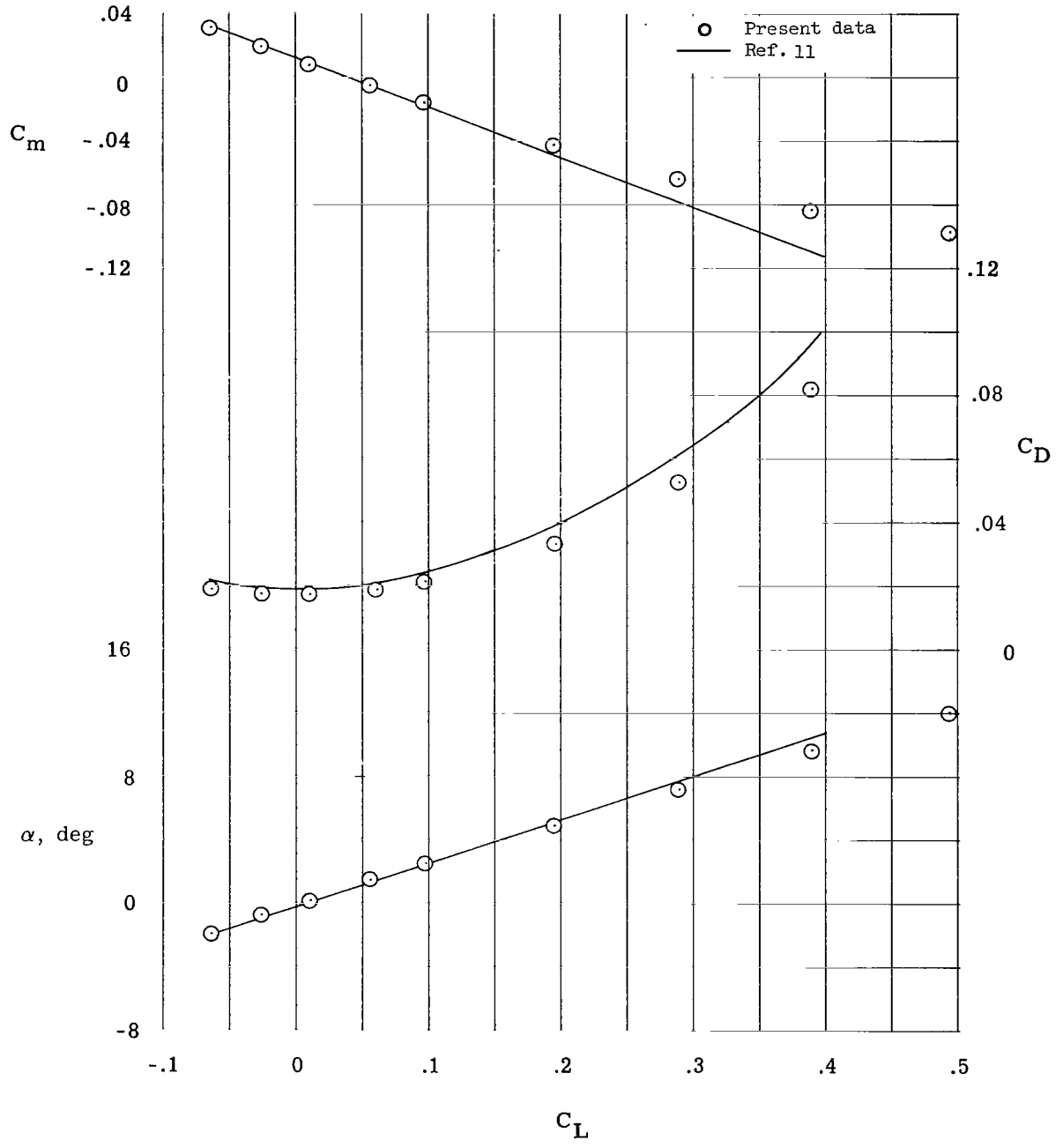

(b) M = 1.50.

Figure 13.- Continued.

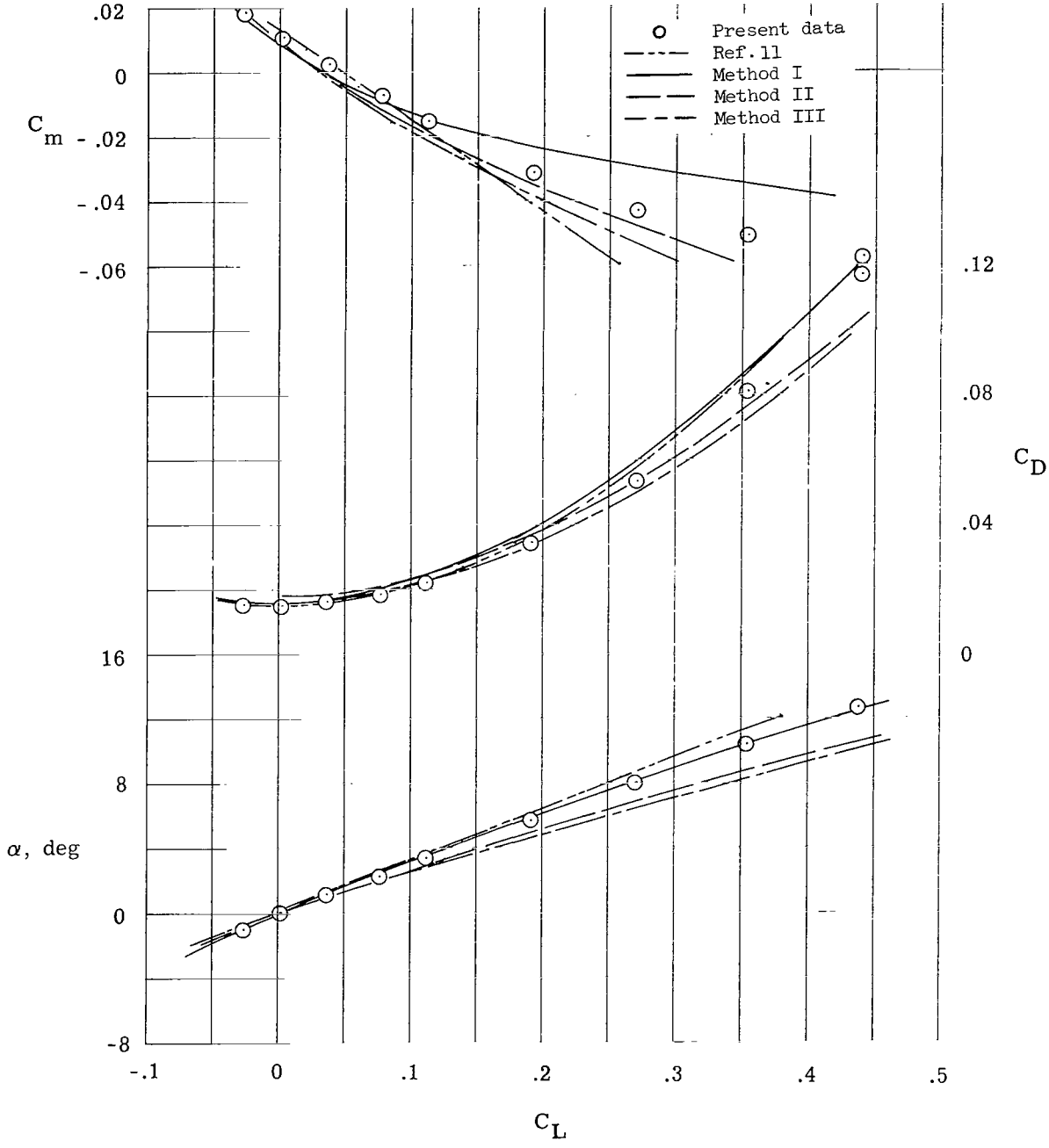

(c) M = 2.00.

Figure 13.- Continued.

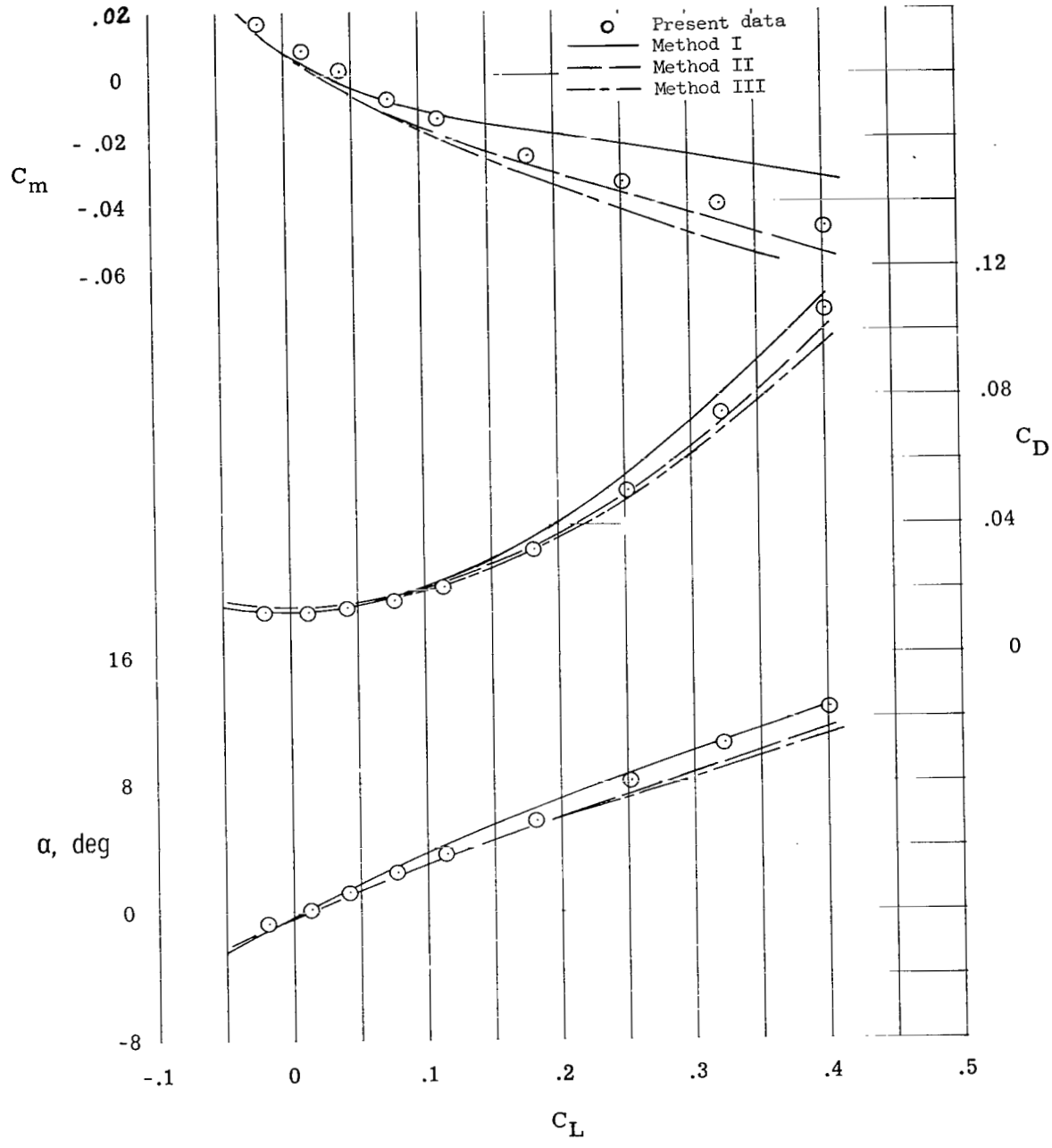

(d) M = 2.36.

Figure 13.- Continued.

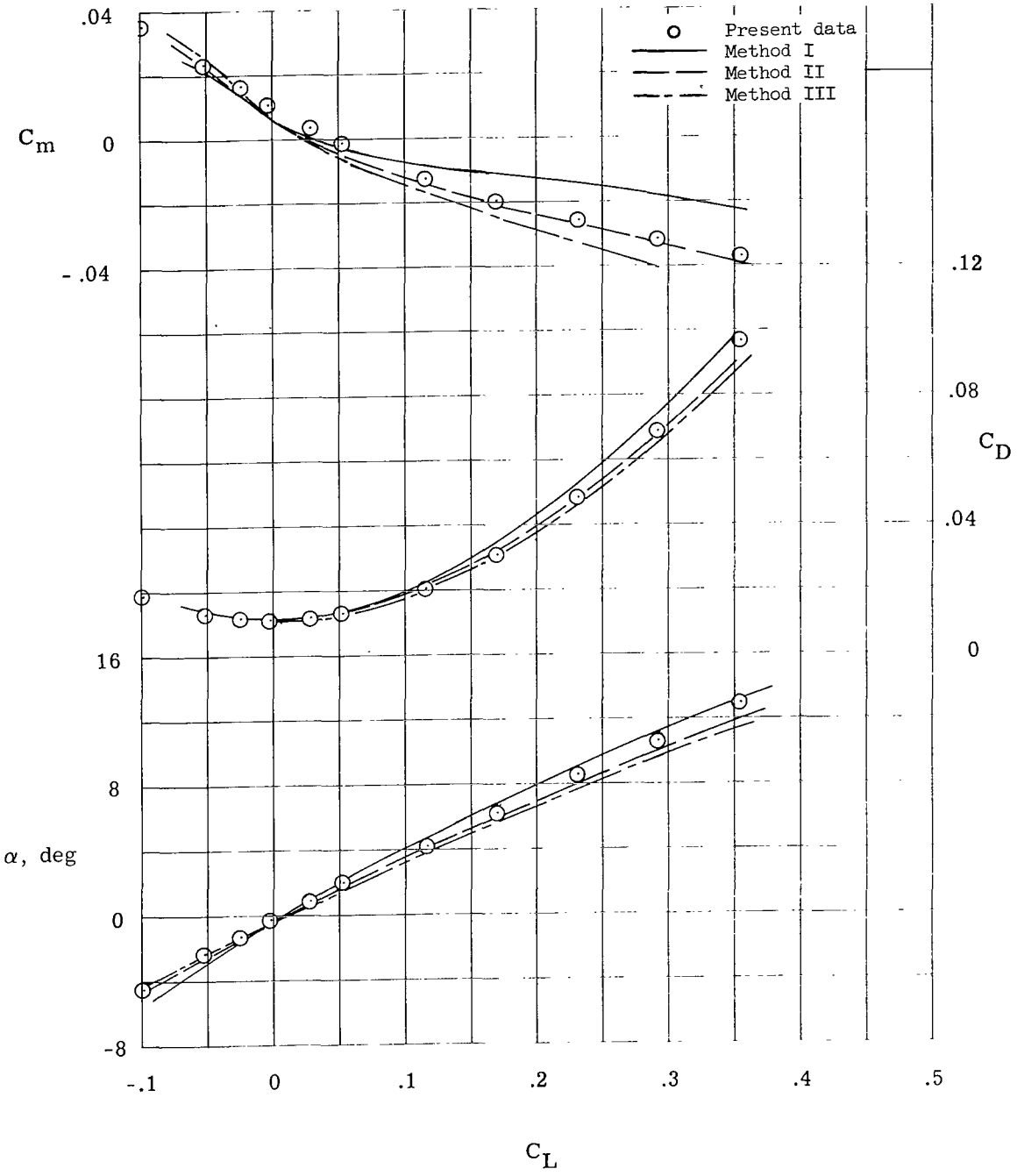

(e) M = 2.86.

Figure 13.- Continued.

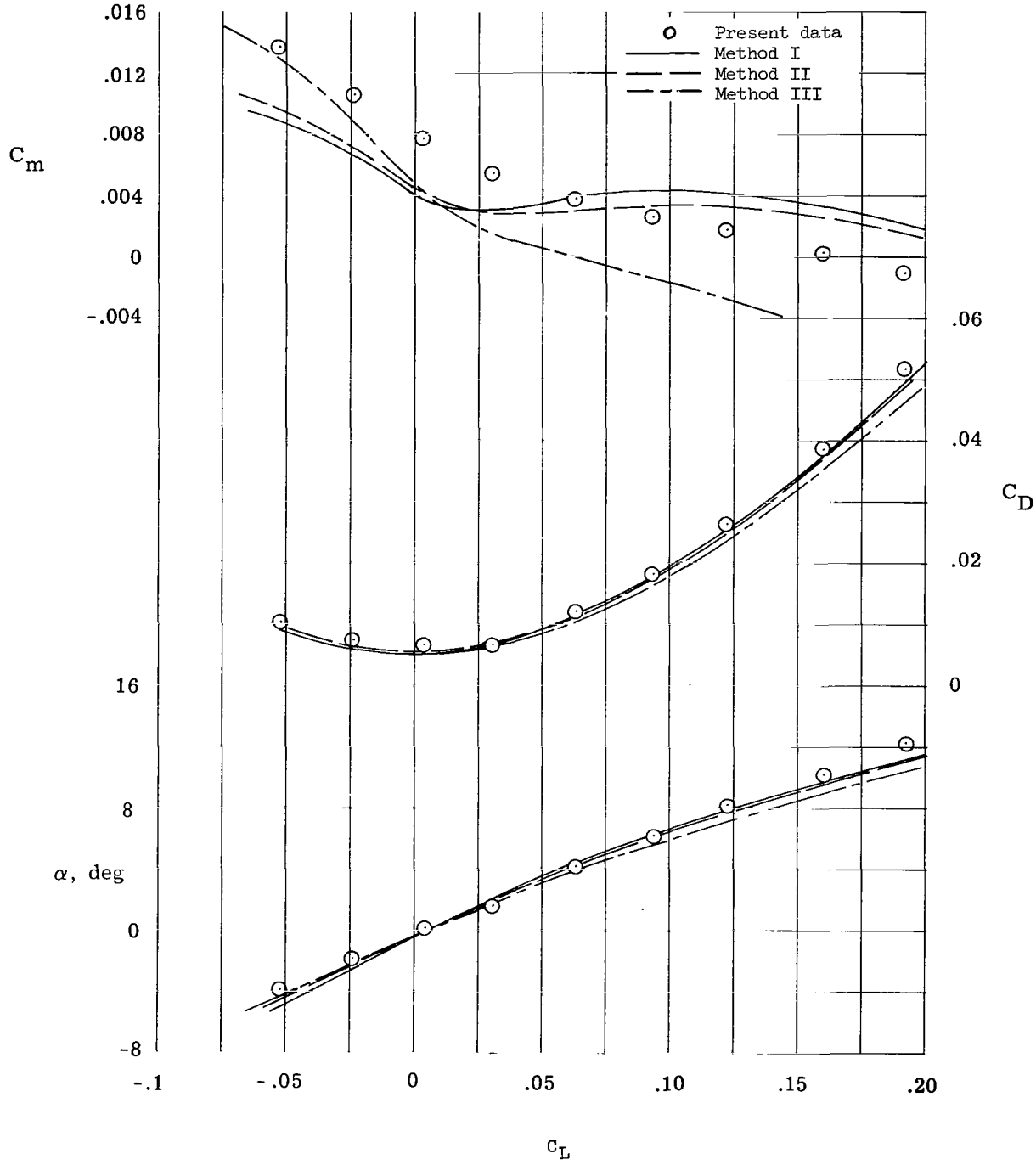

(f) M = 6.00.

Figure 13.- Concluded.

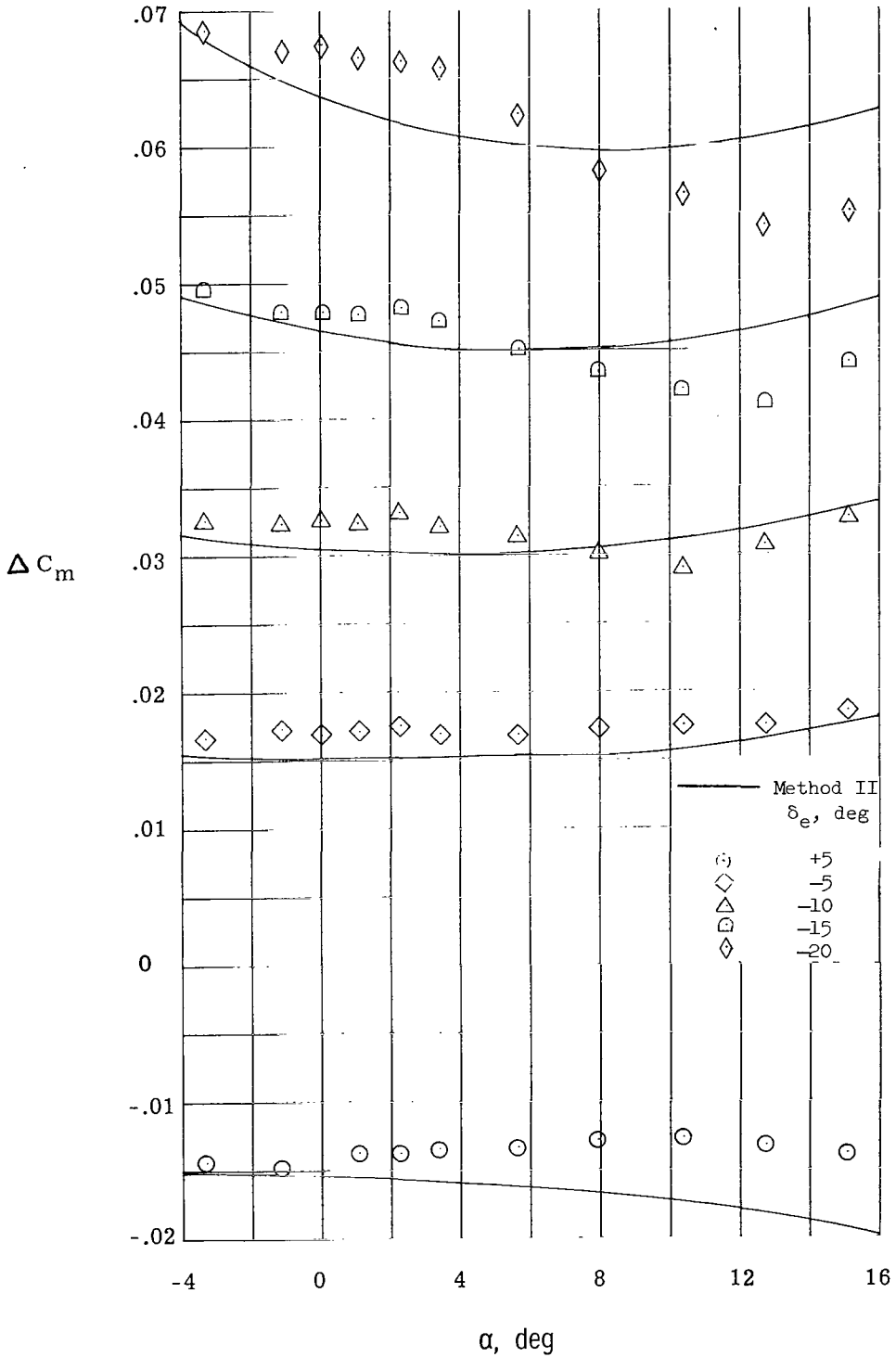

(a) M = 2.00.

Figure 14.- Effect of elevon deflection on pitching-moment-coefficient increment at angles of attack for configuration without inlet.

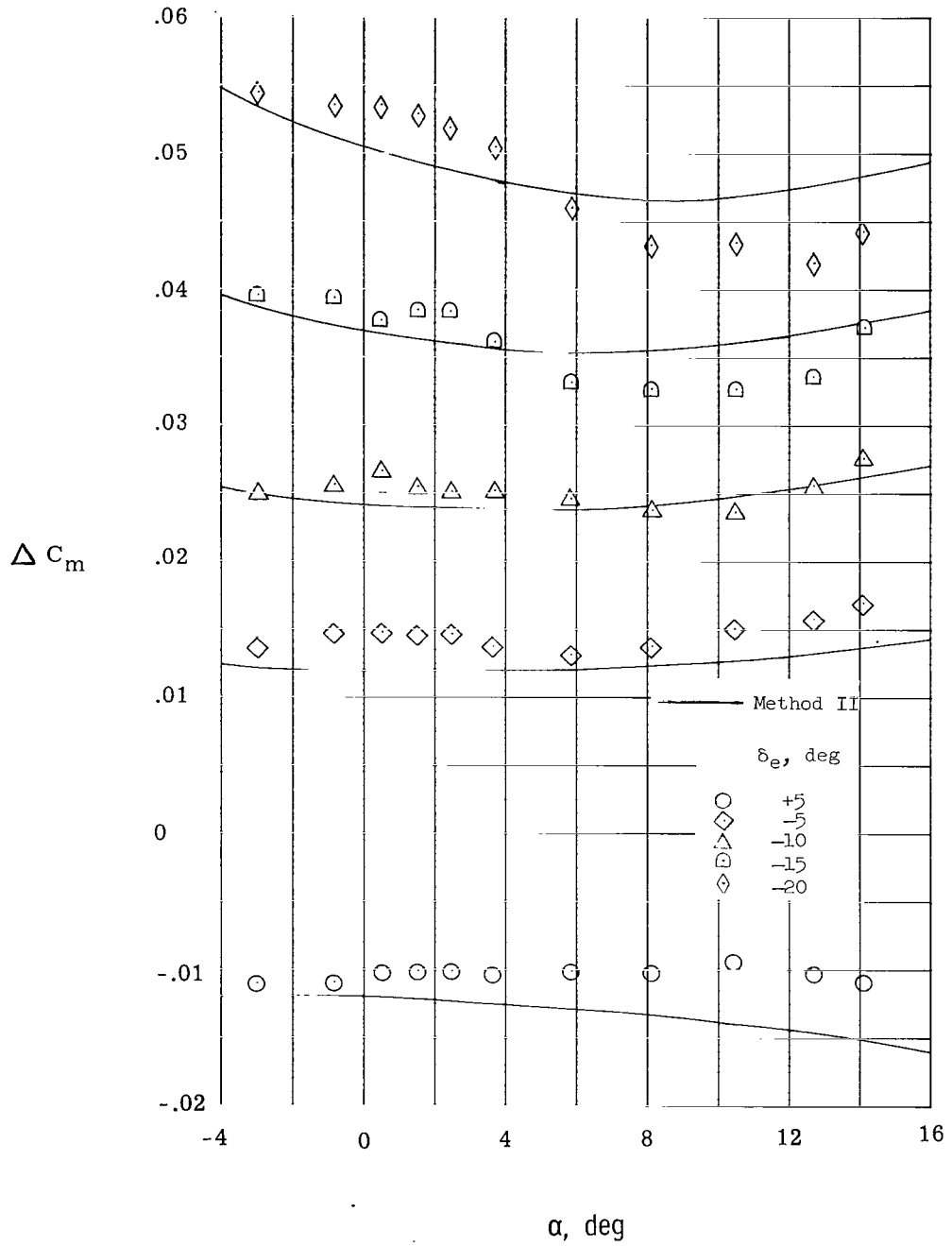

(b) M = 2.36.

Figure 14.- Continued.

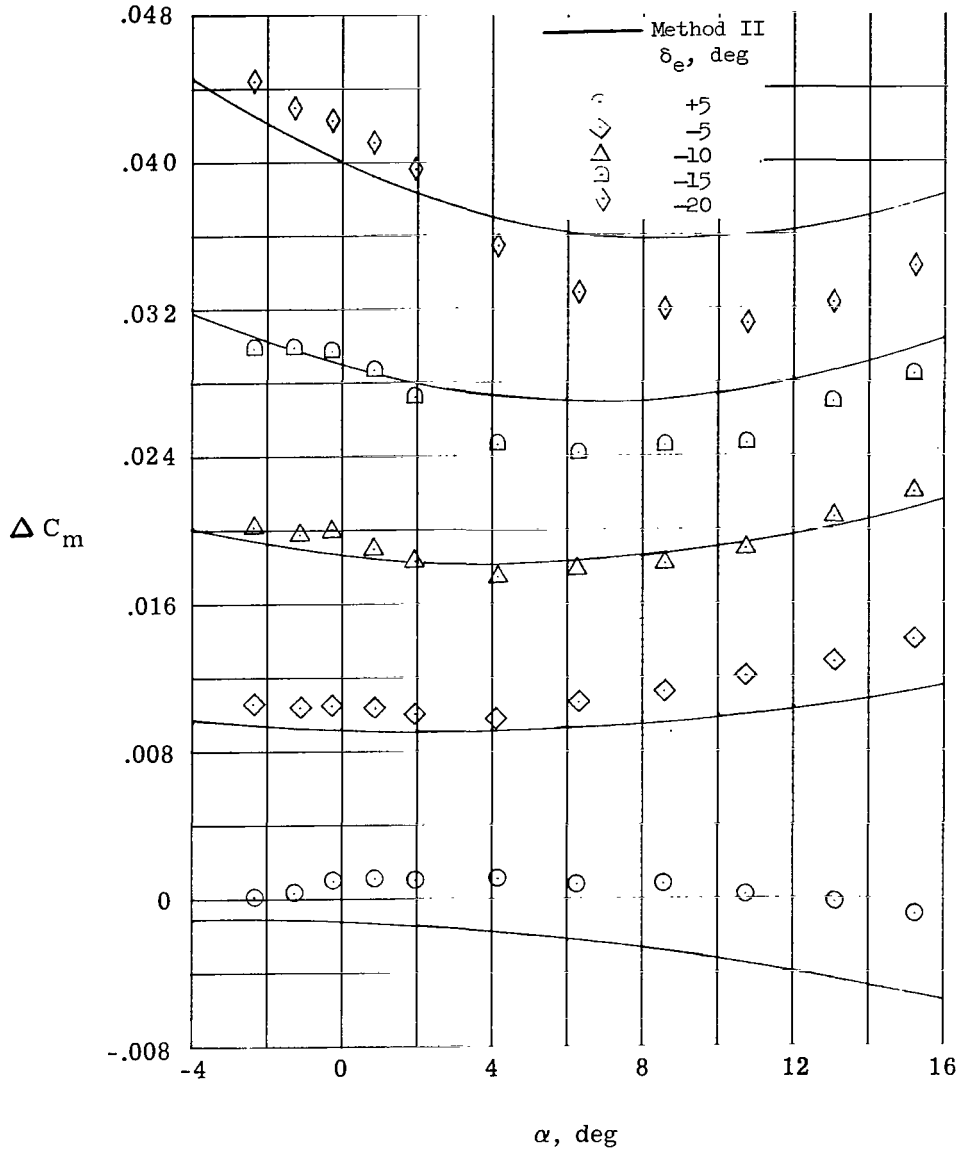

(c) M = 2.86.

Figure 14.- Continued.

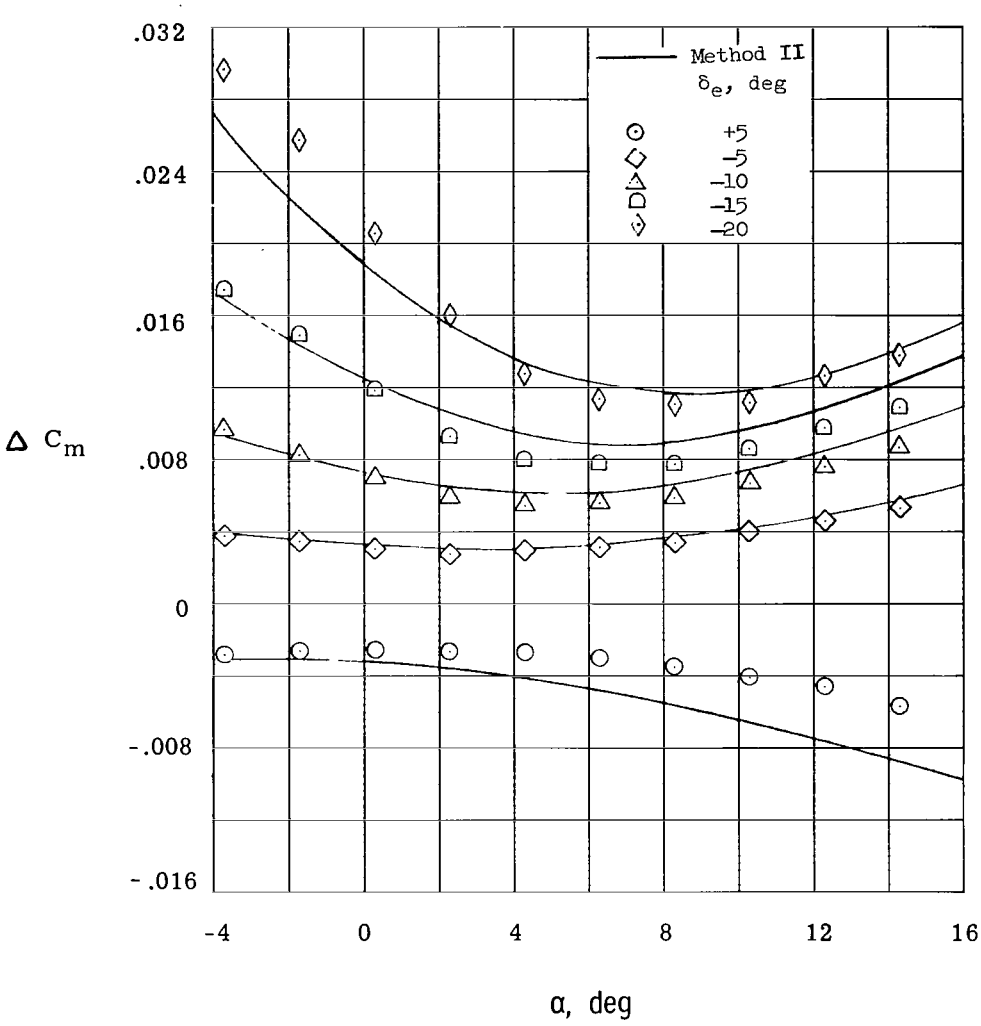

(d) M = 6.00.

Figure 14.- Concluded.

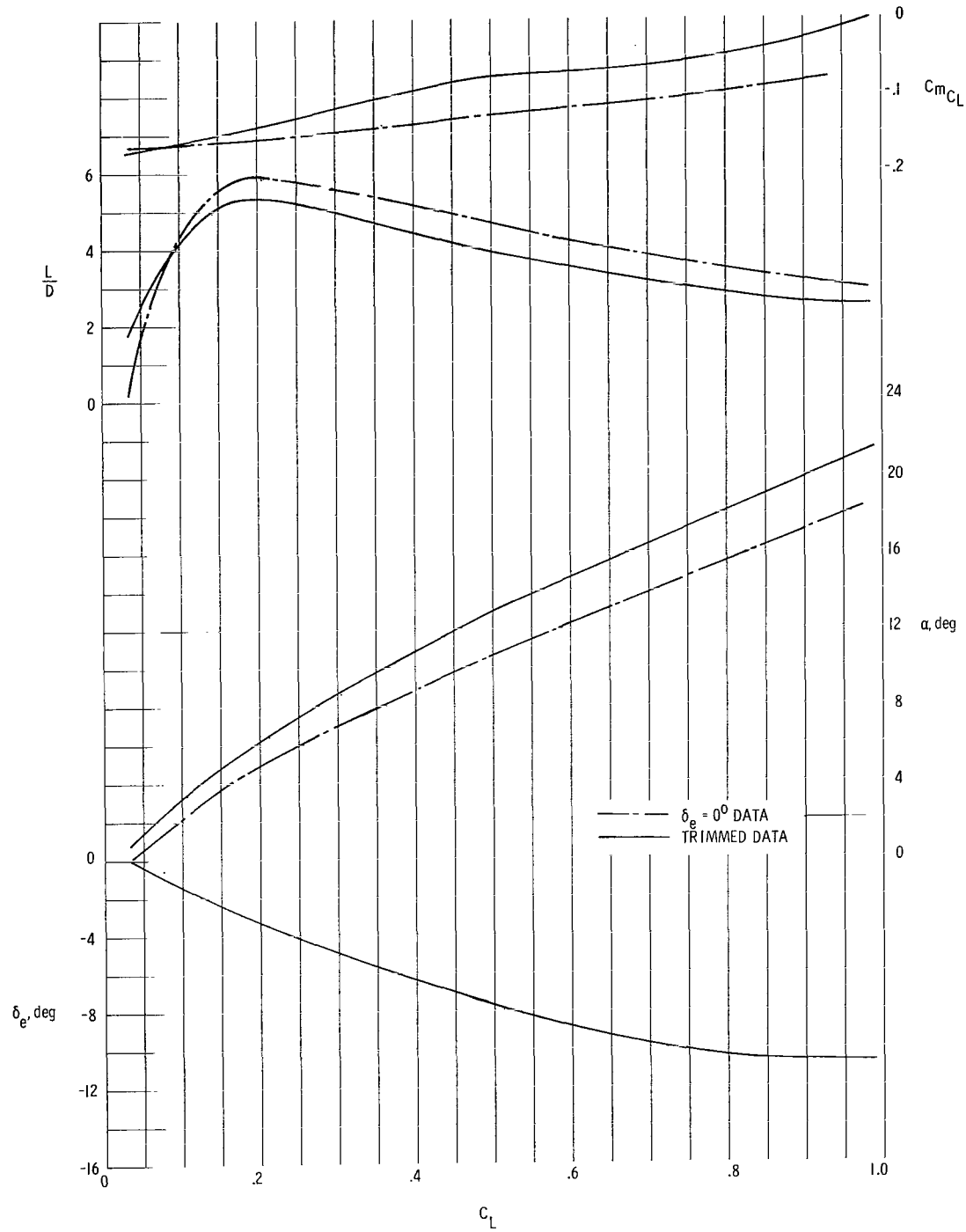

(a) M = 0.36.

Figure 15.- Trimmed and untrimmed aerodynamic characteristics for complete configuration.

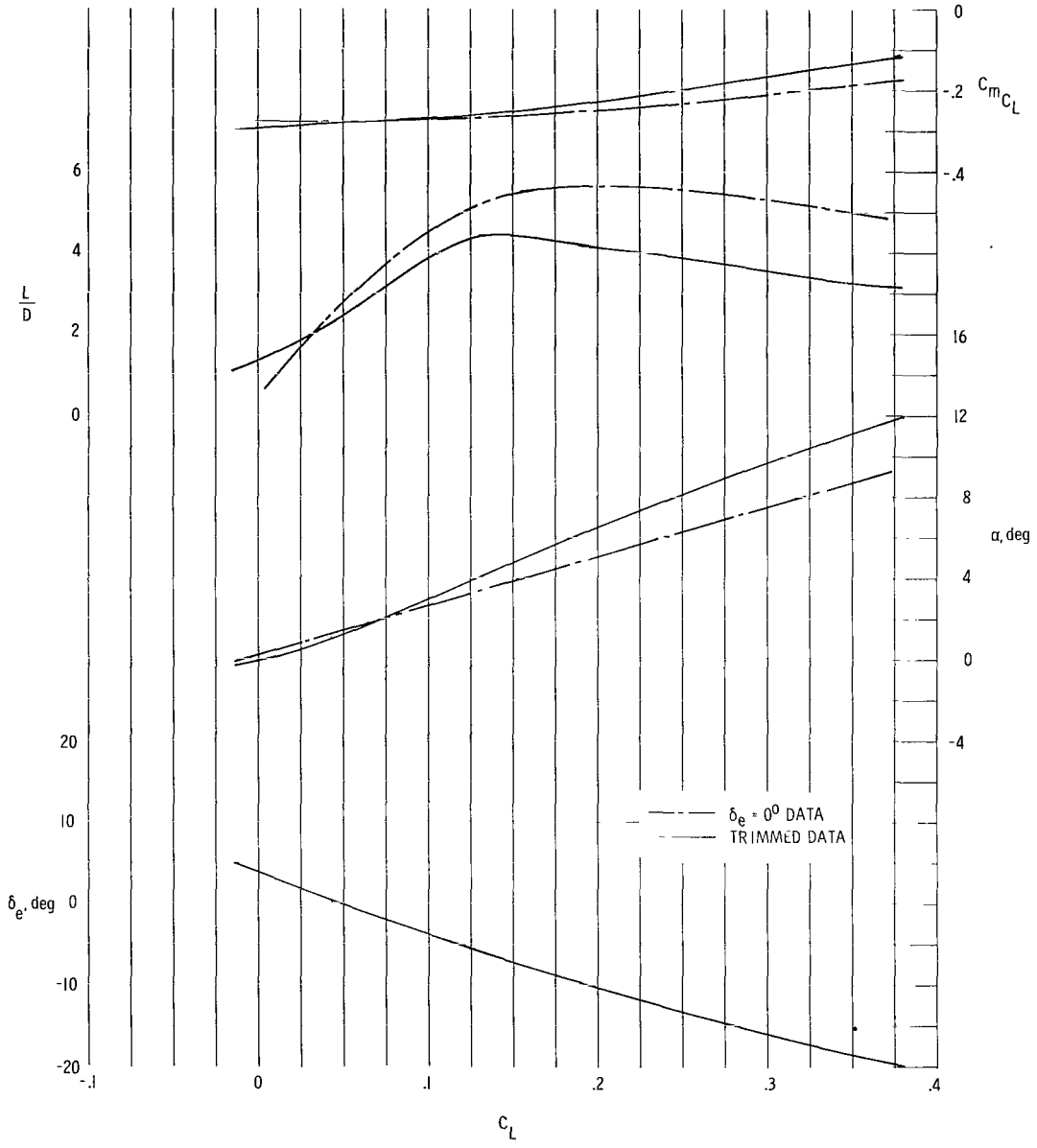

(b) M = 1.50.

Figure 15.- Continued.

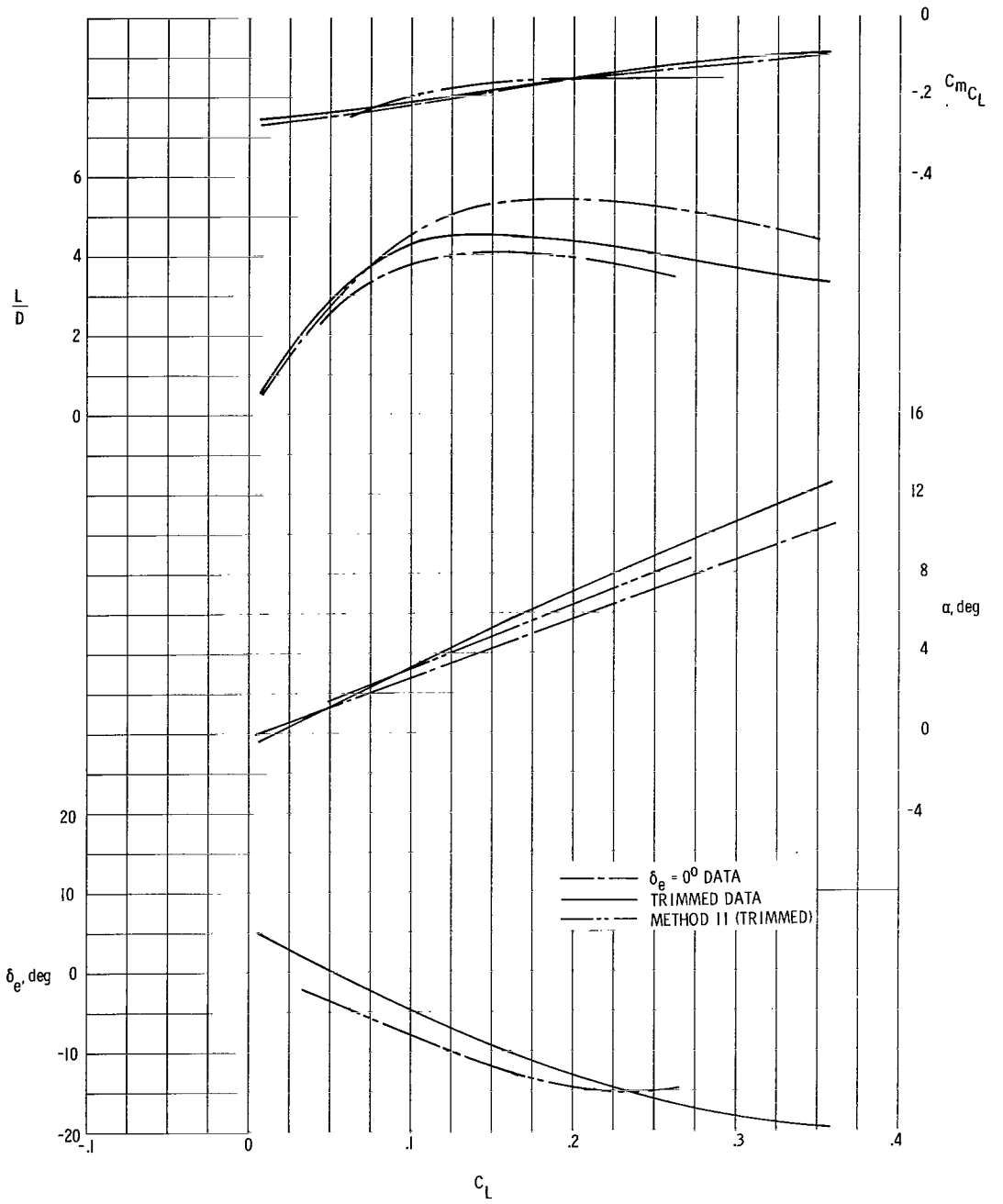

(c) M = 2.00.

Figure 15.- Continued.

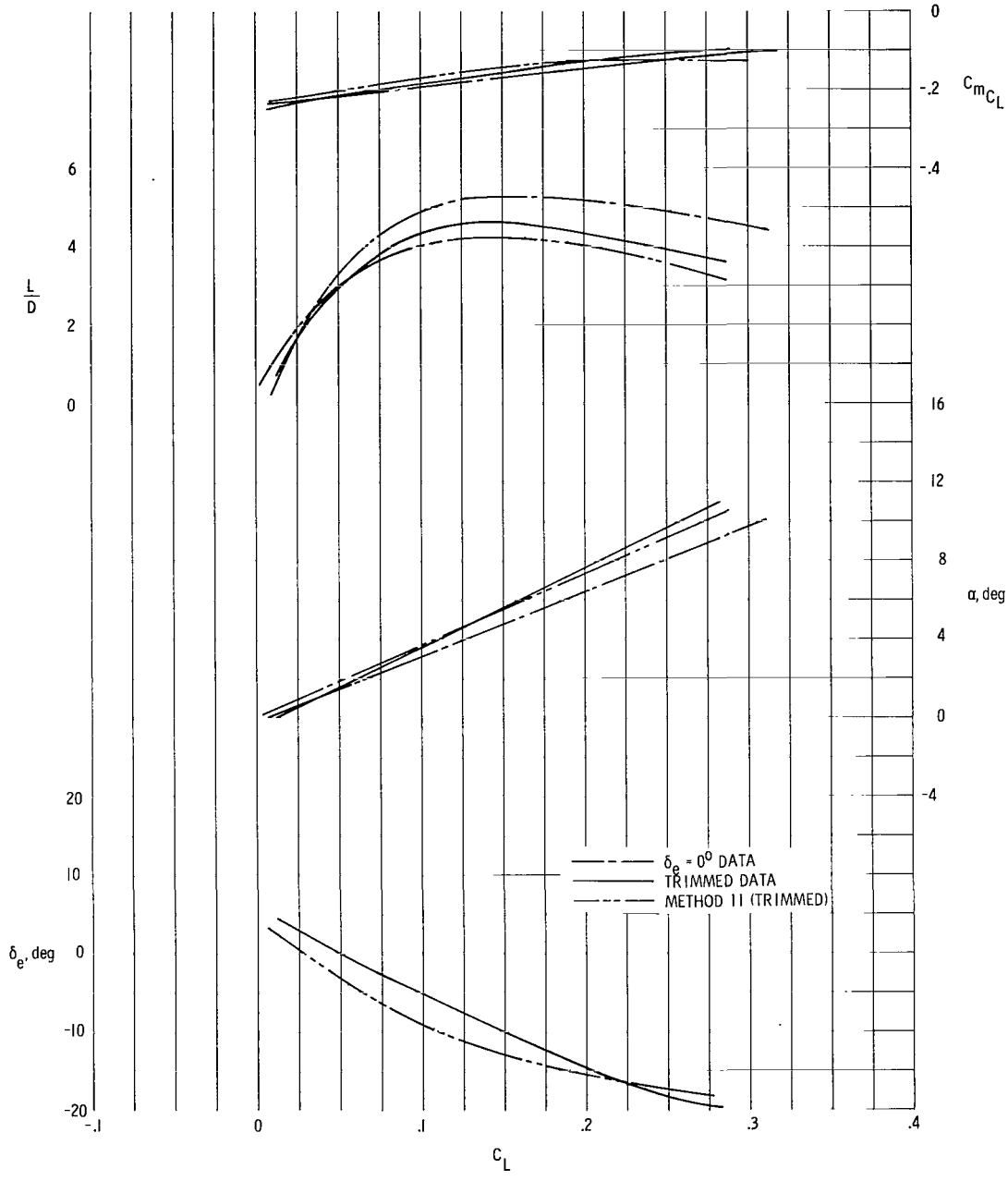

(d) M = 2.36.

Figure 15.- Continued.

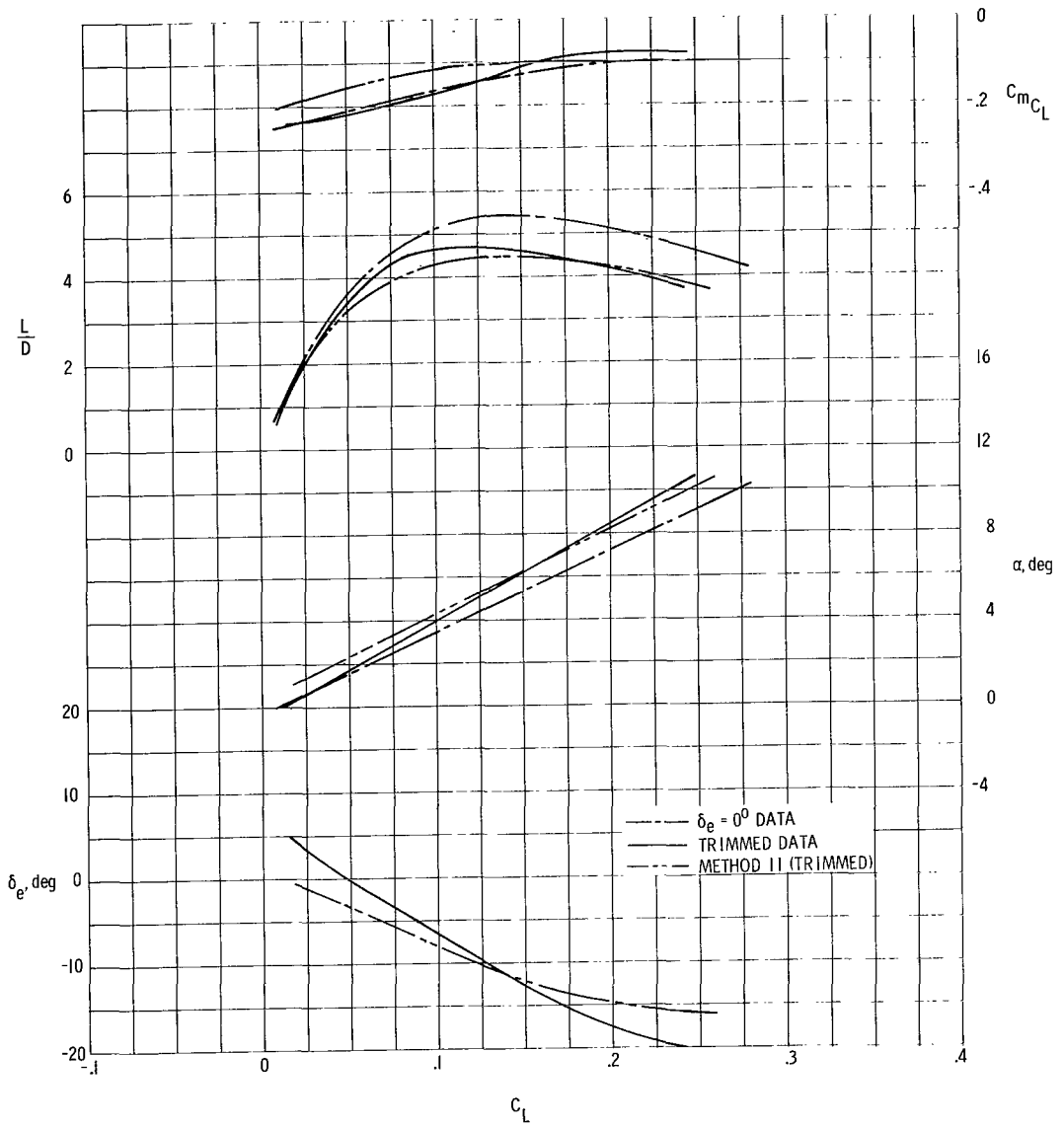

(e) M = 2.86.

Figure 15.- Continued.

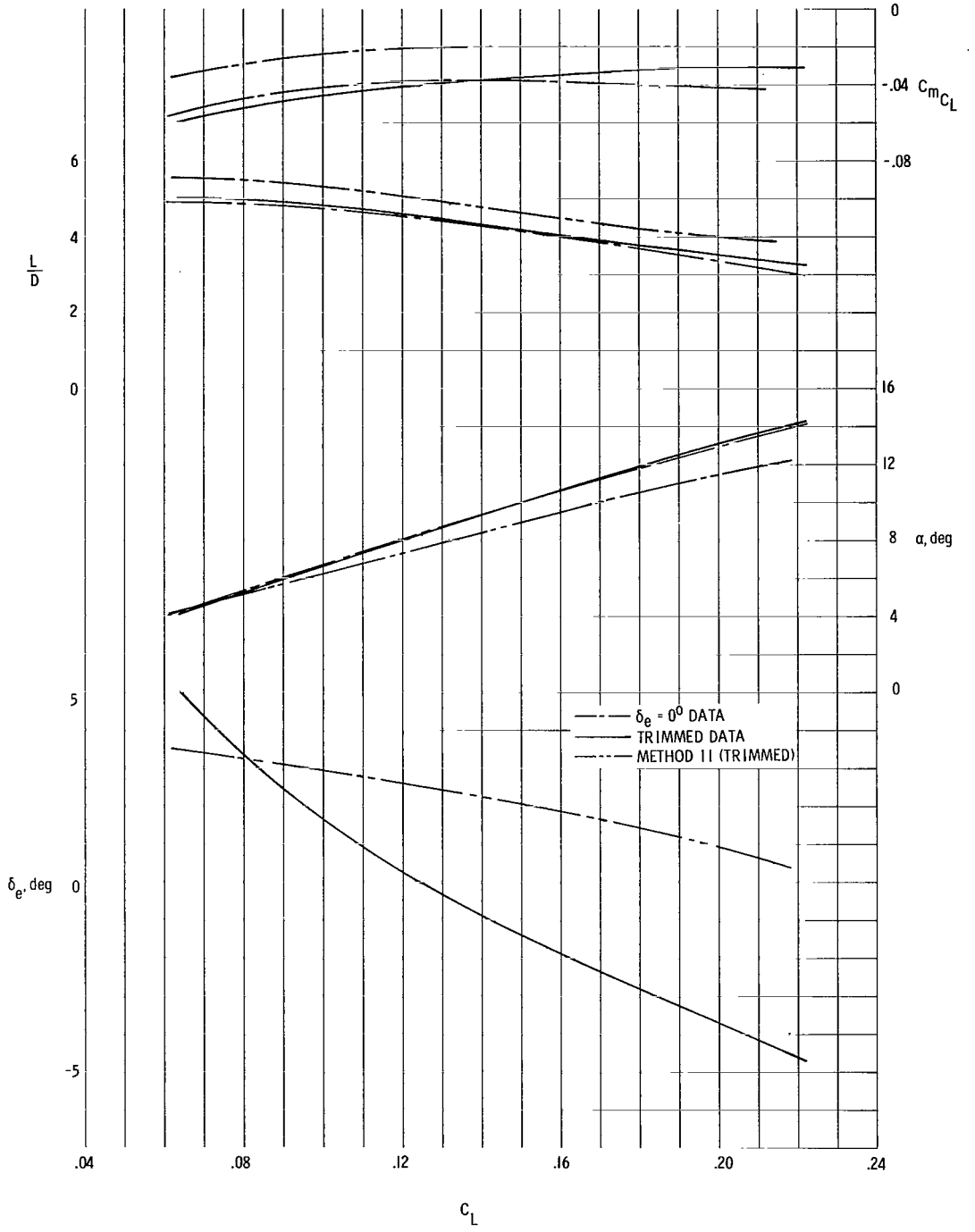

(f) M = 6.00.

Figure 15.- Concluded.

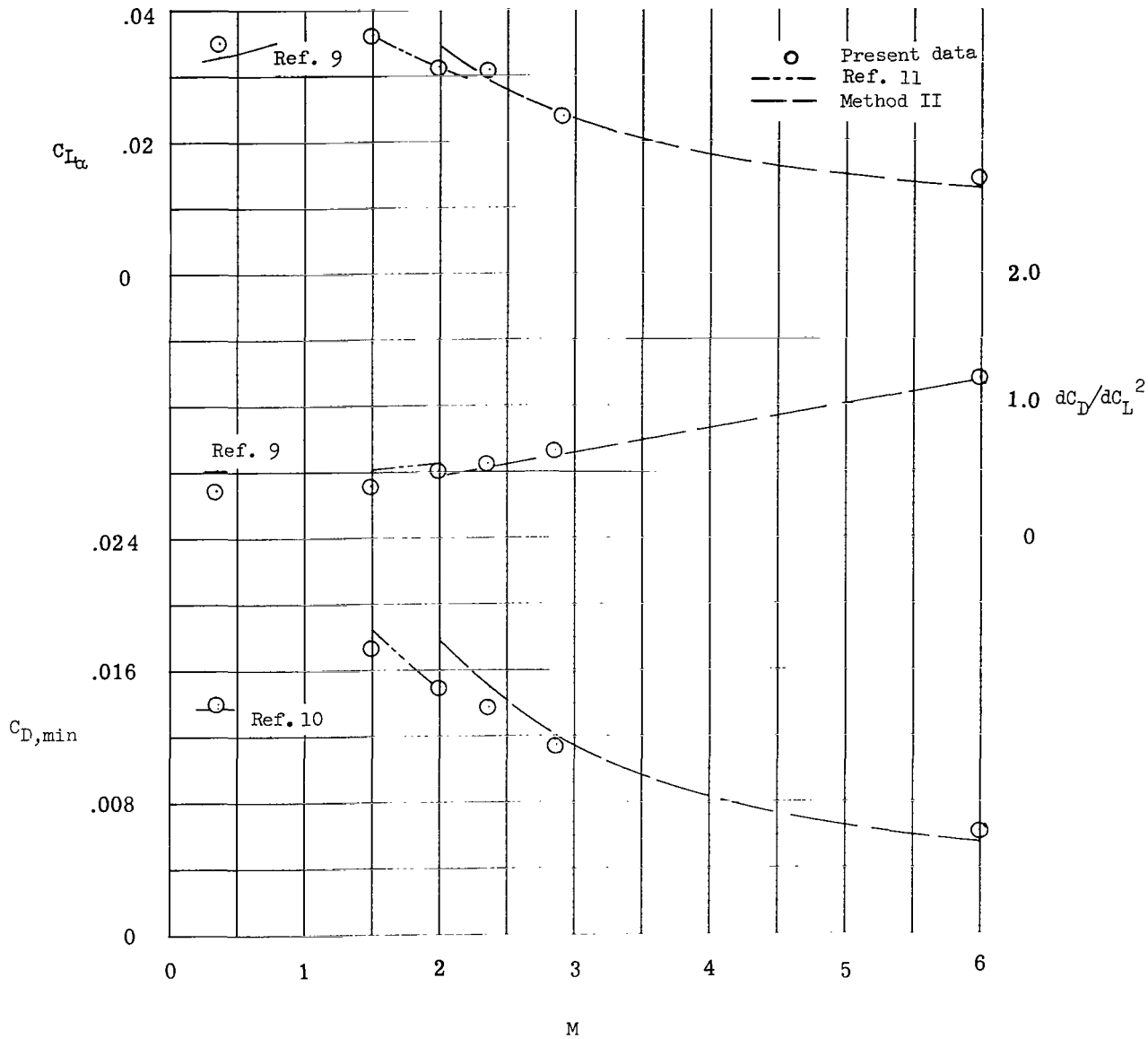

Figure 16.- Summary of aerodynamic characteristics for configuration without inlet. $\delta_e = 0^o$.

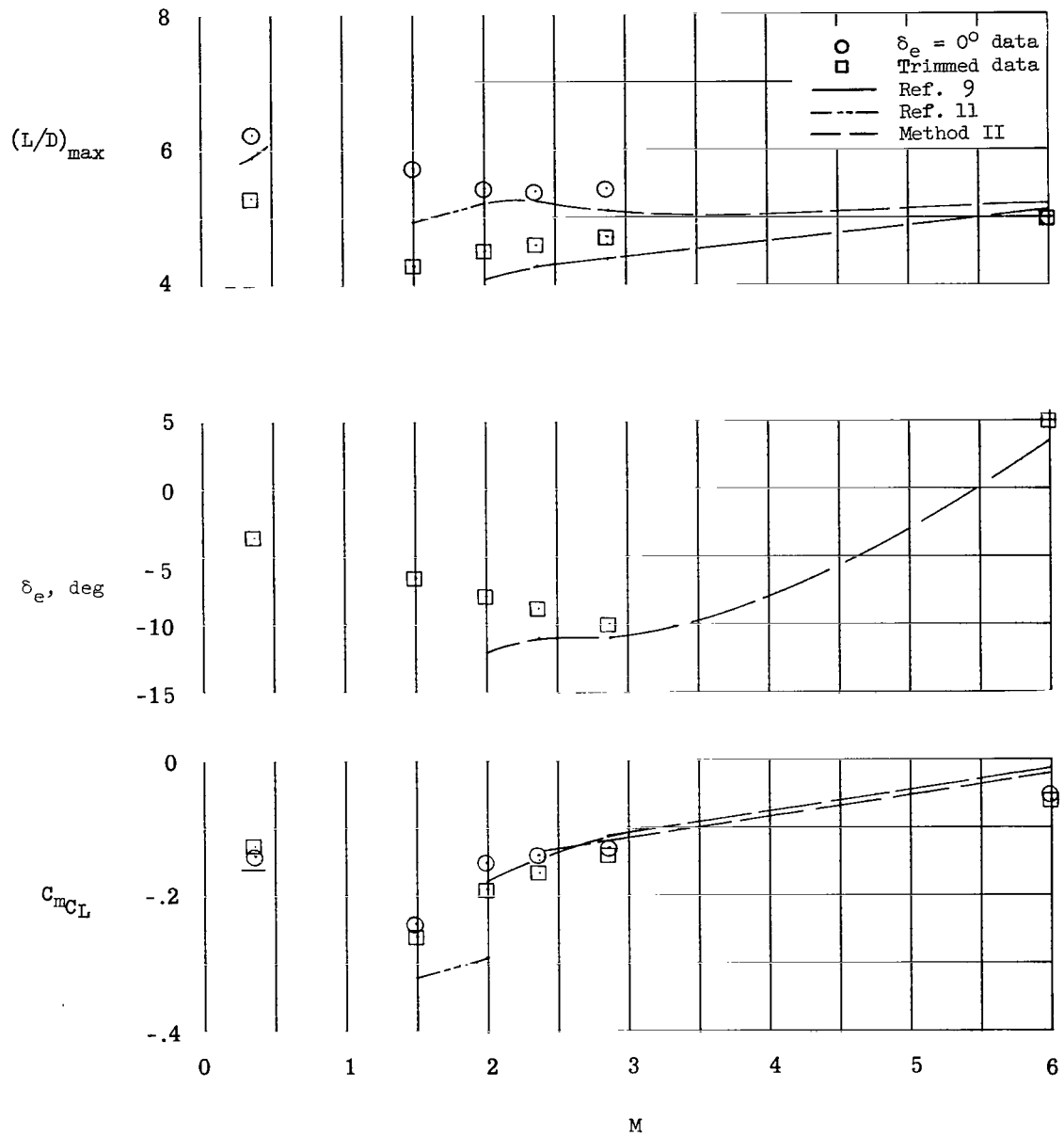

Figure 17.- Summary of performance and stability characteristics for configuration without inlet.

03U 001 26 51 3DS 71.10 00903
AIR FORCE WEAPONS LABORATORY /WLOL/
KIRTLAND AFB, NEW MEXICO 87117

ATT E. LOU BOWMAN, CHIEF,TECH. LIBRARY

"The aeronautical and space activities of the United States shall be conducted so as to contribute . . . to the expansion of human knowledge of phenomena in the atmosphere and space. The Administration shall provide for the widest practicable and appropriate dissemination of information concerning its activities and the results thereof."

—NATIONAL AERONAUTICS AND SPACE ACT OF 1958

NASA SCIENTIFIC AND TECHNICAL PUBLICATIONS

TECHNICAL REPORTS: Scientific and technical information considered important, complete, and a lasting contribution to existing knowledge.

TECHNICAL NOTES: Information less broad in scope but nevertheless of importance as a contribution to existing knowledge.

TECHNICAL MEMORANDUMS: Information receiving limited distribution because of preliminary data, security classification, or other reasons.

CONTRACTOR REPORTS: Scientific and technical information generated under a NASA contract or grant and considered an important contribution to existing knowledge.

TECHNICAL TRANSLATIONS: Information published in a foreign language considered to merit NASA distribution in English.

SPECIAL PUBLICATIONS: Information derived from or of value to NASA activities. Publications include conference proceedings, monographs, data compilations, handbooks, sourcebooks, and special bibliographies.

TECHNOLOGY UTILIZATION PUBLICATIONS: Information on technology used by NASA that may be of particular interest in commercial and other non-aerospace applications. Publications include Tech Briefs, Technology Utilization Reports and Technology Surveys.

Details on the availability of these publications may be obtained from:

SCIENTIFIC AND TECHNICAL INFORMATION OFFICE

NATIONAL AERONAUTICS AND SPACE ADMINISTRATION

Washington, D.C. 20546